UNIVERSITÉ DE MONTRÉAL

LARGE SCALE PRODUCTION, PURIFICATION, AND MODIFICATION OF CHITOSAN-BASED COMPLEXES FOR GENE THERAPY

ASHKAN TAVAKOLINAEINI

INSTITUT DE GÉNIE BIOMÉDICAL

ÉCOLE POLYTECHNIQUE DE MONTRÉAL

THÈSE PRÉSENTÉE EN VUE DE L'OBTENTION

DU DIPLÔME DE PHILOSOPHIAE DOCTOR

(GÉNIE BIOMÉDICAL)

JUIN 2017

© Ashkan TavakoliNaeini, 2017.

UNIVERSITÉ DE MONTRÉAL

ÉCOLE POLYTECHNIQUE DE MONTRÉAL

Cette thèse intitulée:

LARGE SCALE PRODUCTION, PURIFICATION, AND MODIFICATION OF CHITOSAN-BASED COMPLEXES FOR GENE THERAPY

présentée par : TAVAKOLINAEINI Ashkan

en vue de l'obtention du diplôme de : Philosophiae Doctor

a été dûment acceptée par le jury d'examen constitué de :

M. FRADETTE Louis, Ph. D., président

M. BUSCHMANN Michael, Ph. D., membre et directeur de recherche

M. LAVERTU Marc, Ph. D., membre et codirecteur de recherche

M. DE CRESCENZO Gregory, Ph. D., membre

M. PRAKASH Satya, Ph. D., membre externe

DEDICATION

I would like to dedicate this thesis to my wife, Naghmeh, the beautiful melody of my life, for her endless love, support, and encouragement

ACKNOWLEDGEMENTS

First and foremost, I would like to express my special thanks to my supervisor, Professor Michael Buschmann, for giving me the opportunity to join his team. He introduced me to the exciting field of gene delivery and taught me how to be a successful scientist. I appreciate his fabulous support, great feedbacks and recommendations during my Ph.D. Working with Mike was a real inspiration.

I would also like to thank my co-supervisor, Dr. Marc Lavertu, a great scientist and a passionate problem solver. He was always there in hard moments of my research. His critical insights, patience and constructive ideas were instrumental for my project. Throughout this long journey, I enjoyed the countless and constructive conversations we had, whether on the phone or in person.

I would also like to sincerely thank professors Satya Prakash, Louis Fradette, and Gregory De Crescenzo for agreeing to evaluate my work and take part of the defense jury.

A million thanks are accorded to Mohamad-Gabriel Alameh who contributed to the bio-related parts in my research. I appreciate his invaluable knowledge. The credit goes to him for offering to spend time on "bioparts" of this research meticulously, and providing helpful pointers to improve the dissertation during its final stages.

Very special thanks goes to my lovable fellow, Ousamah, a talented young researcher who I have spent most of my time with during this long journey and countless hours in the laboratory. Ousamah is a real friend that was always present in the time of need. His help has been crucial for the success of several critical and challenging experiments presented throughout this thesis.

I would like to thank my colleagues, Jean-Phillip, Anik, Martine, Daniel, Rajesh, Yuan, Vincent D, Vincent P, David, Nicolas, Leili, Colleen, Gabrielle, and Julie for the helpful insights into my project and the fun time on and out of campus.

My exceptional and grateful appreciations are accorded to my beloved wife, Naghmeh, for her support and patience during the days and nights I had to spend in the lab or in front of my desk. I am immensely indebted to you, Naghmeh!

My deepest admiration to my wonderful parents, Mr. Hassan Tavakoli and Mrs. Sima Amini, who have steadfastly prayed and faithfully sought God’s grace and guidance for me to finish this research. I owe my success to their selfless sacrifices, love and constant encouragement.

Last but not least, I would also like to express heartfelt gratitude to my grandparents for their unconditional love and warmth throughout life which has constantly driven me towards achieving my goals.

Thank you all

RÉSUMÉ

Le chitosane (CS) est un polymère cationique naturel qui s'associe aux acides nucléiques (AN), tels que les ARN interférents courts (siRNA), l'ADN plasmidique (pDNA) ou l'ARN messager (mRNA), pour former des complexes polyélectrolytes ou polyplexes non-solubles. Au cours des dernières années, les formulations de polyplexes à base de chitosane ont suscité un intérêt croissant en tant que systèmes de livraison d'acides nucléiques efficaces et sécuritaires, et ce pour des applications *in vitro* et *in vivo*. Les polyplexes CS/AN se forment par association électrostatique lorsque des solutions de CS et NA sont mélangées l'une avec l'autre. On utilise généralement le CS en excès par rapport aux AN, de telle sorte que les polyplexes portent une charge nette positive et suffisante pour assurer leur stabilité colloïdale. Malgré leur grand potentiel thérapeutique, les polyplexes à base de chitosane et leurs méthodes de production doivent être développés/optimisés davantage avant de pouvoir être utilisés pour des applications cliniques.

Le mélange manuel est la méthode de production la plus courante des polyplexes CS/NA. Une telle méthode ne permet cependant pas un contrôle précis du processus de formation des complexes, pose donc des problèmes de variabilité/répétabilité entre utilisateurs/expérimentateurs et ne peut évidemment pas être utilisée à grande échelle. D'un autre côté, une fraction significative du CS utilisé en excès lors de la préparation des polyplexes demeure libre (non-lié aux polyplexes). Cette fraction de chitosane libre ainsi que la charge électrique positive des polyplexes favorisent les interactions avec les composants du sang et des systèmes physiologiques qui sont chargés négativement, ce qui limite la dose applicable de ces systèmes de livraison. L'application clinique de cette technologie de livraison par voie intravasculaire requièrt donc le développement de formulations avec une hémocompatibilité accrue. Le développement de telles formulations nécessite l'élimination de la fraction de CS libre et la modification des polyplexes avec, par exemple, le recouvrement de leur surface avec des polymères hydrophiles neutres ou des polyanions, de façon à neutraliser ou inverser le signe de la charge de ces complexes et ainsi éliminer/limiter les interactions avec les composantes du sang et améliorer leur pharmacocinétique.

Dans le cadre de ce projet de doctorat, un système de mélange en ligne automatisé (SMLA) pour la production contrôlée et reproductible de larges volumes de polyplexes CS/AN a d'abord été développé. Le SMLA a permis la production de polyplexes CS/siRNA plus petits et plus homogènes par rapport à ceux obtenus par mélange manuel. Les polyplexes CS/siRNA produits à

l'aide du SMLA en utilisant la vitesse de mélange maximale de 300 mL/min et une concentration de siRNA de 0.2 mg/mL, sont sphériques, plus petits et homogènes avec un diamètre hydrodynamique (Z-average) et un indice de polydispersite (PdI) de 47 nm et 0.12, respectivement, comparativement à des complexes préparés manuellement dont la taille est de l'ordre de 100 nm et le PdI de l'ordre de 0.2. Ces travaux de recherche ont permis de démontrer que les polyplexes CS/siRNA préparés à l'aide du SMLA ont une efficacité de silençage du gene de l'apolipoprotéine B (ApoB) in vitro équivalente ou supérieure à celle des polyplexes préparés par mélange manuel. Cette plate-forme de production à grande échelle automatisée permet de surmonter les limitations associées au mélange manuel des polyplexes et rend possible leur production contrôlée en grandes quantités pour des applications précliniques/cliniques.

Afin de purifier de grands volumes de polyplexes à base de CS préparés à l'aide du SMLA, la filtration à flux tangentiel (TFF) basée sur l'utilisation de la technologie de fibres creuses a été adoptée et optimisée. Les paramètres d'opération optimaux de la TFF opérée en mode diafiltration ont été déterminés en utilisant des fibres creuses de polyethersulfone modifié (mPES) avec un poids moléculaire de coupure (MWCO) de 100 kDa: pression transmembranaire (TMP) de 0.9-1.0 psi, taux de cisaillement relativement faible allant de 7000 à 11000 s^{-1}. Le rendement du procédé optimisé est de l'ordre de 85% avec une élimination du chitosane libre de plus de 98% et les résultats démontrent que les propriétés physico-chimiques des complexes ne sont pas altérées par la diafiltration. Les complexes de CS/siRNA ainsi purifiés ont été recouverts avec une librairie de molécules d'acide hyaluronique (HA) afin d'accroitre leur hémocompatibilité. Des HAs de masse molaire et degré de sulfatation (densité de charge) différents ont été utilisés. Les résultats démontrent que l'utilisation de HAs sulfatés ou non-sulfatés dans des proportions molaires de charges négatives du HA : charges négatives du siRNA supérieures ou égales à 2 :1 permet la production de polyplexes homogènes de faible taille et chargés négativement. De plus, l'utilisation de HA sulfatés permet d'obtenir des complexes plus stables par rapport à ceux préparés avec des HAs non-sulfatés. Finalement, nous avons déterminé que les polyplexes recouverts avec de HA non-sulfaté de masse molaire 10 kDa et de HA sulfaté de masse molaire 12 kDa (diamètres hydrodynamiques de 125 – 129 nm, PdI de 0.09 – 0.18 et potentiel zeta de 17 mV) possèdent une efficacité de silençage in vitro aussi élevée que celle de polyplexes CS/siRNA non recouverts de HA (non modifiés) et présentent une hémocompatibilité accrue par rapport aux complexes non-recouverts.

Globalement, ce travail de recherche a mené au développement d'une méthode contrôlée et reproductible de production à grande échelle de polyplexes à base de chitosane. Ces polyplexes possèdent une bioactivité équivalente ou supérieure en comparaison à celle de polyplexes préparés par mélange manuel. La purification de larges volumes de polyplexes par TFF, tout en préservant leurs propriétés physico-chimiques et leur bioactivité, constitue une autre réalisation importante de ce projet. L'ajout de molécules de HA à la surface de polyplexes suite à leur purification par TFF a mené au développement d'une nouvelles classe de complexes bioactifs avec une hémocompatibilité accrue. L'ensemble des résultats et développements de ce travail de recherche représentent un pas important pour l'utilisation future de polyplexes CS/AN dans des applications précliniques et cliniques.

ABSTRACT

Chitosan (CS) is a naturally derived cationic polysaccharide which simply self-assembles with nucleic acids (NAs) to form non-soluble polyelectrolyte complexes. In recent years, CS-based polyplex formulations have gained increasing interest as safe and efficient non-viral gene delivery systems both *in vitro* and *in vivo*. CS/NA polyplexes are produced by electrostatic-mediated association upon mixing of CS and NA solutions while CS is in excess *versus* NA. Thus, the final polyplexes bear a net positive charge that electrostatically stabilize them. Despite their great therapeutic potential, CS-based polyplexes must be further improved before transferring for clinical applications. Manual mixing is the most common method to produce CS-based polyplexes. However, this method varies in implementation, which raises concerns regarding comparability of the final polyplexes. Nonetheless, independent of the adopted approach, the conventional manual mixing is not only a poorly controlled method that results in irreproducibility but it is also restricted to relatively small volumes, which poses risks of batch to batch and inter-user variability. On the other hand, upon mixing of CS and NA, a significant portion of CS remains unbound to polyplexes. Due to interactions with negatively charged blood components, the unbound CS as well as the positive surface of polyplexes limit the applicable dosage of these therapeutics. Hence, clinical application of this technology requires development of hemocompatible formulations for intravenous (IV) delivery systems. Development of formulations with increased hemocompatibility involves coating the polyplexes either with another hydrophilic neutral polymer, e.g. polyethylene glycol (PEG), or with another polyanion, e.g. Hyaluronic Acid (HA), to switch the surface charge in order to eliminate the interactions with blood cells, and finally enhance the pharmacokinetics of CS-based polyplexes. Before these polyplexes can be used for further surface modifications, and studied clinically for IV administration they must be purified. Purification of CS-based polyplexes relies on elimination of the unbound CS molecules from the polyplexes.

This work initially established a fully automated in-line mixing system (AIMS) for production of large batches of CS-based polyplexes. CS/siRNA polyplexes produced via AIMS were predominantly spherical, with z-average diameter as small as 47 nm, polydispersity index (PDI) as low as 0.12, and zeta potential of +16 mV, when prepared at the highest possible mixing speed (300mL/min), and siRNA concentration of 0.2mg/mL. Thus, AIMS was capable to deliver even smaller and more monodisperse CS/siRNA polyplexes compared to manual polyplexes with z-

average of 100 nm and PDI of 0.20). It was also demonstrated that the in-line mixed CS/siRNA polyplexes have equivalent or higher silencing efficiency of Apolipoprotein B (ApoB) in HepG2 cells, compared to manually prepared polyplexes. This scaled-up platform addressed the risk of batch to batch inter-user and intra-user variability, resulting in a controlled quality of large quantities of polyplexes intended for pre-clinical and clinical applications.

Furthermore, to concentrate and purify large batches of CS-based polyplexes, tangential flow filtration (TFF) was adopted based on hollow fiber technology. Optimal TFF operational conditions were established using 100kD modified polyethersulfone (mPES) hollow fibers: trans-membrane pressure (TMP) of 0.9-1.0 psid, and relatively low shear rates of 7000-11000 s^{-1}. Upon establishment of the operational conditions, it was demonstrated that TFF is capable in concentration of polyplexes up to sevenfold while preserving their physico-chemical properties. Optimal number of diafiltration volumes (DV) for diafiltration of polyplexes was also studied. Our data showed that when system ran at the shear rate of 7000 s^{-1}, more than 98% of the unbound CS was removed with a DV of 5, while recovery yield was as high as 85%. Moreover, no marked changes in physico-chemical properties and morphology of polyplexes were observed post-diafiltration. Purified CS/siRNA eGFP polyplexes were then coated by a library of HA molecules to enhance their hemocompatibility. HAs with different molecular weights and degrees of sulfation, at different phosphate to carboxyl ratios (C:P) were tested. It was found that a high molecular weight HA (866 kDa) results in macroscopic flocculations at every C:P ratio tested. Moreover, for low molecular weight HA (10-40 kDa) or moderate molecular weight HA (148-168 kDa), C:P$\geq$ 2 is needed to effectively coat the polyplexes and switch the surface charge of complexes. Our data showed that polyplexes coated with lower molecular weight HAs, non-sulfated 10kDa and sulfated 12 kDa have have even higher knockdown efficiency of eGFP in H1299 cells (75-82%), compared to the uncoated polyplexes (53-63%). Furthermore, it was shown that although both sulfated and non-sulfated HAs result in small sized, homogenous and bioactive complexes, sulfated HA molecules present higher stability during filtration process. However, for both non-sulfated and sulfated HAs, coated formulations demonstrated improved hemocompatibility compared to the uncoated polyplexes.

This work allowed to develop a controlled method for reproducible production of large batches of CS-based polyplexes with equivalent bioactivity as compared to manually prepared polyplexes. Purification of large batches of polyplexes *via* TFF while preserving their physicochemical

properties, and their biological activity was another accomplishment of this work. Moreover, adding a HA-coating to polyplexes led to the development of a new class of bioactive complexes with increased hemocompatibility. These results represent an important step towards future clinical use of CS-based intravenous gene therapies.

TABLE OF CONTENTS

DEDICATION III

ACKNOWLEDGEMENTS IV

RÉSUMÉ VI

ABSTRACT IX

TABLE OF CONTENTS XII

LIST OF TABLES XVII

LIST OF FIGURES XVIII

LIST OF SYMBOLS AND ABBREVIATIONS XXIII

CHAPTER 1 INTRODUCTION 1

1.1 Objectives 6

1.2 Architecture of the thesis 6

CHAPTER 2 LITERATURE REVIEW 7

2.1 Polyelectrolyte complexes (PECs) 7

2.1.1 Soluble and colloidal PECs 7

2.1.2 Polyelectrolyte complex structure 8

2.2 Chitosan as a polycation for gene delivery applications 9

2.2.1 Influential factors on CS/NA polyplex formation and its properties 11

2.3 Chitosan-based polyplexes 14

2.3.1 Chitosan/pDNA polyplexes 15

2.3.2 Chitosan/siRNA polyplexes 16

2.3.3 Coated polyplexes: surface modification using hyaluronic acid 16

2.4 Techniques used for mixing NA with polycations 18

2.4.1 Manual mixing 18

2.4.2 Jet mixer 19

2.4.3 Y or T-shaped mixer 19

2.4.4 Static mixer 20

2.4.5 Staggered herringbone micromixer 20

2.5 Purification and concentration techniques 22

2.5.1 Dialysis 22

2.5.2 Gel filtration chromatography 23

2.5.3 Ultracentrifugation 23

2.5.4 Freeze-drying 23

2.5.5 Ultrafiltration 24

2.6 Parameters that influence a TFF process 29

2.6.1 Membrane material and molecular weight cut off 29

2.6.2 Membrane geometry 30

2.6.3 Cross flow rate 32

2.6.4 Trans-membrane pressure 32

CHAPTER 3 APPROACH OF THE RESEARCH WORK AND GENERAL STRUCTURE OF THE THESIS 35

CHAPTER 4 ARTICLE 1: AUTOMATED IN-LINE MIXING SYSTEM FOR LARGE SCALE PRODUCTION OF CHITOSAN-BASED POLYPLEXES 37

4.1 Abstract 37

4.2 Graphical abstract 38

4.3 Keywords 38

4.4 Introduction 38

4.5 Material and Methods 41

4.5.1 Materials 41

4.5.2 Preparation of CS, plasmid DNA and siRNA for mixing 42

4.5.3 Preparation of CS/NA polyplexes by Manual Mixing (classical pipetteing).....42

4.5.4 Preparation of CS/NA polyplexes by In-line Mixing.....43

4.5.5 Polyplex Size, Polydispersity, and Surface Charge Analysis 43

4.5.6 Transmission Electron Microscopy Imaging 43

4.5.7 Sterile and RNase free production via AIMS.....44

4.5.8 Cell culture and transfection 44

4.5.9 Assessment of silencing efficiency 44

4.5.10 Statistical analyses.....45

4.6 Results and Discussion.....46

4.6.1 Design and Establishment of the Up-scaled Automated In-line Mixing System (AIMS). 46

4.6.2 Influence of mixing speed on the properties of CS/NA polyplexes.....47

4.6.3 Mixing patterns and tube length have no impact on the properties of CS/NA polyplexes.....51

4.6.4 Influence of NA concentration on the properties of CS/NA polyplexes.....51

4.6.5 Surface charge density of CS/NA polyplexes increases with NA mixing concentration.. 54

4.6.6 Morphology of the CS/pDNA and CS/siRNA polyplexes.....56

4.6.7 CS/siRNA polyplexes produced in-line are as bioactive as manual polyplexes.....57

4.7 Conclusion.....60

4.8 Acknowledgements 60

4.9 Supplementary material.....60

4.9.1 Investigation of the impact of mixing in the acceleration phase of the peristaltic pump… 60

4.9.2 Calculation of overlap concentration (C*) for pDNA, siRNA, CS solutions 62

4.9.3 Verification of the effect of overlap concentration (C*) on the maximum NA starting concentration to produce homogeneous small sized polyplexes.....63

4.9.4 MIQE compliant qPCR 64

CHAPTER 5 PURIFICATION AND MODIFICATION OF CHITOSAN-BASED POLYPLEXES USING TANGENTIAL FLOW FILTRATION 69

5.1 Objective 69

5.2 Summary 69

5.3 Introduction 70

5.4 Materials and Methods 73

5.4.1 Materials.....73

5.4.2 Preparation of CS, ODN, and siRNA formulations for mixings.....74

5.4.3 Preparation of polyplexes by in-line mixing 74

5.4.4 Preparation of HA-coated polyplexes by manual mixing 74

5.4.5 Preparation of HA-coated polyplexes by in-line mixing 75

5.4.6 Tangential flow filtration 75

5.4.7 Polyplex size, polydispersity, and surface charge analysis 76

5.4.8 Orange II assay.....76

5.4.9 Transmission electron microscopy imaging.....77

5.4.10 Cell culture and transfection 77

5.4.11 Assessment of in vitro silencing efficiency.....78

5.4.12 Hemocompatibility assays.....78

5.4.13 Statistical analysis 79

5.5 Results and discussion.....79

5.5.1 Establishment of TFF operational parameters 79

5.5.2 Diafiltration of CS-based polyplexes is optimized at 5 diavolume.....83

5.5.3 TFF is capable in concentration of CS-based polyplexes 85

5.5.4 Influence of molecular weight and degree of sulfation of HA, as well as the mixing C:P ratio on the physico-chemical properties of complexes 86

5.5.5 Morphology of the uncoated and HA-coated CS/siRNA polyplexes 90

5.5.6 HA-coated complexes are as bioactive as uncoated CS/siRNA polyplexes 92

5.5.7 HA-coated complexes have increased hemocompatibilty 94

5.6 Conclusion.....98

CHAPTER 6 GENERAL DISCUSSION.....99

CHAPTER 7 CONCLUSION AND RECOMMENDATIONS.....104

BIBLIOGRAPHY 106

LIST OF TABLES

Table 2.1 Common membrane materials used for TFF, their physical and performance attributes and limitations 30

Table 4.1. The sequence of the forward, reverse and the probe for each assay used.....65

Table 4.2 Assay efficiency for the two experiments 65

Table 4.3 Total RNA quality, integrity, and quantity for the two experiments 67

Table 5.1 Hemolysis (%) and hemagglutination of RBCs following incubation with serial dilutions of uncoated CS/siRNA polyplexes (N:P=5), and HA-coated (sulfated or non-sulfated) both pre- and post-diafiltration. Maximum final siRNA concentration was of 0.1 mg/mL and 0.066 mg/mL for uncoated and HA-coated complexes, respectively. siRNA (0.1 mg/mL), HAs (1 mg/mL), and PEG (40% w/v) were used as negative controls. PLL (10mg/mL) and TX-100 (10% v/v) were used as positive controls. Uncoated polyplexes at N:P=5 and HA-coated polyplexes were all nonhemolytic (< 2% hemolysis) for all the concentrations. Mean ± standard deviation (n = 2).....94

LIST OF FIGURES

Figure 2.1 Polyelectrolyte formation as the consequence of attractive electrostatic interactions, which is associated with an increase in entropy due to liberation of low molecular counter-ions. 7

Figure 2.2 Snapshots of PECs with different levels of stiffness: from very stiff chains (a), relatively stiff (b), relatively flexible (c), and completely flexible (d). PECs were derived from two identical polyions: equal degree of polymerization and equal numbers of charged groups. Taken from (Lazutin et al., 2012). Copyright 2017, with Elsevier's permission.....9

Figure 2.3 Chemical structure of chitosan (A and D units represent N-acetyl-D-glucosamine and D-glucosamine, respectively). Adapted from (Buschmann et al., 2013). Copyright 2017, with Elsevier's permission. 10

Figure 2.4 Chemical structure of hyaluronic acid. Adapted from (Dosio et al., 2016). Copyright 2017, with Elsevier's permission. 17

Figure 2.5 Y and T shaped connectors, used in several studies for in-line mixing of two solutions. 20

Figure 2.6 Comparison of NFF and TFF. Due to tangential movement of flow over the membrane, risk of cake formation, fouling and concentration polarization in a TFF process is much lower than a NFF process. Taken from Spectrumlabs filtration handbook (Ballew, Martinez, Markee, & Eddleman, 2002) with permission. 25

Figure 2.7 Schematic of a TFF system in concentration mode. During recirculation, the permeate is being generated (blue liquid), therefore, the volume of the sample reduces and the retentate (red liquid) becomes concentrated. Taken from Spectrumlabs filtration handbook (Ballew et al., 2002) with permission. 26

Figure 2.8 Schematic of a TFF system in diafiltration mode. While the permeate leaves the system, the new buffer is replaced based on the established vacuum. Taken from Spectrumlabs filtration handbook (Ballew et al., 2002) with permission.....28

Figure 2.9 Schematic of a typical hollow fiber module (A), and the performance of a hollow fiber membrane (B).....31

Figure 2.10 TFF performance when TMP=0 (A), TMP is balanced in a range where the is a linear trend between TMP and permeate flux (B), TMP is above the optimal threshold which causes membrane fouling. 33

Figure 4.1 Graphical abstract: large scale production of chitosan based polyplexes using the automated in-line mixing system 38

Figure 4.2 Schematic of Automated In-line Mixing System (AIMS): initial version (configuration a), and advanced version (configuration b). 47

Figure 4.3 Influence of mixing speed on size and polydispersity of CS/siRNA polyplexes (a) and CS/pDNA polyplexes (b) produced by initial and advanced versions of AIMS. pDNA and siRNA concentration prior to mixing were 0.1 mg/mL, and 0.2 mg/mL, respectively, at molar ratio of CS amine to NA phosphate ratio of 5 (N:P=5). In-line mixing was done using 2 mL of CS and 2 mL of NA. Manual mixing was done by addition of 100µL of CS into 100µL of NA, followed by pipetting up and down ten times. Error bars represent standard deviation between the duplicates. 48

Figure 4.4 Influence of NA mixing concentration on size and polydispersity of CS/siRNA polyplexes (a) and CS/pDNA polyplexes (b) produced manually and by AIMS (using both initial and advanced versions), at molar ratio of CS amine to NA phosphate ratio of 5 (N:P=5). In-line mixing was done using 2 mL of CS and 2 mL of NA at Re=4,000. Manual mixing was done by addition of 100µL of CS into 100µL of NA, followed by pipetting up and down for ten times. CS/pDNA polyplexes severely aggregate at ≥0.4 mg/mL. Error bars represent standard deviation between the duplicates. 52

Figure 4.5 Influence of NA mixing concentration on zeta potential of CS/pDNA polyplexes (a) and CS/siRNA polyplexes (b). In-line mixing was done using the advanced version of AIMS: 2 mL of CS and 2 mL of NA at Re=4,000. Manual mixing: pipetting 100µL of CS into 100µL of NA. Zeta potential measurements were done in 0.5% trehalose and 3.5mM histidine (Ionic strength =1mM). Error bars represent standard deviation between the duplicates. 55

Figure 4.6 Transmission Electron Microscopy (TEM) images of CS/pDNA polyplexes (a and b) and CS/siRNA polyplexes (c and d), produced both manually (a and c) and using the advanced version of AIMS (b and d). pDNA and siRNA concentration prior to mixing were 0.1 mg/mL and 0.2 mg/mL, respectively. In-line mixing was done by mixing 2 mL of CS and 2 mL of

NA at 150 mL/min. Manual mixing was done by pipetting 100µL of CS into 100µL of NA. 56

Figure 4.7 Bioactivity of In-line and manually mixed CS/siRNA polyplexes. HepG2 cells were transfected with either inline or manually mixed anti-ApoB CS/siRNA polyplexes at a final siRNA concentration of 100 nM/well. Apob mRNA knockdown was assessed by qPCR using geometric averaging of the most stable reference genes (GAPDH and B2M) and expressed relative to non-treated cells. Data represent the mean of two independent experiments (N=2) with two technical replicate per experiment (n=2). Analysis of Variance (ANOVA) was performed using the SigmaPlot 13.0 statistical package. 58

Figure 4.8 Correlation between bioactivity and physico-chemical parameters of in-line and manually prepared polyplexes. a) correlation between ApoB mRNA knockdown (average) and polyplexe size (average). b) correlation between ApoB mRNA kncockdown (average) and polyplexe zeta potential (average). Regression and pearson correlation analysis was performed with SigmaPlot 13.0 statistical package. 59

Figure 4.9 Influence of mixing during and after (white circles), and only after (black circles) the acceleration phase of the peristaltic pump on size and PDI of ODN/CS polyplexes produced using AIMS. In-line mixing was done using 2 mL of CS and 2 mL of NA at 150 mL/min. Error bars represent standard deviation between the duplicates. 61

Figure 4.10 Influence of chitosan C* on size and PDI of siRNA/CS polyplexes produced manually. Two CS with the same DDA (92%), but different molecular weights (10 kDa and 2 kDa) were tested.....63

Figure 4.11 Comparison of knockdown detected by two different primer-probe pairs targeting the ApoB mRNA. The IDT primer-probe pair detect the ApoB mRNA at 996-1115 (amplicon 120 bp). The UPL primer-probe pair (#55) detect the ApoB mRNA at 12177-12254 (amplicon 78 bp).....68

Figure 5.1 Distribution of CS/ODN polyplexes post-diafiltration by 300 kDa mPES (A), and 100 kDa mPES (B) membranes. Diafiltration was done at shear rate of 11000 s^{-1}, and TMP of 1.0 psid at 5DV.....81

Figure 5.2 Relationship between permeate flux and TMP at five different shear rates using 100 kDa mPES hollow fibers. CS/ODN polyplexe solution prepared at ODN concentration of 0.2 mg/mL and N:P=5 via AIMS. Filtration of polyplexes was kept in total recirculation mode (TRM). For each curve, a fresh polyplex solution (10 mL) was loaded and a brand new 100 kDa hollow fiber was used. 82

Figure 5.3 Mass percentage of chitosan removed, and mass percentage of polyplexes recovered (a), as well as the size and PDI of polyplexes (b) at each diavolume. Diafiltration was performed using 100 kDa mPES hollow fibers at shear rates of 7000 s^{-1} (TMP=0.9 psid) and 11000 s^{-1} (TMP=1.0 psid). CS/ODN polyplexe solution prepared at ODN concentration of 0.2 mg/mL and N:P=5 via AIMS. 84

Figure 5.4 Z-average and PDI of uncoated CS/ODN polyplexes at each VCF (a), Deviation between volume concentration factor (VCF) and the real concentration factor (CF) (b). Concentration of 60 mL of CS/ODN polyplexes was done up to sevenfold using 100 kDa mPES hollow fibers in shear rate=7000 s^{-1}, TMP=0.9 psid. 85

Figure 5.5 Effect of HA molecular weight, HA degree of sufation, and C:P ratio on the size and PDI (a), as well as zeta potential (b) of polyplexes post HA-coating. Uncoated CS/siRNA polyplexes were prepared at N:P=5, then diafiltered against HCl at pH=4 to remove the unbound CS. Diafiltered polyplexes were then coated by different HAs. HA was added manually to the polyplex solutions (200 µL of HA into 400 µL of diafiltered polyplexes). Error bars represent standard deviation between the duplicates. 87

Figure 5.6 Effect of diafiltration on the size and PDI (a), and zeta potential (b) of HA-coated complexes prepared at C:P=3. Both non-sulfated 10 kDa and sulfated 12 kDa HAs were tested. Diafiltration of HA-coated complexes was done at 5DV against HCl at pH=5 using 100 kDa mPES hollow fibers at shear rate=7000 s^{-1}, and TMP=0.9 psid. Error bars represent standard deviation between the duplicates.....89

Figure 5.7 TEM images of uncoated polyplexes (prepared at N:P=5), pre-diaifltration (a) and post-diafiltration agiast HCl at pH=4 (b). HA-coated complexes were prepared using the diafiltered polyplexes via AIMS at C:P=3 (c is non-sulfated 10 kDa HA, and e is sulfated 12 kDa HA with 1.4DS). HA-coated complexes were diafiltered against HCl at pH=5 (d is non-sulfated 10 kDa HA, and f is sulfated 12 kDa HA with 1.4DS). Diafiltration of HA-coated complexes

was done at 5DV using 100 kDa mPES hollow fibers at shear rate=7000 s^{-1}, and TMP=0.9 psid. 91

Figure 5.8 Bioactivity of CS/siRNA polyplexes as well as HA-coated complexes both pre-diafiltration and post-diafiltration. $eGFP^{+}$ H1299 cells were transfected with either uncoated or HA-coated anti-eGFP CS/siRNA polyplexes at a final siRNA concentration of 100 nM/well. eGFP silencing was assessed by fluorescence measurement at 410 nm, and normalized to total protein content and expressed relative to non-treated cell. Data represent the mean of two independent experiments (N=2) with three technical replicates per experiment (n=3). 93

Figure 5.9 Hemagglutination assay of uncoated CS/siRNA polyplexes prepared at N:P=5 at 0.1, 0.05, and 0.025 mg siRNA/mL pre-diafiltration (A, B, C), and post-diafiltration (D, E, F). Note that 1 mg siRNA/mL equals to 1 mg/kg injectable dose for a mouse of 10g (for an injection of 10 µL/g). Highest dose of uncoated polyplexes cuased hemagglutination both pre- (A) and post-diafiltration (D). 95

Figure 5.10 Hemagglutination assay of non-sulfated HA-coated complexes prepared at P:C=3 at 0.067, 0.0335, and 0.0167 mg siRNA/mL pre-diafiltration (A, B, C), and post-diafiltration (D, E, F). Note that 1 mg siRNA/mL equals to 1 mg/kg injectable dose for a mouse of 10g (for an injection of 10 µL/g). None of the samples caused hemagglutination. 96

Figure 5.11 Hemagglutination assay of sulfated HA-coated complexes prepared at P:C=3 at 0.067, 0.0335, and 0.0167 mg siRNA/mL pre-diafiltration (A, B, C), and post-diafiltration (D, E, F). Note that 1 mg siRNA/mL equals to 1 mg/kg injectable dose for a mouse of 10g (for an injection of 10 µL/g). None of the samples caused hemagglutination. 97

LIST OF SYMBOLS AND ABBREVIATIONS

μ	Micro
^{1}H-NMR	Nuclear magnetic resonance
AIMS	Automated in-line mixing system
ANOVA	Analysis of Variance
ApoB	Apolipoprotein B
ASTM	American Section of the International Association for Testing Materials
BSA	Bovine serum albumin
CF	Concentration factor
CIJ	Confined Impinging Jet
C:P ratio	Carboxyl to phosphate molar ratio
CS	Chitosan
Da	Dalton, molar mass unit
DDA	Degree of deacetylation
DLS	Dynamic light Scattering
DMEM-HG	Dulbecco's Minimal Essential Media with high glucose content (4.5g/L)
DS	Degree of sulfation
DV	Diavolume, diafiltration volume
EGFP	Enhanced Green Fluorescent Protein
ESEM	Environmental Scanning Electron Microscopy

FBS	Fetal bovine serum
FD	Freeze-dried, freeze drying
GPC	Gel permeation chromatography
H1299	Human adenocarcinoma lung cell line
HA	Hyaluronic acid
Hb	Hemoglobin
kDa	Kilo Dalton, 1000 dalton
LMH	Flux unit, litre per hour per squer meter of membrane surface area
LNP	Lipid nanoparticles
MIQE	Minimum Information for Publication of Quantitative Real-Time PCR Experiments
Mn	Average number molecular weight
MW	Molecular weight
mRNA	Messenger RNA
mV	Milli-volt
Mw	Molecular weight
NFF	Normal flow filtration
N:P ratio	Amine to phosphate molar ratio
NA	Nucleic acid
nm	Nanometer

mPES	Modified Polyethersulfone
MWCO	molecular weight cut off
NCBI	National Center for Biotechnology Information
NP	Nanoparticles
NT	Non-treated
OD	Optical density
ODN	Oligonucleotides
PAA	Polyacrylic acid
PAH	Polyallyl amine hydrochloride
PBS	Phosphate buffered Saline
PDI	Polydispersity index
pDNA	Plasmid DNA
PEC	polyelectrolyte complexes
PEG	Polyethylene glycol
PEI	Polyethylenimine
PES	Polyethersulfone
PLGA	Poly lactide-co-glycolide
POPC	1-palmitoyl, 2-oleoyl phosphatidylcholine
PP	Polypropylene

psid	Pressure unit, pounds per square inch differential
PVA	Polyvinyle alcohol
qPCR	Quantitative real time PCR
R^2	Pearson correlation coefficient
RFU	Relative fluorescence units
RNA	Ribonucleic acid
RPMI-1640	Roswell Park Memorial Institute medium number 1640
RT	Room temprature
siRNA	Small interfering RNA
TAE	Tris-Acetate-EDTA
TBH	Total blood hemoglobin
TEM	Transmission electron microscopy
TMP	Trans-membrane pressure
TFF	Tangential flow filtration
VCF	Volumetric concentration factor
VFR	Volumetric flow rate
ZP	Zeta potential

CHAPTER 1 INTRODUCTION

Gene therapy involves introduction of nucleic acids (NAs) into cells to either promote or inhibit expression of a protein. While deoxyribonucleic acids (DNA) and messenger ribonucleic acids (mRNA) are used to express proteins, short interfering ribonucleic acids (siRNA) are used to inhibit the expression of a specific protein in host cells. Suppressing or promoting a gene expression requires successful delivery of NA into the cells. However, several extracellular and intracellular barriers limit the effectiveness of the delivery of an unprotected genetic material. For instance, the NA must be protected from nucleases; it must penetrate various structures including the endothelium and the plasma membrane; it must resist degradation during endolysosomal transit, and then be released into the cytoplasm; and, in the case of DNA, it must even migrate into the nucleus (Al-Dosari & Gao, 2009a). Therefore, for a successful delivery of a gene, an appropriate carrier is required. Depending on the nature of the carrier, delivery of NA can be accomplished using two major approaches: viral and non-viral. Viral gene delivery uses a virus as a vehicle to deliver therapeutic NAs. Although viral vectors show higher efficiency, they involve safety concerns such as immunogenicity, possible toxicity, inflammatory potential (Lim et al., 2006), and insertional mutagenesis (Dewey et al., 1999; Fox, 2000). In spite of a relatively large number of trials for viral products, only a few are marketed which is due to the safety issues. Therefore, viral-based vectors need to be carefully assessed with regard to their safety for human gene therapy (S. R. Mao, W. Sun, & T. Kissel, 2010). On the other hand, non-viral vectors can present certain advantages over viral vectors such as large scale production and low host immunogenicity as well as formulation flexibility and lower manufacturing cost. Non-viral gene delivery mainly relies on the use of cationic compounds binding to negatively charged NAs by means of electrostatic interactions. Interest in this field has risen due to the lack of delivery systems for siRNA. Non-viral vectors are broadly classified into two categories: i) cationic lipids such as DOTAP (*N*-[1-(2,3-dioleoyloxy)propyl]-*N*,*N*,*N*-trimethylammonium) (Tousignant et al., 2000); and ii) cationic polymers such as polyethylenimine (PEI) and chitosan (CS) that form electrostatic complexes with NA. Complexes formed with cationic lipids and cationic polymers are referred to as lipoplexes and polyplexes, respectively. Lipoplexes are the most studied non-viral gene delivery systems, and have demonstrated ability for delivering siRNA, however, they are still associated with *in vitro* and *in vivo* toxicity issues (Basha et al., 2011; Ewert et al., 2004; M. C. Filion & Phillips, 1998; Lee et

al., 2012; Lv, Zhang, Wang, Cui, & Yan, 2006; Mortimer et al., 1999). On the other hand, cationic polymers present less toxicity compared to their cationic lipid counterparts (Al-Dosari & Gao, 2009b), and have been shown to be particularly promising vectors and demonstrated successful nucleotide delivery both *in vitro* and *in vivo* (Aliabadi, Landry, Sun, Tang, & Uludag, 2012; Boussif et al., 1995; Chaturvedi et al., 2011; Davis et al., 2004; Heidel, Hu, Liu, Triche, & Davis, 2004; Howard, 2009; Howard et al., 2006b; Ikonen, Murtomaki, & Kontturi, 2008; Ishii, Okahata, & Sato, 2001; Issa et al., 2006; Pun et al., 2004). Hence, significant effort has been devoted to develop biomolecular conjugates and cationic polymers as delivery systems (Al-Dosari & Gao, 2009a; Prakash, Malhotra, & Rengaswamy, 2010; Winkler, 2013). There is also an increasing interest in cationic polymers as a non-viral carrier because of the virtually unlimited size of genes that they can complex and the possibility to easily functionalize such vectors. Among the cationic polymers, CS has gained interest for the safe delivery of NA in the past decade.

CS is a naturally derived polycation, and a biocompatible and biodegradable linear polysaccharide. It has been demonstrated that CS-based delivery systems are efficient for the delivery of plasmid DNA, pDNA (Buschmann et al., 2013; Jean, Alameh, Buschmann, & Merzouki, 2011; Jean et al., 2009; Lavertu, Methot, Tran-Khanh, & Buschmann, 2006; Mao et al., 2001; Nimesh, Thibault, Lavertu, & Buschmann, 2010a; Thibault, Nimesh, Lavertu, & Buschmann, 2010b) and siRNA (Alameh et al., 2012; Alameh et al., 2017; Corbet et al., 2016; Gao et al., 2014; Holzerny et al., 2012; Howard et al., 2006a; X. Liu et al., 2007; Malhotra et al., 2009; Malhotra, Tomaro-Duchesneau, Saha, Kahouli, & Prakash, 2013; Malmo, Sorgard, Varum, & Strand, 2012a; S. Mao, W. Sun, & T. Kissel, 2010; Ragelle et al., 2014; Ragelle, Vandermeulen, & Preat, 2013; Raja, Katas, & Jing Wen, 2015; Yang et al., 2015) both *in vitro* and *in vivo*. CS/NA polyplexes can be simply produced by electrostatic-mediated association upon mixing of CS and NA solutions in dilute conditions, while CS is used in excess *versus* NA. Thus, the final polyplexes bear a net positive charge which electrostatically stabilize them. Despite the promising potential of CS-based polyplexe formulations, some factors currently limit the use of these complexes in the clinic.

Preparation of CS-based polyplexes is most commonly done by simple manual addition of CS and NA. However, this method is not established between research groups, which raises some concerns regarding comparability of the properties of such complexes. On the other hand, independent of the adopted approach, manual mixing is not only a poorly controlled method, which can result in formation of inconsistent complexes (C. Ankerfors, Ondaral, Wagberg, & Odberg, 2010a; Lu et

al., 2014), but is also restricted to relatively small preparation volumes, which seriously limit their applicability. Small scale day to day preparation of complexes poses the risk of batch to batch and inter-user variability of these polyplexes (Kasper, Schaffert, Ogris, Wagner, & Friess, 2011; Lu et al., 2014; Zelphati et al., 1998). Thus, a controlled and reproducible production process (ideally, an automated platform) is a prerequisite to tackle the drawbacks of manual method before transferring CS-based polyplexes to clinical applications. To date, there is no report on establishment of an automated platform for production of large batches of CS-based polyplexes. Here, we introduced an automated in-line mixing system for reproducible production of CS-based polyplexes in large batches, as we hypothesized that by controlling the process parameters, it is possible to control the physico-chemical properties and bioactivity of the polyplexes.

On the other hand, in order to produce stable colloidal suspensions of relatively small sized and homogeneous polyplexes, preparation must take place in dilute conditions, ~50 to 100 μg nucleic acid/mL (MacLaughlin et al., 1998a; Xu & Anchordoquy, 2011a). The low concentration regime limits the concentration of the final product in such systems. However, higher doses of polyplexes per injection are required for clinical applications. Thus, it is necessary to increase the concentration of polyplexes post-mixing. In addition, being in excess during mixing, a significant portion of CS remains free (unbound to polyplexes) in the final polyplex solution. It was reported that in CS/NA formulations prepared at an N:P ratio of 5, around 70% of added CS stays free in the final soluiton (P. L. Ma, Lavertu, Winnik, & Buschmann, 2009). Moreover, in almost all of the reported studies, a very high N:P ratio (>25) was used to produce CS/siRNA formulations. The unbound CS as well as the cationic surface of the polyplexes limit *in vivo* application of these formulations due to interaction with negatively charged blood components, *e.g.* proteins and red blood cells (RBCs). Despite promising results for different administration routes (*i.e.* intramuscular, oral, intranasal, etc.), intravenous (IV) administration of high doses of CS-based polyplexes remains problematic due to the interactions with blood components, which cause hemolysis and hemagglutination (Carreno-Gomez & Duncan, 1997; Rao & Sharma, 1997). To overcome this challenge, several types of surface modification can be used to eliminate the hemotoxicity of these polyplexes.

Effective approach involves either PEGylation of CS before mixing with NA (Malhotra, Lane, Tomaro-Duchesneau, Saha, & Prakash, 2011; Pickenhahn et al., 2015), or PEGylation of polyplexes (Corbet et al., 2016), where the polyplexes become neutralized by addition of PEG

though chemical modification of CS on the surface of the polyplexes. PEG not only provides nanoparticles (NPs) with a hydrophilic layer that stablizes and protects them from further intractions due to steric repulsions, but also increases the circulation time of NPs in the blood (Buschmann et al., 2013; Torchilin & Trubetskoy, 1995). However, PEGylation of polyplexes involves several chemical modifications that potentiates toxicity concerns. A relatively simple approach involves coating the CS/NA polyplexes with another biocompatible polyanion, *i.e.* hyaluronic acid (HA). Hyaluronic acid is a highly hydrophilic glycosaminoglycan with a broad range of molecular weight (Karbownik & Nowak, 2013; Tripodo et al., 2015). HA is a polyanion formed of N-acetyl-D-glucosamine and D-glucuronic acid units, which are linked by alternating β-(1,4) and β-(1,3) glycosidic bonds. HA is involve in several biological functions including maintenance of the elastoviscosity of joint liquids, hydration and water transport to tissues, as well as numerous receptor-mediated roles (Hascall et al., 2004; Necas, Bartosikova, Brauner, & Kolar, 2008; Turley, Noble, & Bourguignon, 2002), *e.g.* HA binds to the CD44 receptor, which is overexpressed in a wide variety of cancer cells (Dosio, Arpicco, Stella, & Fattal, 2016; Karbownik & Nowak, 2013; Platt & Szoka, 2008). HA can be used to modify the surface of CS-based complexes to improve their hemocompatibility. The carboxyl functions of the D-glucuronic acid units have an acidic pKa of ~3-4. Thus, HA is negatively charged at physiological pHs (Dosio et al., 2016), and therefore can bind spontaneously to the cationic amine groups of CS by electrostatic interactions. However, before CS-based polyplexes can be either studied clinically for IV administration, or used for further surface modifications, they must be concentrated and purified. Purification of CS-based NPs relies on elimination of the unbound chitosan molecules from the polyplex solution. Several conventional techniques have been reported for the purification of NPs such as ultracentrifugation (Correa et al., 2016; Dalwadi, Benson, & Chen, 2005), dialysis (Kwon, Lee, Choi, Jang, & Kim, 2001), and gel separation (Beck, Scherer, & Kreuter, 1990; Hanauer, Pierrat, Zins, Lotz, & Sonnichsen, 2007). However, these traditional techniques are either invasive, expensive, or time-consuming and relatively inefficient, or difficult to scale-up. Ultracentrifugation is associated with irreversible aggregation due to the high centrifugal forces, and particle loss in the supernatant during the washing steps (Dalwadi et al., 2005). Such drawbacks become much more problematic when transitioning from small scale to large scale purifications (Correa et al., 2016). Dialysis involves the risk of product loss through manual manipulations of the dialysis bags, requires a large amount of exchange buffer, which produces large volumes of aqueous waste, and can take up to

several days (Sweeney, Woehrle, & Hutchison, 2006). Moreover, due to the lengthy process, dialysis can result in release of NP's payload (Dalwadi et al., 2005). Gel filtration is relatively, a faster purification technique, however, irreversible adsorption of molecules onto the column, and not a perfect selectivity of small and bigger NPs can restrict the application of this technique for purification of drug or gene-loaded particulates. Moreover, gel separation is not scalable since only a small volume of NP solution can be processed at a time (Dalwadi et al., 2005). Tangential flow filtration (TFF), on the other hand, is a rapid and efficient method which is used for purification and concentration of biomolecules, and NPs. TFF overcomes the main limitations of the other conventional purification techniques. The exceptional feature of TFF is its capablility to purify and concentrate polyplexes in a single process. During TFF, molecules smaller than membrane pores pass through the membrane (generating the permeate) and larger molecules are retained and re-circulated in the system (generating the retentate) until the desired purity is reached. Diafiltration is a TFF process that involves washing out the original buffer by continuously adding water (or a new buffer) to the sample at the same rate as permeate is being removed from the system (Larry Schwartz, 2003). In the past decade diafiltration has been applied frequently for purification and buffer exchange purposes. It has been used to purify pDNA (Kahn et al., 2000), indomethacin loaded NPs (Limayem, Charcosset, & Fessi, 2004), poly(lactide-co-glycolide) (PLGA) NPs containing polyvinyle alcohol (PVA) (Dalwadi et al., 2005), DNA-loaded nanospheres (Hammady, Nadeau, & Hildgen, 2006), hyaluronic acid (Zhoua, Ni, Huanga, & Zhang, 2006), Gold NPs (Sweeney et al., 2006), PEGylated NPs (Dalwadi & Sunderland, 2007), Silver NPs (Anders et al., 2012; Trefry et al., 2010), lauric acid/albumin-coated iron oxide NPs (Zaloga et al., 2015), and polymersome NPs (Robertson et al., 2016). Recently, Correa et al. applied TFF to synthesize layer by layer (LBL) NPs (Correa et al., 2016). They managed the intermediate purification steps by using TFF in diafiltration mode to produce nanoscale LbL formulations. Despite its widespread use, to date, there is no report on using TFF to purify and concentrate CS-based polyplexes. Therefore, it would be relevant to validate and establish TFF technique for processing these polyplexes. We hypothesized that TFF is capable to remove the unbound CS, and to concentrate the polyplexes as well. Another hypothesis of this study is that HA-coating improves hemocompatibility and targeting capability of CS-based polyplexes.

1.1 Objectives

The first objective of the thesis is to set up an automated mixing system for reproducible production of large batches of CS-based polyplexes, while preserving their physicochemical properties and biological activity. Another objective is to establish TFF technique and optimize its operational conditions for purification and concentration of CS-based polyplexes. The final objective of the thesis is to develop HA-coated complexes, upon purification of polyplexes, to enhance their hemocompatibility for intravenous clinical applications.

1.2 Architecture of the thesis

The thesis begins with a critical literature review, presented in Chapter 2, which covers topics relevant to different mixing strategies for scaled up production of nanoparticles, and drug formulations. This chapter continues with a literature review of several conventional purification techniques as well as TFF which have been used for purification of various biomolecules and nanoparticles. Chapter 3 presents the approach to all the work carried out in order to achieve the objectives of the thesis mentioned in section 1.1. The following two chapters constitute the body of the thesis; they are presented in the form of a published article summarizing the in-line mixing system for large scale production of chitosan-based polyplexes (chapter 4), and a chapter describing purification of polyplexes *via* TFF, and finally coating of the chitosan-based polyplexes using hyaluronic acid (chapter 5). A general discussion of the results is then presented in chapter 6, followed by a conclusion and recommendations (chapter 7).

CHAPTER 2 LITERATURE REVIEW

2.1 Polyelectrolyte complexes (PECs)

Mixing of anionic and cationic polyelectrolytes results in the formation of polyelectrolyte complexes (PECs) as a consequence of attractive electrostatic interactions. The formation of PECs is associated with an increase in entropy due to liberation of low molecular counter-ions (C. B. Bucur, Z. Sui, & J. B. Schlenoff, 2006; Claudiu B. Bucur, Zhijie Sui, & Joseph B. Schlenoff, 2006; Ou & Muthukumar, 2006). Figure 2.1 displays a schematic diagram of the complexation of two oppositely charged polyelectrolytes. The simple formation mechanism of PECs avoids the use of chemical manipulations, therefore minimizes the possible toxicity and other undesirable effects of the reagents (Lankalapalli & Kolapalli, 2009). These advantages represent a great potential for PECs in gene therapy and drug delivery applications. Complexes of cationic polymers and NA (as the polyanion) are called polyplexes which are considered as a type of PECs. There are two different types of PECs, soluble and non-soluble (colloidal) that are described further below.

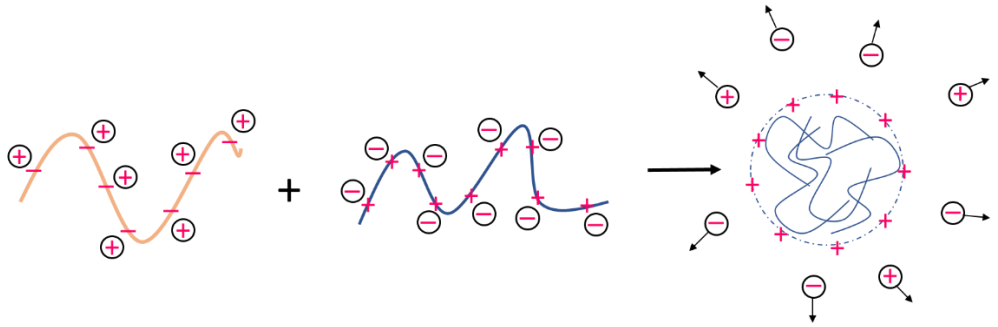

Figure 2.1 Polyelectrolyte formation as the consequence of attractive electrostatic interactions, which is associated with an increase in entropy due to liberation of low molecular counter-ions.

2.1.1 Soluble and colloidal PECs

Depending on the nature of the polyelectrolytes and mixing conditions such as media composition, mixing stoichiometry, and concentration of polyelectrolytes, water-soluble PECs (on a molecular level) or non-soluble PECs (on a colloidal level) may be formed. The first synthetic PEC was prepared by Michaels and Miekka dealing with the stoichiometry of PECs (Michaels & Miekka, 1961). They investigated the formation of non-soluble PECs resulting from the mixing of two oppositely charged polyelectrolytes at a 1:1 charge ratio. Later, preparation of nonstoichiometric

water-soluble PECs was studied and developed by groups of Kabanov and Tsuchida and Dautzenberg (Bindig et al., 1998; Tsuchida, 1994). Soluble complexes can be formed under special conditions: 1) one component has weak ionic groups, 2) there is a significant difference in the molecular weight of the oppositely charged chains, 3) the mixture contains a high excess of the long chain component, and 4) a minimal amount of salt is present in mixing medium (Thunemann, Muller, Dautzenberg, Joanny, & Lowen, 2004b). If one or more of the above conditions are not met, complex formation results in particles in the colloidal range (Dautzenberg et al., 2001; Shovsky, Varga, Makuska, & Claesson, 2009; Zintchenko, Rother, & Dautzenberg, 2003). The structure of colloidal PECs is in fact aggregated particles comprising many polyelectrolytes. While in very dilute solutions, the formed PECs stop at colloidal level and resist secondary aggregation, PEC formation between strong polyelectrolytes in a concentrated regime continues with association of more polyelectrolytes into the previously formed PEC and creates highly aggregated or macroscopic flocculated systems. In highly diluted solutions (<0.1 mg/mL) PEC formation leads to non-aggregated, quasi-soluble particles on a colloidal level with nearly spherical morphology (Dautzenberg, Hartmann, Grunewald, & Brand, 1996; Muller, 1974; Muller, Kessler, Frohlich, Poeschla, & Torger, 2011; Thunemann, Muller, Dautzenberg, Joanny, & Lowen, 2004a). Aggregation, flocculation and macroscopic phase separation take place at higher concentrations (>1 mg/mL) (Dautzenberg et al., 1996).

2.1.2 Polyelectrolyte complex structure

Depending on the characteristics of the polyelectrolyte groups and external conditions, PEC formation leads to two different structural models known as ladder-like and scrambled egg structure (Michaels & Miekka, 1961). The ladder-like structure (Figure 2.2a) in which complex formation takes place on a molecular level consists of hydrophilic single-stranded and hydrophobic double-stranded segments. This structure results from the mixing of two polyelectrolytes with weak ionic groups and large differences in molecular weights in nonstoichiometric systems. In the ladder-like architecture, the two polyelectrolyte are relatively stiff and have low charge densities (Chen, Heitmann, & Hubbe, 2003). The ladder-like structure corresponds to the soluble PECs and was found as a successful model in explaining the behaviour of certain PECs formed from a “guest” polyelectrolyte added into a “host” polyelectrolyte with much higher molecular weight (Chen et al., 2003; Kabanov et al., 2003; Philipp, Dautzenberg, Linow, Kotz, & Dawydoff, 1989). However,

the scrambled-egg model Figure 2.2d), where a large number of chains are incorporated into a particle, is formed from mixing of polyelectrolytes with relatively strong charge densities (or at least one of the two polyelectrolytes with strong charge density) and similar molecular weights. Ankerfors *et al.* showed that mixing polyelectrolytes at 1:1 stoichiometry yields in insoluble and highly aggregated complexes (Caroline Ankerfors, 2008). When the two polyions are very dilute, the complex will be controlled at the colloidal level. While the ladder-like structure is realized in the case of relatively stiff chains, flexible chains form globular scrambled-egg structure with disordered position of monomer units (Lazutin, Semenov, & Vasilevskaya, 2012).

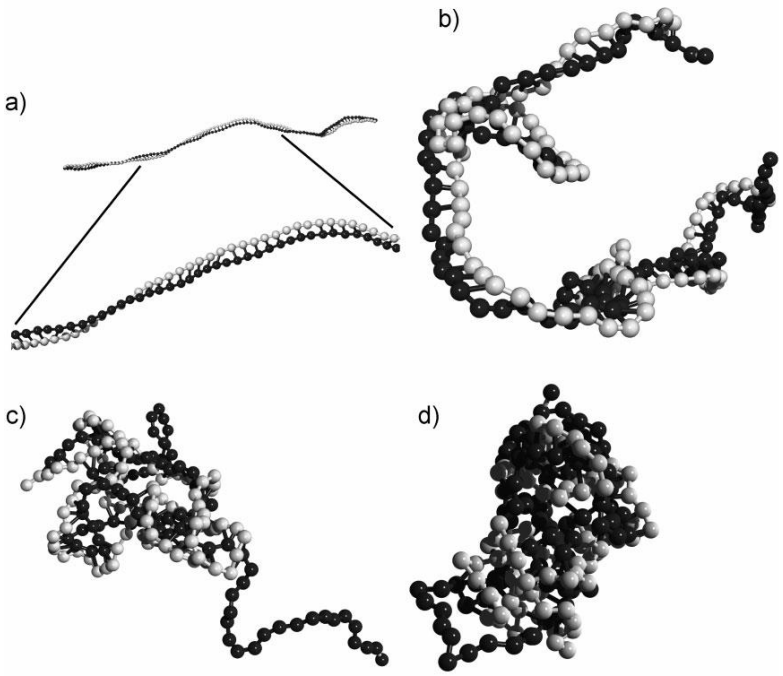

Figure 2.2 Snapshots of PECs with different levels of stiffness: from very stiff chains (a), relatively stiff (b), relatively flexible (c), and completely flexible (d). PECs were derived from two identical polyions: equal degree of polymerization and equal numbers of charged groups. Taken from (Lazutin et al., 2012). Copyright 2017, with Elsevier's permission.

2.2 Chitosan as a polycation for gene delivery applications

As mentioned previously, the simple formation mechanism of PECs makes them great candidates for gene delivery systems when a NA is condensed by a suitable polycation as the carrier. A positively charged polymeric carrier should have well defined physicochemical properties, enough NA packaging capacity, a high molecular weight diversity that allows multiple formulations to

potentially overcome extracellular and intracellular obstacles of gene delivery (Jeong, Kim, & Park, 2007), and form stable complexes in physiological conditions. In addition, it should have the potential to avoid the host surveillance systems, and deliver the therapeutic NA to the desired cell population and provide appropriate functionalities to escape from endolysosomal pathways, after being localized within the cells (S. R. Mao et al., 2010). Chitosan (CS) is a naturally derived polycation obtained by deacetylation of chitin, which is a structural element in the exoskeleton of crustaceans (crabs, shrimp, etc.) and cell walls of fungi (S. R. Mao et al., 2010). Composed of *β*-(1-4)-linked D-glucosamine (D unit) and N-acetyl-D-glucosamine (A unit) (Figure 2.3), CS is a biocompatible and biodegradable polymer (Garcia-Fuentes & Alonso, 2012; Kean & Thanou, 2010) with positive charge groups.

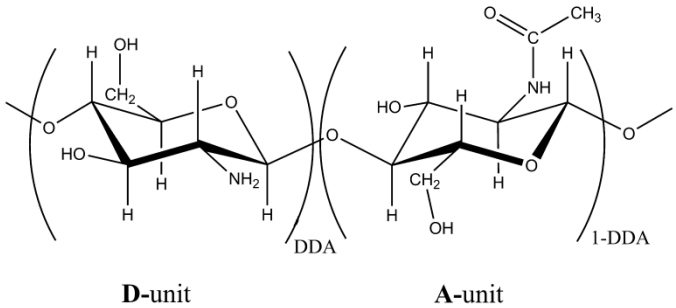

Figure 2.3 Chemical structure of chitosan (A and D units represent N-acetyl-D-glucosamine and D-glucosamine, respectively). Adapted from (Buschmann et al., 2013). Copyright 2017, with Elsevier's permission.

CS is characterized by its physicochemical properties such as molecular weight (MW) and degree of deacetylation (DDA). DDA corresponds to the molar fraction of D unit in the linear chain of chitosan, calculated as below:

$$DDA = (D/(D+A)\times 100 \qquad \text{Eq. 2.1}$$

The solubility of CS is greatly influenced by the DDA, MW, as well as pH and ionic strength of the solution. Each deacetylated unit of chitosan (D unit) contains an amine group with an intrinsic dissociation constant, pKa, near 6.5 (D. Filion, Lavertu, & Buschmann, 2007). CS is soluble in acidic conditions where sufficient protonation of D units occurs and is insoluble at neutral and alkaline pH values. CS can be hydrolyzed either by lysozymes or by chitinases and chitosanases that are produced by human intestine (Aiba, 1992; Zhang & Neau, 2002), or exist in the blood

(Escott & Adams, 1995). Furthermore, the protonated amine functions of CS also allow it to interact spontaneously with negatively charged phosphate groups of NAs, thus, forming a PEC, namely a polyplex. Due to its NA packaging capability, CS has been widely used in biomedical and pharmaceutical research as a safe alternative to other non-viral vectors such as cationic lipids for gene delivery applications (W. G. Liu & De Yao, 2002; S. R. Mao et al., 2010). In recent years, CS-based polyplexes have gained increasing interest for safe delivery of gene materials including pDNA and siRNA (Alameh et al., 2012; Alameh et al., 2017; Buschmann et al., 2013; Corbet et al., 2016; Gao et al., 2014; Holzerny et al., 2012; Howard et al., 2006a; Jean et al., 2012b; Katas & Alpar, 2006; Lavertu et al., 2006; X. Liu et al., 2007; MacLaughlin et al., 1998a; Malhotra et al., 2009; Malhotra et al., 2013; Malmo et al., 2012a; Mao et al., 2001; S. Mao et al., 2010; Ragelle et al., 2014; Ragelle et al., 2013; Raja et al., 2015; Thibault et al., 2010b; Veilleux, 2016; Yang et al., 2015).

Due to the intrinsic high charge density of NAs and relatively high charge density of CS (at low pHs where it is fully ionized), PECs prepared by addition of CS and NA are non-soluble and expected to have the scrambled-egg structure when mixed in dilute conditions. At low concentrations, the non-soluble particles can be stable at the colloidal level and protected from flocculation (Dautzenberg et al., 1996; Muller, 1974; Muller et al., 2011; Thunemann et al., 2004a).

2.2.1 Influential factors on CS/NA polyplex formation and its properties

Generally, several parameters influence the properties of PECs such as polyelectrolyte concentration, structural properties (*i.e.* length and charge spacing), molar mixing ratio (Dautzenberg et al., 1996), pH of the medium (Rungsardthong et al., 2003), and ionic strength (Dautzenberg, 1997; Oupicky, Konak, Ulbrich, Wolfert, & Seymour, 2000). In the case of CS/NA polyplexes, the influential parameters could be described by the formulation parameters such as molecular weight of NA, molecular weight and DDA of CS, as well as the molar ratio of amine groups of CS to the phosphate group of NA (N:P ratio) as the indicators of length, charge spacing and the mixing ratio, respectively. Reducing the ionization degree of the polyelectrolytes by changing pH reduces the binding affinity and influences the structure of the PECs (Rungsardthong et al., 2003; Strand, Danielsen, Christensen, & Varum, 2005). In CS/NA polyplex formation, lowering the pH of the solution increases the degree of ionization for the aminated cationic polymer of CS leading to greater binding affinity with NA (P. L. Ma et al., 2009). For example, the variation

in pH at the time of transfection can influence the size, charge, colloidal stability, and transfection efficiency of CS/pDNA polyplexes (Lavertu et al., 2006). In the pH range from 4 to 8, DNA has a constant anionic charge density since the pK_a of its phosphate group is near 1. Therefore, adjusting the solution pH only influences the degree of ionization of CS due to the pKa (~6.5) of the amine group in the glucosamine units (D. Filion et al., 2007). According to Ma *et al.*, there is a stronger interaction of CS and DNA at low pH compared to that at high pH. A lower binding affinity is found at pH of 7.4 *versus* 6.5 and 5.5 due to a lower level of CS ionization and lower electrostatic attraction between CS and NA (P. L. Ma et al., 2009). The MW of CS is another important factor that influences the size, stability, the dissociation of DNA from the complex after endocytosis, and therefore the transfection efficiency of the CS/NA polyplexes (MacLaughlin et al., 1998b; Sato, Ishii, & Okahata, 2001). There is a contradiction for the relationship between the MW of chitosan and the size of polyplexes. Many reports show that the size of CS/pDNA polyplexes increase as chitosan MW increases (M. Huang, Fong, Khor, & Lim, 2005; Q. G. Huang, Zhu, Wu, & Lin, 2001; MacLaughlin et al., 1998b) as they found an increase from about 100 nm to 500 nm when CS's MW goes from a few kDa to around 500 kDa. In contrast, in few reports it is shown that by increasing CS's MW, the size of polyplexes is decreased (M. Huang et al., 2005; Romoren, Pedersen, Smistad, Evensen, & Thu, 2003) or remained unchanged (Lavertu et al., 2006; Romoren et al., 2003). Transfection efficiency of CS/DNA polyplexes may depend on the size of the particles (M. Huang et al., 2005; Nafee, Taetz, Schneider, Schaefer, & Lehr, 2007). CS's degree of deacetylation (DDA) corresponds to the percentage of deacetylated amine groups and thus the fraction of glucosamine monomers *versus* total glucosamine and N-acetyl glucosamine, along the molecular chain of CS. DDA is proportional to the positive charge density when CS is dissolved and ionized in strong acidic conditions. The DDA of CS influences its solubility, crystallinity, and degradation (Aiba, 1989). A higher DDA results in an increased charge density enabling a greater DNA binding capacity and cellular uptake (Kiang, Wen, Lim, & Leong, 2004). According to Koping-Hoggard *et. al.*, in order to obtain stable complexes with pDNA that transfect target cells *in vitro* the DDA of chitosan must exceed 65% (Koping-Hoggard et al., 2001). According to Lavertu *et al.*, the *in vitro* transgene expression of CS/pDNA polyplexes is maximized either by reducing the DDA and increasing MW, or by increasing the DDA and decreasing MW. This could be described by the desired intermediate level of stability of NPs, that should be high enough to condense and protect DNA extracellularly but low enough to allow intracellular DNA release from

the vector for gene expression (Lavertu et al., 2006). Also, Jean *et al.* found higher pDNA transfection efficiency using chitosan of 92% DDA compared to 80% *in vitro* (Jean et al., 2012a). The influence of DDA of CS on its binding affinity to DNA was studied by Ma *et al.* (P. L. Ma et al., 2009). They showed that an increase in the DDA of chitosan results in an increase in the charge density along the molecular chain of CS and increased affinity for DNA that also results in fewer chitosan chains bound to DNA at saturation of the binding sites. The N:P ratio is defined as the mixing molar ratio of amine groups of chitosan to the phosphate of NA. At a sufficient N:P charge ratio, CS can condense DNA and siRNA to the sizes compatible with cellular uptake while preventing nucleases from accessing the enclosed NA by steric protection (M. Huang et al., 2005). However, it should be noted that when the DDA of CS is high, using very high N:P ratio may lead to difficulties of NA release once the polyplex arrives at the site of action because of the strong electrostatic interaction (Thibault, Nimesh, Lavertu, & Buschmann, 2010a); therefore, a good balance needs to be chosen for appropriate cellular uptake. It has been proven that an excess CS *versus* NA (Thibault et al., 2010a) is needed for an efficient transfection. Part of the excess CS creates a positive charge to the polyplex surface and an additional part of the excess CS remains free and unassociated with the polyplexes. It has been demonstrated that an N:P ratio of 5 is generally optimal for a highly efficient transfection of NAs (Lavertu et al., 2006; Thibault et al., 2010a). In addition to the above-mentioned parameters, concentration of the two polyelectrolytes to be mixed (CS and NA) plays a very important role on the size and the transfection efficiency of the produced polyplexes. In fact, there is a very significant difference between the characteristics of a dilute polymer solution (where polymer chains are completely separate) and a concentrated solution (where polymer chains are overlapped). When the distance between polyelectrolyte chains becomes on the order of their size, they begin to overlap. Generally, the transition concentration of polyelectrolyte solutions from dilute to semi-dilute regimes is defined as the overlap concentration (de Gennes, 1979). It is well established that for production of non-aggregated PECs, the mixing of the two polyions has to be done in dilute regime. Accordingly, for producing stable and non-aggregated CS-NA polyplexes, the formation of PECs should take place in dilute regime (Klausner, Zhang, Chapman, Multack, & Volin, 2010; Lavertu et al., 2006; Malmo, Sorgard, Varum, & Strand, 2012b; Mao et al., 2001). It is reported that the diameter of the polyplexes increased as the plasmid concentration increased (MacLaughlin et al., 1998b). Also, the transfection efficiency will increase when the dosage of NA increased up to a critical point, thereafter; the transfection will

decrease significantly (S. R. Mao et al., 2010), which can be described by a sharp increase in the size of polyplexes and aggregation of NPs, resulting in impaired cell uptake. Although, according to the literature the maximum concentration of NA for preparation of non-aggregated and uniform CS/NA polyplexes is roughly 0.1 mg/mL (Xu & Anchordoquy, 2011b), it is important to be aware of the overlap concentration (C*) of the two polyions to have an estimation of the applicable range of mixing concentrations of polyions and how far the mixing conditions are from the semi-dilute regime. C* of a polymer solution could be either measured or calculated. Several techniques are used to determine the overlap concentration of polymeric solutions, such as small angle light scattering, osmometry, viscometry, light scattering and nuclear magnetic resonance (Wandrey, 1999; Zhu & Choo, 2008). For example, Calero *et. al.* measured the overlap concentration of chitosan with the molecular weight of 200 kDa by viscometry technique and reported a C* of 2.6 mg/mL. C* depends on the degree of polymerization of polyelectrolye (N, number of monomers in a chain), mass of a monomer (M_{mon}) and the radius of gyration (Rg, chain size in salt-free solution) (de Gennes, 1979):

$$C^* \approx (N \times Mmon)/R_g^3 \qquad \text{Eq. 2.2}$$

2.3 Chitosan-based polyplexes

CS/NA polyplexes are generally prepared by fast addition of CS to NA solutions under dilute conditions (~0.1 mg/mL or below). NPs prepared this way constitute a colloidal type of PEC (Klausner et al., 2010; Lavertu et al., 2006; Malmo et al., 2012b; Mao et al., 2001). Studies of colloidal PEC formation indicate that such PECs are mainly spherical and consist of a neutral stoichiometric core that is surrounded by a charged stabilizing shell composed of the excess polyion (Dautzenberg et al., 1996; Philipp et al., 1989; Rungsardthong et al., 2003). CS-based polyplexes have been shown to be efficient for the delivery of pDNA (Buschmann et al., 2013; Jean et al., 2012b; Jean et al., 2009; Lavertu et al., 2006; Mao et al., 2001; Nimesh et al., 2010a; Thibault et al., 2010b) and siRNA (Alameh et al., 2012; Alameh et al., 2017; Corbet et al., 2016; Gao et al., 2014; Holzerny et al., 2012; Howard et al., 2006a; X. Liu et al., 2007; Malhotra et al., 2011; Malmo et al., 2012a; S. Mao et al., 2010; Ragelle et al., 2014; Ragelle et al., 2013; Raja et al., 2015; Yang et al., 2015) both *in vitro* and *in vivo*.

Despite the potential of these polyplexes *in vivo*, intravenous (IV) administration remains problematic for high doses due to hemolysis and haemagglutination of erythrocytes in contact with CS (Carreno-Gomez & Duncan, 1997). In fact, CS binds to the red blood cells (RBCs), and causes haemagglutination, even at very low concentrations (Rao & Sharma, 1997). The interactions between the cationic charges of CS molecules and the anionic charges on the surface of the erythrocytes results in haemagglutination, thus inducing stresses on the cell membranes which eventually leads to their rupture (Carreno-Gomez & Duncan, 1997; Rao & Sharma, 1997).

2.3.1 Chitosan/pDNA polyplexes

As mentioned above, molecular weight (MW in kDa) and the degree of deacetylation (DDA in %) of CS together with the concentration and molar ratio of amine group of CS to the phosphate group of NAs (N:P ratio) are the key factors in preparation of CS/NA complexes (M. Huang et al., 2005; Lavertu et al., 2006; S. R. Mao et al., 2010). It has been shown that while CS with relatively high MW is needed to achieve the extracellular NA protection, efficient intracellular unpackaging of NAs inside the cells is obtainable using relatively low MW chitosan (Koping-Hoggard et al., 2004). Lavertu *et al.* also reported that the transgene expression of CS/pDNA polyplexes is maximized *in vitro* by either reducing the DDA and increasing MW, or increasing the DDA and decreasing MW (Lavertu et al., 2006). It has been reported that the 10 kDa chitosan with DDA of 92% at N:P of 5 (CS 92-10-5 DDA-MW-N:P ratio) form stable complexes and also dissociates effectively upon release from lysosomes, maximizing the level of transfection (Thibault et al., 2010a). Transfection in a slightly acidic medium (pH 6.5) can also maximize the *in vitro* transfection of CS92-10-5/pDNA complexes (Ishii et al., 2001; Lavertu et al., 2006; Nimesh, Thibault, Lavertu, & Buschmann, 2010b; Sato et al., 2001). This can be explained by the fact that in the media of lower pH the zeta potential of the polyplexes increases, due to ionization of CS, which improves their affinity to the negatively charged cell membranes and consequently enhance cellular uptake (Lavertu et al., 2006). In another study, Veilleux *et al.* demonstrated that CS/pDNA polyplexes prepared at pH=6.5 maintained their physico-chemical properties and transfection efficiency post freeze-drying and (Veilleux, Nelea, Biniecki, Lavertu, & Buschmann, 2016).

2.3.2 Chitosan/siRNA polyplexes

In recent years, chitosan/siRNA formulations have gained momentum as a safe and efficient delivery system (Alameh et al., 2012; Corbet et al., 2016; Gao et al., 2014; Holzerny et al., 2012; Howard et al., 2006a; X. Liu et al., 2007; Malmo et al., 2012a; S. Mao et al., 2010; Ragelle et al., 2014; Ragelle et al., 2013; Raja et al., 2015; Yang et al., 2015). Several groups studied key factors (i. e. DDA and MW of CS, as well as N:P ratio) to produce CS/siRNA polyplexes with highest bioactivity. In one of the early studies, Liu *et al.* showed that using CS with MW of 65-170 kDa (78 to 84% DDA) results in CS/siRNA polyplexes of around 200 nm. It was demonstrated that the zeta potential of CS/siRNA polyplexes increases with the DDA, and they are more efficient when DDA≥ 80% (X. D. Liu et al., 2007). It was shown that CS/siRNA polyplexes prepared at N:P=50 with different CSs had a silencing efficiency of 45 to 65% 48 h after transfection of $EGFP^+$ H1299 cells with 50 nM of siRNA (X. D. Liu et al., 2007). Moreover, as observed previously for CS/pDNA polyplexes, Howard *et al.* demonstrated that the size of the CS/siRNA polyplexes increases with the final concentration of siRNA in the formulations (Howard et al., 2006a). However, producing small polyplexes at low concentrations limits the injectable doses (1 mg of siRNA/mL) for clinical administrations. It was demonstrated that CS/siRNA polyplexes prepared by CS with MW of 114kDa (DDA=84%) have *in vitro* silencing efficiency as high as ~ 80% (Howard et al., 2006a). Malmo *et al.* showed that when CS is fully deacetylated, MW and N:P ratio have not a marked impact on the silencing efficiency of the CS/siRNA polyplexes (Malmo et al., 2012a). They reported that the size of polyplexes increased from 34 nm to 95 nm with increasing the MW of CS from 16.4 kDa to 141.6 kDa, and increasing the N:P ratio from 10 to 60. Generally, DDA of CS was found to have a low impact on silencing efficiency of CS/siRNA polyplexes (Holzerny et al., 2012; Howard et al., 2006a; Ji et al., 2009; X. Liu et al., 2007; Malmo et al., 2012a). Therefore, most of the studies involving CS/siRNA polyplexes were conducted at moderate DDA (80-85 %) (Holzerny et al., 2012; Howard et al., 2006a; Katas & Alpar, 2006; X. Liu et al., 2007; Ragelle et al., 2014).

2.3.3 Coated polyplexes: surface modification using hyaluronic acid

Hyaluronic Acid (HA) is a member of glycosaminoglycans. As a natural polyelectrolyte, HA is constituted by alternating and repeating units of D-glucuronic acid and N-acetyld-glucosamine linked at 1, 3 and 1, 4 position to form a linear chain (Figure 2.4) (Kakehi, Kinoshita, & Yasueda,

2003). HA is a non-toxic and non-immunogenic material, and is generally associated with anti-inflammatory properties (Necas et al., 2008). The pharmacokinetics of HA upon intravenous (IV) injection in human adults was documented by Necas *et al.* It was demonstrated that HA has a circulating half-life of 2 to 6 min, and it is mainly eliminated in the liver by a mechanism of endocytosis (Necas et al., 2008). HA is also an important CD44 receptor ligand, which is expressed in almost every cell type in human and in mouse (Liang, Jiang, & Noble, 2016; Sherman, Sleeman, Herrlich, & Ponta, 1994; Tripodo et al., 2015) and overexpressed in several cancer cells, and has been extensively studied as a therapeutic targeting agent (Dosio et al., 2016; Karbownik & Nowak, 2013; Platt & Szoka, 2008).

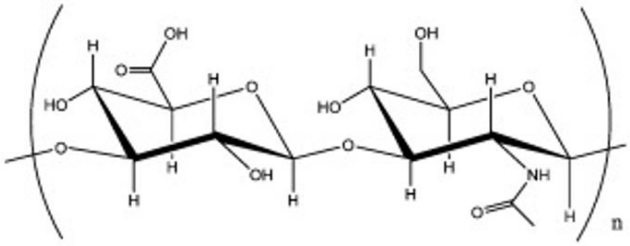

Figure 2.4 Chemical structure of hyaluronic acid. Adapted from (Dosio et al., 2016). Copyright 2017, with Elsevier's permission.

The distributions of the molecular size of HA are of wide range (Karbownik & Nowak, 2013; Tripodo et al., 2015). HA can also be modified by the insertion of ionic sulfate ($SO3^{-}$) groups in the polysaccharide chain. Sulfated HAs have been reported with different degrees of sulfation, ranging from 1 to 4 sulfate groups per disaccharide (Magnani, Silvestri, & Barbucci, 1999). While non-sulfated HA contains only one ionizable group per disaccharide (carboxylate moiety, COO^{-}, of the D-glucuronic acid units with pKa of ~3-4), sulfated HAs have ionic groups that are charged negatively. In one of the very early studies, Magnani *et al.* showed that compared to non-sulfated HA, the sulfate groups provide with stronger electrostatic attraction to the metal ions (Cu^{2+} and Zn^{2+}), which is due to increased negative charge along the polymer chain (Magnani et al., 1999). In another study, recently, Feng *et al.* demonstrated a stronger binding affinity of sulfated HA with proteins due to higher charged density of the HA chains. Moreover, they demonstrated that sulfated HA has significantly slower degradation by hyaluronidase compared to the non-sulfated HA (Feng et al., 2017). HA is highly hydrophilic, and the charged groups of this anionic glycosaminoglycan can form electrostatic bonds with the amine functions of CS on the surface of the polyplexes. Since

the binding constant of HA and CS is ~200 fold lower than that of CS and NA, HA would not cause NA release when it is added to the CS/NA polyplexes (Pei Lian Ma, 2010). The presence of HA would promote the formation of more hemocompatible formulations with increased solubility at higher pHs. Moreover, since HA binds to the CD44 receptor, which is often overexpressed on the surface and in the matrix of cancer cells, it can act as the addressing molecule of polyplexes (Platt & Szoka, 2008).

2.4 Techniques used for mixing NA with polycations

NA and CS solutions are miscible aqueous solutions. Mixing miscible liquids can be simply seen as blending two fluids to get a specified degree of homogeneity. Aiming to develop a method to reproducibly mix large volumes of CS and NA solutions, this part of the thesis reviews different methods reported in the literature through which a NA solution was mixed with a polycation solution.

2.4.1 Manual mixing

Direct manual mixing is the simplest method that can be used to mix two miscible liquids. This is the most often used technique to produce CS-based polyplexes. However, this method is not established between research groups (varies from a lab to another and from paper to another) which raises some concerns regarding comparability of the properties of such complexes. Order of addition of the two solutions, experience of the user, speed of mixing are among the factors that affect the properties of the prepared polyplexes. The most frequently reported mixing method involves manual addition of CS solution into the NA solution followed by homogenization by pipetting the mixture up and down (Alameh et al., 2012; Jean et al., 2011; Lavertu et al., 2006; MacLaughlin et al., 1998a; Malmo et al., 2012a; Mao et al., 2001; Nimesh et al., 2010a; Veilleux et al., 2016). Independent of the method used, manual mixing is restricted to relatively small preparation volumes and seriously limits the quantity and applicability of the prepared complexes. Small scale day to day preparation by manual mixing poses the risk of batch to batch and inter-user variability. Aside from the manual mixing, a few mixing techniques or devices have been proposed in the literature to prepare large volumes of polyplexes. These techniques rely on in-line mixing of the two polyelectrolyte solutions in jet mixers *via* Y or T-shaped connectors or in a static mixer coupled to a dual syringe.

2.4.2 Jet mixer

A jet mixer generates two opposing high velocity linear jets of polyelectrolyte solutions which collide in a chamber in a few milliseconds. Johnson and Prud'homme invented a novel Confined Impinging Jet mixing (CIJ mixer) apparatus for the preparation of nanoparticles (NPs) through which rapid mixing takes place in a time less than the nucleation and growth time of NPs (Brian K. Johnson & Prud'homme, 2003). Ankerfors *et al.* applied the CIJ system to investigate the influence of mixing time on the size of PECs produced by mixing of two low MW polyelectrolytes in dilute regime (C. Ankerfors, Ondaral, Wagberg, & Odberg, 2010b). PECs were prepared at pH=7 using NaCl concentration of 10 mM. For polyacrylic acid (PAA) and polyallyl amine hydrochloride (PAH), smaller particles were obtained (ranging from 45 nm to 60 nm prepared in very short time of 20 and 65 ms, respectively), as compared to larger particles when the two solutions were added slowly, ranging from 80 to 140nm (C. Ankerfors et al., 2010b). Although CIJ resulted in very small PECs, it is a very sophisticated device.

2.4.3 Y or T-shaped mixer

The easier and probably the most basic design for in-line mixing of two solutions is mixing in a Y or T-shaped connector, where mixing takes place by pumping the two solutions simultaneously to contact each other and mix in the connector. Clement *et al.* designed an in-line mixing platform based on two peristaltic pumps, and a Y-connector. (Clement, Kiefer, Kimpfler, Garidel, & Peschka-Suss, 2005). They showed that in-line mixed pDNA lipoplexes retained their full biological function *in vivo*. Also, they investigated the influence of mixing speed and reported no marked change in the size and surface charge of NPs in moderate flow rates. In 2011, Kasper *et. al.* claimed reproducible production of small and homogeneous polyethyleneimine (PEI)/pDNA polyplexes by means of an up-scaled micro-mixer system (Kasper et al., 2011). Kasper *et al.* showed that small and homogeneous PEI/pDNA polyplexes could be reproducibly prepared using this technique. They developed a micro-mixer consisting of two syringes that are connected to each other heading oppositely by a T-connector. They also investigated the influence of mixing flow rate and concentration of NA solution on the size and polydispersity of the polyplexes. It has been shown that by increasing the mixing speed (from 0.1 to 1.0 cm/min, using 2.5 mL syringes), the size of polyplexes is reduced (from 197 to 59nm), however, polydispersity index (PDI) increased significantly (from 0.05 to 0.19). Moreover, by increasing the concentration of pDNA (20-400

μg/mL), the z-average diameter (65-170 nm) and PDI (0.05-0.22) of the polyplexes increased (Kasper et al., 2011).

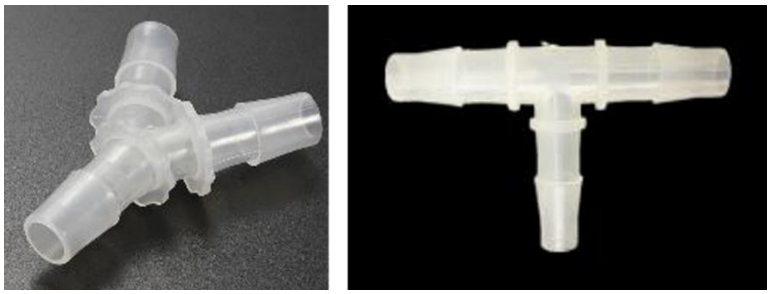

Figure 2.5 Y and T shaped connectors, used in several studies for in-line mixing of two solutions.

2.4.4 Static mixer

A static mixer, also known as a motionless mixer, is a mixing device consisting of a series of identical, motionless elements. The purpose of the elements is to redistribute fluid in directions transverse to the main flow (since in a simple empty cylinder, there is no radial mixing). The effectiveness of static mixers is due to its ability to perform radial mixing so that mass transfer become rapid. Static mixers can be coupled to Y connectors or a jet mixer to increase the homogeneity of polyplexes. Davies *et al.* used dual syringes attached to a static mixer driven by a cylindrical pneumatic actuator for preparation of PEI/pDNA polyplexes for gene therapy application (Davies et al., 2010). They obtained small and homogeneous polyplexes using a static mixer in both laminar and turbulent regimes. They also found that by increasing the mixing flow rate (from 1 to 20 mL/sec), the hydrodynamic diameter of produced polyplexes increased slightly from 70 to 95 nm.

2.4.5 Staggered herringbone micromixer

A very recently introduced device used for in-line mixing of two solutions is a micro-mixer called “staggered herringbone microfluidic mixing device”. Staggered herringbone micromixer (SHM) is a chaotic mixer that works based on rapid microfluidic mixing in a laminar regime to produce well-defined NPs (Belliveau et al., 2012; A. K. K. Leung et al., 2012; Zhigaltsev et al., 2012b). The device comes with two inlets which are connected to each other through a Y connector, where the output is a herringbone shape channel with asymmetric grooves on its floor. This mixing method makes continuous rotational and extensional flows resulting in a high speed mixing of the two

fluids that are injected through syringes driven by a dual syringe pump. Zhigaltsev *et al.* used the SHM device to drive lipid nanoparticle (LNP) formation (consisting of 1-palmitoyl, 2-oleoyl phosphatidylcholine (POPC), cholesterol and the triglyceride triolein) by high speed mixing of lipids dissolved in ethanol, injecting into the first inlet, with an aqueous buffer stream (saline, 154 mM NaCl), injected into the second inlet of the micromixer, using 1 to 5 mL syringes and connections with inner diameters of 1/32" (Zhigaltsev et al., 2012b). They found two factors influencing the size of the produced LNP: the mixing flow rate and the volumetric ratio of aqueous to ethanol solutions that are being mixed. They reported that as the mixing flow rate increased (0.5−4.5 mL/min), polydispersity of the produced LNP decreased that could be described by the fact that at a very high speed, mixing time (approximately 3 ms) is much shorter than the time for mass transfer that causes heterogeneous lipid aggregation. In addition, by increasing the volumetric flow ratio (VFR) of the aqueous stream to the ethanol solution, the size of LNP decreases as the final concentration of ethanol decreases which results in reduced production of larger LNP at the output (the size reduced from 120nm to around 30nm for both POPC and POPC/cholesterol mixture by changing the VFR from 1 to 7, and from 65 nm to 15 nm for the POPC/triolein by changing the VFR from 1 to 9). The staggered herringbone microfluidic mixing technique is a reproducible method that produces NPs in the sub-100 nm size range which are stable after purification for several months (Zhigaltsev et al., 2012b). In another study, Belliveau et. al. investigated the ability of SHM in preparation of monodisperse LNP/siRNA complexes in different flow rates of the range 0.02 to 4 mL/min (in laminar flow regime, $2<Re<500$) (Belliveau et al., 2012). They reported that although the size of LNP remained constant (at ~55 nm) over the range of the tested flow rates, by increasing the mixing flow rate the PDI of produced LNP-siRNA decreases. In addition, reducing the concentration of siRNA results in a decrease in polydispersity. They showed that the lowest polydispersity was obtained at the highest mixing flow rate (4 mL/min), with a PDI of 0.03 over the concentration range of siRNA from 0.25 to 0.59 mg/mL.

Each of the above-mentioned methods might produce particles that have different physico-chemical properties, but there is no clear indication to date that any of these techniques can produce CS-based polyplexes that are reproducible and approperiate in terms of their physico-chemical characteristics and transfection efficiency.

2.5 Purification and concentration techniques

As mentioned before, in order to produce stable colloidal suspensions of relatively small and homogeneous polyplex NPs, the mixing process must take place i) in excess chitosan *versus* NA, and ii) in dilute conditions. However, for further surface modifications and clinical applications, these polyplexes must be purified (to remove the unbound chitosan), and concentrated (to achieve higher doses per injection). Hence, investigation of an appropriate technique is required to treat polyplexes post-mixing. The following section summarizes techniques used for purification and concentration of NPs in biopharmaceuticals.

2.5.1 Dialysis

Dialysis is one of the methods used for purification and concentration of NPs and proteins (Andrew, Titus, & Zumstein, 2001; Degerli & Akpinar, 2001; Shire, Shahrokh, & Liu, 2004). In dialysis, the concentration of NP suspensions is performed using a dialysis bag against a counter-dialysing (concentrator) solution. Concentrator solution could be an aqueous polymer solution that can be supplemented with additives, including buffering agents, denaturants, salts and detergents to maintain the integrity of the sample during concentration by dialysis. Due to osmotic pressure, water is displaced from the inside of the dialysis bag towards the concentrator solution until equilibrium is achieved. Once the desired volume of the solution is achieved, the excess concentrator solution is removed from the dialysis membrane and the sample is recovered. Concentration of NPs using dialysis against a polymer solution, dextran (Stella et al., 2007; Vauthier, Cabane, & Labarre, 2008), and Aquacide II, sodium salt of carboxymethyl cellulose, (Andrew, Titus, & Zumstein, 2002) has been reported. Concentration of NPs in pharmaceutical suspensions can be done *via* dialysis without causing any aggregation of NPs (Vauthier et al., 2008). As a low-shear rate method, dialysis prevents DNA degradation and protein denaturation during the concentration process (Shire et al., 2004). However, dialysis requires preparation of an appropriate counter-dialysing solution at an optimized concentration to obtain the desired concentration factor. Dialysis procedures require large volumes of exchange buffer for equilibration which can take up to several days and involve the risk of product loss through manual manipulations of the dialysis bags (Sweeney et al., 2006). These drawbacks limit the applicability of this method for purification of large volumes of NPs.

2.5.2 Gel filtration chromatography

Compared to dialysis, gel filtration is a relatively faster process; however, only a small volume of NP solution can be processed at a time which makes it difficult to scale-up. Moreover, selectivity of small and bigger NPs, and irreversible adsorption of molecules onto the column can restrict the application of this approach in pharmaceuticals (Dalwadi et al., 2005). In addition, gel filtration results in a dilution of the sample and often requires an additional step to concentrate it back. While time consuming, gel filtration is not scalable since only a small volume of NP solution can be processed at a time (Dalwadi et al., 2005).

2.5.3 Ultracentrifugation

Ultracentrifugation is probably the most common approach to remove impurities. This process is typically followed by a subsequent resuspension in a fresh buffer. Although simple, this technique is time-intensive and results in aggregation of NPs due to high centrifugal forces (Correa et al., 2016). Moreover, resuspension as a following step might also cause loss of smaller NPs in the supernatant liquid, resulting in a low recovery (Chiellini, Orsini, & Solaro, 2003; Dalwadi et al., 2005). Ultracentrifugation is considered as a simple and relatively fast approach to remove impurities from small batches of NPs, however, is not a suitable for large scale applications (Correa et al., 2016).

2.5.4 Freeze-drying

Freeze-drying (FD), also known as lyophilization, is a technique used to attain long term stability of pharmaceutical and biological products preserving their original properties. The principle of FD is to remove water content of a sample from its frozen form by sublimation and desorption under vacuum (Abdelwahed, Degobert, Stainmesse, & Fessi, 2006; Hirsjarvi, Peltonen, & Hirvonen, 2009; Vauthier & Bouchemal, 2009). FD is not a purification technique, but can be used for producing concentrated NPs by rehydration in a volume smaller than the original volume. Anchordoquy *et al.* demonstrated that PEI/DNA complexes can be concentrated tenfold (DNA concentration of 1 mg/mL) using FD technique (Anchordoquy, Armstrong, & Molina, 2005). In another study, Veilleux *et al.* showed that CS/pDNA polyplexes can be concentrated up to 20-fold (to ~1 mg/mL) using this method, while maintaining isotonicity (Veilleux et al., 2016). Excipients are used in FD in order to increase the stability and to protect NPs against either freezing or drying

stresses, called cryoprotectants and lyoprotectants respectively. The commonly used excipients for FD are sugars such as sucrose, trehalose and glucose. Moreover, in order to control pH during freezing, buffers such as histidine (Veilleux et al., 2016), phosphate and citrate can be used (Abdelwahed et al., 2006). A maximum concentration limit, difficulties of carrying FD and subsequent rehydration in large scales and maintaining the isotonicity of solutions after rehydration are among limitations of lyophilization technique for concentration purposes. Moreover, FD is not applicable for purification of materials.

2.5.5 Ultrafiltration

Filtration is a pressure driven process of separating the components of a solution based on their size and charge differences using a membrane. Filtration is an important process in biopharmaceutical industry which is also used to concentrate the products to the desired final concentration. In contrast to the above mentioned techniques (dialysis, gel separation and ultracentrifugation), ultrafiltration is a fast and highly cost effective purification method for processing large batches of solutions, thus, suitable to implement in industrial processes (Sweeney et al., 2006). Based on the direction of the fluid flow on the filter membrane, filtration can be of two different types: 1) Normal Flow Filtration (NFF) and 2) Tangential Flow Filtration (TFF).

2.5.5.1 Normal Flow Filtration

In NFF, also know as dead end filtration, the fluid flows directly towards the filter under the influence of pressure. Normal flow indicates that the fluid flow is perpendicular (normal) to the filter surface and there is no recirculation of the feed stream. Basically, particles that are smaller than the pore size of the filter pass through the membrane, and all of the particles that are larger accumulate on the surface of the filter, as their size prevents them from passing through the filter medium. The normal pressure of the flow pushes the particles on the surface. As the process continues, more particles accumulate on the filter. The trapped particles start to build up a “filter cake” on the membrane, thus the filtration flow rate per unit membrane area decreases over time (Figure 2.6b). Although more efficient than other conventional purification techniques, NFF can cause aggeregation of NPs. Cake formation, fouling and concentration polarization are the main concerns in a TFF process (Dalwadi et al., 2005).

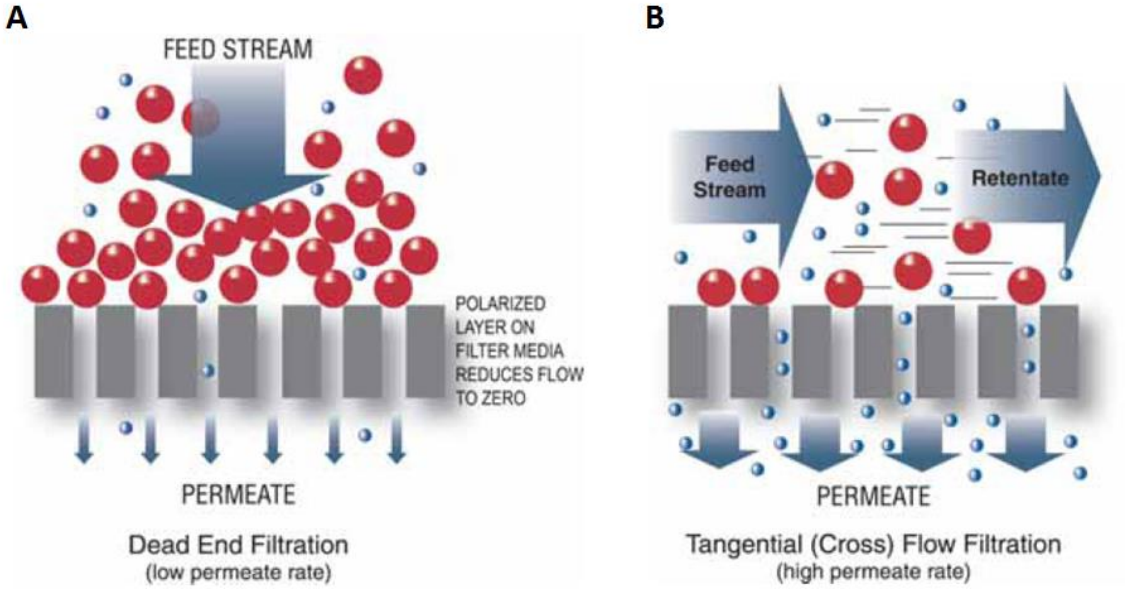

Figure 2.6 Comparison of NFF and TFF. Due to tangential movement of flow over the membrane, risk of cake formation, fouling and concentration polarization in a TFF process is much lower than a NFF process. Taken from Spectrumlabs filtration handbook (Ballew, Martinez, Markee, & Eddleman, 2002) with permission.

2.5.5.2 Tangential Flow Filtration

TFF, sometimes referred to as cross flow filtration, generally involves the circulation of the fluid parallel to the surface of a semi-permeable filter under pressure. Filtrate is pushed through the membrane by the pressure applied on the feed. While some of the feed solution passes through the membrane filter, most of the solution is circulated back to the feed tank. The solution retained by the membrane is known as the concentrate (or retentate) and the solution that passes through the membrane is known as the permeate (or filtrate). Figure 2.6 illustrates the fluid flow in TFF mode compared to the NFF mode. In TFF equipment, a pump is used to supply enough pressure on the feed flow and to generate feed recirculation. In each pass of the feed fluid over the surface of the filter, the applied pressure forces a portion of the fluid through the filter to the permeate stream, thus concentrating the solution. The continuous movement of the feed solution across the membrane surface helps to remove the built-up cake on the surface. During TFF molecules smaller than membrane pores (sugar, salt and water) pass simply through the membrane and larger molecules (*e.g.* NPs) are retained and re-circulated in the system until the desired concentration of

the solution is reached. TFF overcomes the main limitations of the NFF such as rapid flux decrease over time and particle trapping on the surface of the filter (Ralf Kuriyel, 2008). TFF is usually used in biopharmaceutical downstream processes including concentration, clarification, and fractionation (Ralf Kuriyel, 2008), and to concentrate, and separate proteins (Millipore, 2003). As NPs are in the same size range as proteins, TFF has been studied as a possible concentration and purification method for NPs (Anders et al., 2012; Correa et al., 2016; Dalwadi et al., 2005; Dalwadi & Sunderland, 2007; Hammady et al., 2006; Limayem et al., 2004; Robertson et al., 2016; Sweeney et al., 2006; Trefry et al., 2010; Zaloga et al., 2015). Unlike the other purification techniques, TFF can be automated by controlling the pump. This is a very important feature of TFF which stands it out as a convienent technique for large scale applications. TFF in concentration mode is schematically shown in Figure 2.7.

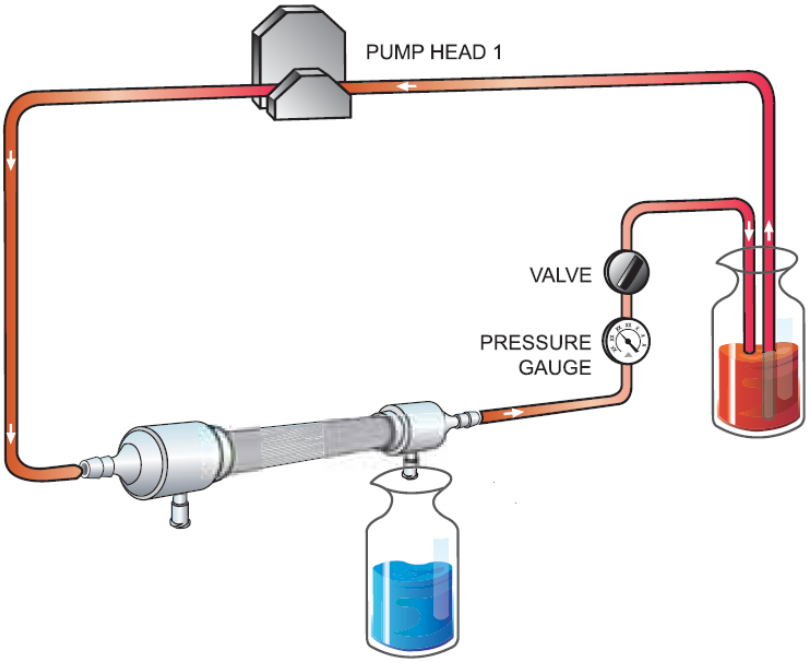

Figure 2.7 Schematic of a TFF system in concentration mode. During recirculation, the permeate is being generated (blue liquid), therefore, the volume of the sample reduces and the retentate (red liquid) becomes concentrated. Taken from Spectrumlabs filtration handbook (Ballew et al., 2002) with permission.

2.5.5.3 Diafiltration

It is possible to use a TFF system for purification or buffer exchange instead of concentration mode. When a new buffer is added into the feed tank while permeate is removed continuously from the system, the process is refered to as diafiltration. Diafiltration is a technique which uses ultrafiltration membranes to completely remove, replace, or lower the concentration of salts or solvents from solutions containing proteins, peptides, nucleic acids, and other biomolecules (L. Schwartz, 2003). Diafiltration technique involves washing out the original buffer in the sample (retentate) by adding water or a new buffer to the sample continuously at the same rate as permeate is being removed from the system. In processes where the products of interest are in the retentate, diafiltration washes and removes other components out of the retentate into the permeate, thus exchanging buffers and gradually reducing the concentration of impurities. The sample volume and product concentration do not change during a diafiltration process. Using diafiltration, the unwanted molecules will be washed out and their concentration is lowered. If a buffer is used for diafiltration aiming buffer exchange, the new buffer concentration will increase gradually at a rate inversely proportional to that of the initial buffer being removed. The amount of buffer exchange is directly related to the permeate volume generated. The permeate volume generated is usually referred to as “diafiltration volumes” (DV). With diafiltration, salt or solvent removal as well as buffer exchange can be performed quickly and conveniently. Another very important advantage of TFF is that the sample can be concentrated on the same system, minimizing the risk of sample loss or contamination. Figure 2.8 illustrates a schematic view of a TFF system in diafiltration mode. When the volume of permeate collected equals the starting retentate volume, one DV has been processed. The number of DV needed for a complete buffer exchange directly depends on the permeability of the molecules of the buffer through the chosen membrane.

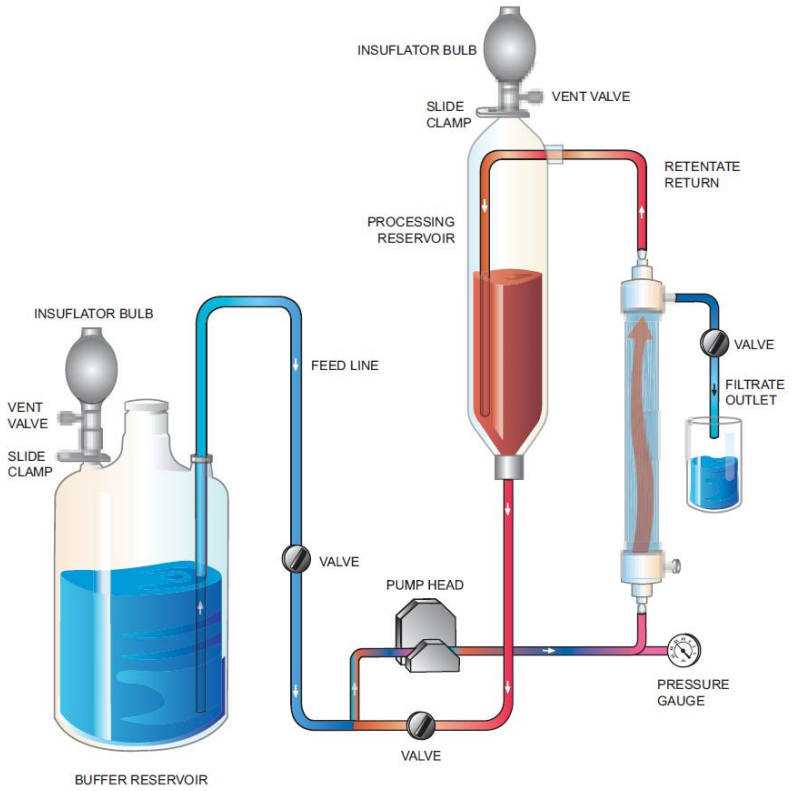

Figure 2.8 Schematic of a TFF system in diafiltration mode. While the permeate leaves the system, the new buffer is replaced based on the established vacuum. Taken from Spectrumlabs filtration handbook (Ballew et al., 2002) with permission.

Theoretically, there will be a linear decrease in solute content in the concentration mode, and an exponential decrease in diafiltration mode. This model is applicable for all solutes to be eliminated, but with different slopes depending on the permeability of the solute. 100% permeability means that all solute freely passes through the membrane, which is the case for salts, solvents and buffers (L. Schwartz, 2003). Permeability can be determined by measuring the concentration of the unwanted molecule in the permeate compared to its concentration in the retentate. According to the technical reports of the TFF instrument from Pall Corporation, greater than 99.5% of a 100% permeable solute can be removed and replaced with a new buffer by washing through 6 diafiltration volumes (6DV). Also, greater than 99.5% of a solute with a 75% permeability can be removed and replaced with the new buffer by washing through 8 diafiltration volumes (8DV) (L. Schwartz, 2003). Permeability can be affected by such factors as transmembrane pressure (TMP), crossflow rate,

retentate concentration, pH, and ionic strength. Therefore, the permeability may change during the process.

2.6 Parameters that influence a TFF process

TFF is the method that was used here for purification and concentration of CS-based polyplex solutions, hence, more details on this technique will be reviewed in this section. Parameters that influence the performance of this technique include membrane properties (material, cut-off, and geometry), as well as operational parameters (cross flow rate and trans-membrane pressure). These parameters are reviewd in the following sections.

2.6.1 Membrane material and molecular weight cut off

Choosing a membrane with appropriate retention characteristics is critical to ensure a high product yield. TFF membranes are rated by molecular weight cut off (MWCO) that refers to the average molecular weight of solutes for which 90% of solute is retained by the membrane. Generally, the membrane for concentration is selected based on its rejection characteristics of the sample to be processed. To assure complete retention, MWCO of the membrane should be $1/6^{th}$ to $1/3^{rd}$ of the molecular weight of the molecule to be retained (L. Schwartz, 2003). The closer the MWCO is to that of the sample, the greater the risk of losing some small product out of the concentrate. Ultrafiltration membranes for TFF are commercially available in a wide range of nominal MWCO from 1-1000 kDa (pore sizes between 0.001 and 0.1 micron). TFF membranes are commercially available in a variety of polymeric materials or ceramic for certain applications. The membranes are constructed from materials with high mechanical strength, chemical and physical compatibility, with the lowest levels of extractable and/or toxic compounds (Cross flow filtration Method Handbook, 2014). Some polymers have modified surfaces to improve their performance (*i.e.* increased hydrophilicity, lower binding). The common materials used for TFF are: i) polysulfone (PS), ii) cellulose based membranes, iii) polyethersulfone (PES), and iv) modified PES (mPES). Polymeric membranes are usually stored in sodium hydroxide solution. PS is hydrophilic membrane with low binding properties. It is more resistant to acids, bases and surfactants than other membrane chemistries. PS filters are common in applications like NP processing and diafiltration. Cellulose based membranes offer high flux and selectivity and because of its hydrophilic nature, this membrane is optimal for processes involving very hydrophilic materials

such as protein. PES membranes are stable against biological and physical degradation due to the unique chemical properties of PES. Due to their extremely low binding properties, PES membranes are significantly resistant to fouling, thus provide with higher recovery yields. Their fouling resistant properties allow higher flux rates and a shorter processing time (Novasep, 2016; "Why You Should Consider Hollow Fibres for Ultrafiltration," 2015). PE, PES, and Cellulose based hollow fibers are limited commercially in terms of cut-off availability. mPES has advanced hydrophilic membrane filtration chemistry. Compared to other membrane chemistries, mPES provides excellent selectivity for separation applications, higher flux rates for faster processing times, and low protein binding for higher product yields. mPES is slightly negatively charged, but due to the modifications it is very close to neutral. mPES hollow fibers are commercially available in a broad range of cut-offs, from 1 kDa to 0.2 µm. Table 2.1 summarizes the performance and limitations of common TFF membranes.

Table 2.1 Common membrane materials used for TFF, their physical and performance attributes and limitations

Material	**Physical attribute**	**Performance attribute**	**Limitations**
Cellulose base	Most neutral membrane	Charge has little effect on separation High filtration flux	No storage in NaOH
Polyethersulfone (PES)	Negatively charged	Charge can affect separation	Protein passage, variable
Polysulfone (PS)	Negatively charged	Can absorb endotoxins, low flux	Hollow fiber most common Lower permeate rate
modified Polyethersulfone (mPES)	Mix of cellulose & PES attributes	High permeate flux	Depends on the specific modification

2.6.2 Membrane geometry

Generally, two different filter configurations are used in TFF processes, cassette filters and hollow fiber filters. Cassette filters refer to filter units containing few sheets of membrane that are held apart in parallel and from the cassette housing by means of supports (called screens). Basically, the feed stream passes into the space between the sheets and the generated permeate is collected from the other side of the membrane. Cassettes are characterized by the thickness of the screen, as well

as the flow path length. On the other hand, hollow fiber filters (also called as cartridge filters), encompass several hollow fibers that are supported next to each other (see Figure 2.9A). In this configuration, the feed stream passes into the fibers and the permeate is collected from outside of the fibers, Figure 2.9B). Hollow fibers are characterized by their length, diameter, as well as number of fibers in a cartridge (Cross flow filtration Method Handbook, 2014). Hollow fibers are less expensive than cassette geometry since packaging of membranes in a module compartment is more cost effective. Moreover, there is no need of a holder in hollow fiber technology which also reduces the capital cost. In addition, hollow fibers are more user friendly as the modules are pre-assembled, pre-sterilized, and disposable ("Why You Should Consider Hollow Fibres for Ultrafiltration," 2015). It is known that for filtration of particles, the tubular geometry of hollow fibers is more beneficial than the cassette geometry. This is due to the migration of particles to the center of the hollow fiber where the flow velocity is the highest. This phenomenon is known as “tubular pinch effect” (Serway & Tamashiro, 2010; Veeken, 2012).

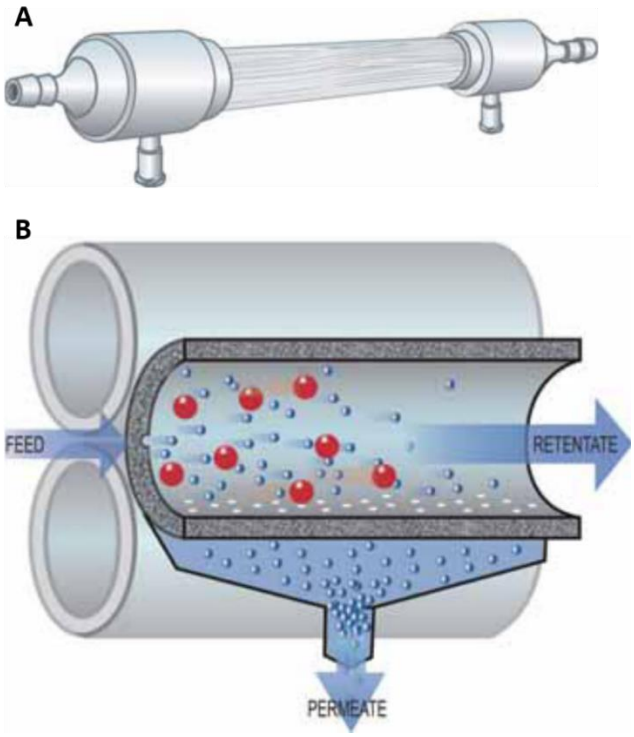

Figure 2.9 Schematic of a typical hollow fiber module (A), and the performance of a hollow fiber membrane (B)

2.6.3 Cross flow rate

Cross flow rate is the recirculating volumetric flow rate in a TFF process. Cross flow rate, also referred to as retentate flow rate, is simply the rate of the fluid that passes parallel to the filter membrane surface. This parameter is important since it produces the force required to sweep away the molecules which tend to accumulate on the filter and cause fouling, thereby restricting the filtrate flow. For hollow fiber filters, the cross flow rate through the fibers is expressed as the shear rate in units of per second (s^{-1}), which is a function of the flow rate per fiber as well as the fiber diameter (d).

$y = \frac{32q}{\pi.d^3}$, where q is the retentate flow rate in each fiber Eq. 2.3

Shear rates are not applicable for cassettes geometry, since calculation is complicated due to the influence of the support screen (Cross flow filtration Method Handbook, 2014). Shear rate plays an important role in scale up or down analysis between the modules. By expressing cross flow rate as shear rate, it would be possible to approximate the flow rate which results in the same shear rate at different scales.

2.6.4 Trans-membrane pressure

Trans-membrane pressure (TMP) is the pressure acting across the membrane which drives the fluid to the permeate side, carrying all permeable components. TMP is basically an average difference in pressure from the feed to the permeate. TMP is defined as follows:

$$\mathrm{TMP} = \frac{\mathrm{P_{feed}} + \mathrm{P_{retentate}}}{2} - \mathrm{P_{permeate}} \qquad \text{Eq. 2.4}$$

As the filtration driving force, TMP plays a very critical role in a TFF process. There is no filtration when the TMP is at zero as a given cross flow rate (no net pressure across the membrane), see Figure 2.10A. As soon as TMP applies across the membrane, permeable components pass through the pores to generate the permeate solution, and the higher the TMP, the higher permeate flux. This is the safe condition during a TFF process, confirming no clogging of the membrane (Figure 2.10B) (H. F. Liu, Ma, Winter, & Bayer, 2010). If a TMP higher than required level is applied, more gel layer and fouling occur on the membrane, which eventually, causes a drop in the TMP and permeate flux (Figure 2.10C). This is associated with high concentration of retained species at the membrane wall (Cross flow filtration Method Handbook, 2014; Paulena, Fikara, Foleyb, Kovácsc, &

Czermakc, 2012). Thus, selecting the optimum operating TMP must be determined through experimentation to prevent membrane fouling and to have an efficient TFF operation through a controlled TMP (Cross flow filtration Method Handbook, 2014; Jornitz, Jornitz, & Meltzer, 2007; Millipore, 2013).

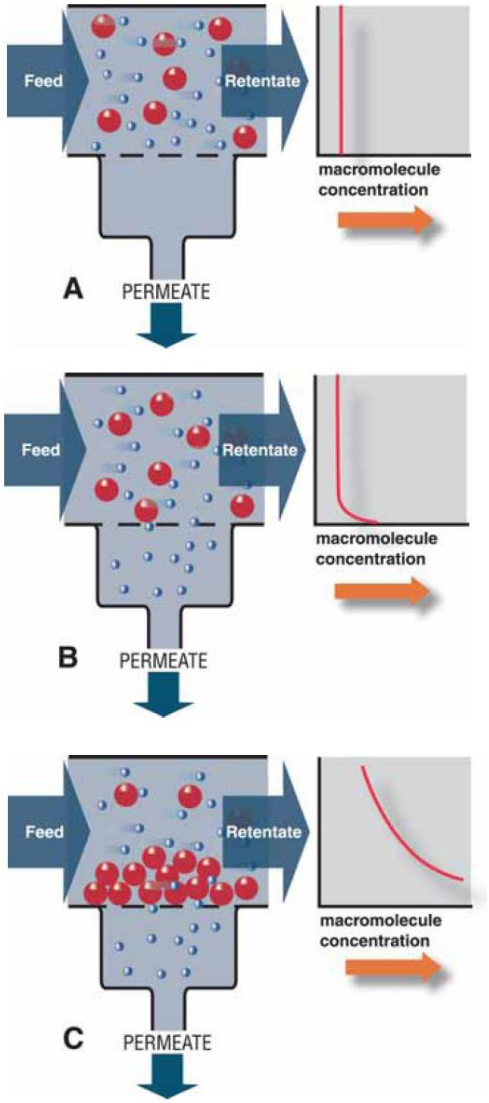

Figure 2.10 TFF performance when TMP=0 (A), TMP is balanced in a range where the is a linear trend between TMP and permeate flux (B), TMP is above the optimal threshold which causes membrane fouling.

Like any other processes, TFF operational parameters (*i.e.* TMP, shear rate, and permeate flux) must be optimized for a robust process, and to have consistent and high product recovery yield.

Despite its high importance, there is no report on a systematic study of these operational parameters. This potentiats lack of consistency, significant drop in permeate flux during the process, and finally low product yield. Therefore, it would be relevant to validate the safe TFF operational parameters prior to its application.

CHAPTER 3 APPROACH OF THE RESEARCH WORK AND GENERAL STRUCTURE OF THE THESIS

The next two chapters, which represent the body of the thesis, will cover the research carried out in order to achieve the objectives of the thesis (see section 1.1). The results and their interpretation are presented in the form of a published article summarizing the in-line mixing system for large scale production of chitosan-based polyplexes (chapter 4), and a chapter describing purification of polyplexes *via* TFF, and coating of the chitosan-based polyplexes using hyaluronic acid (chapter 5). The document finishes with a general discussion (chapter 6), followed by a conclusion and recommendations on future work (chapter 7).

Chapter 4 presents the study on the development of an automated in-line mixing system for the large scale production of CS-based polyplexes. Mixing parameters such as mixing speed, mixing concentration, mixing length, as well as mixing pattern were studied for production of CS/pDNA and CS/siRNA polyplexes. The optimal operation conditions were established to reproducibly deliver small sized homogenuous CS/pDNA and CS/siRNA polyplexes. Size, size distribution (PDI), as well as zeta potential of polyplexes were studied by Dynamic Light Scattering (DLS). The morphology of the polyplexes was studied by transmission electron microscopy (TEM). *In vitro* transfection efficiency of CS/siRNA formulations was measured by quantitative real time polymerase chain reaction (qPCR), quantifying the knockdown percentage of Apolipoprotein B (*ApoB*) mRNA in the HepG2 hepatocellular carcinoma cell line. This study was published: Ashkan Tavakoli Naeini, Ousamah Younoss Soliman, Mohamad Gabriel Alameh, Marc Lavertu, Michael D. Buschmann, "Automated in-line mixing system for large scale production of chitosan based polyplexes", *J Colloid Interface Sci*, vol. 500, pp. 253-263, 2017.

Chapter 5 presents the work done to purify, concentrate, and modify CS-based polyplexes using tangential flow filtration. Optimized mixing conditions, from chapter 4, were used to produce large batches of polyplexes. TFF operational parameters (*i.e.* TMP, permeate flux, and shear rate) were studied in order to establish a safe operational zone where the TMP and permeate flux stay as constant (indicating maximum recovery of polyplexes post-filtration). Since for the TFF optimization study large volumes of polyplexes were needed, double stranded oligodeoxynucleotide (dsODN, 21 bp) encoding the same sequences and mimicking siRNA eGFP physico-chemical properties was used as a lower-cost alternative. Under the established TFF

operational conditions, polyplexes preserved their physico-chemical properties when concentrated up to sevenfold. Furthermore, using the safe operational conditions, the optimized number of diafiltration volumes (DV) for purification of polyplexes (unbound CS removal) was identified at 5 DV. Upon establishement of TFF operational conditions as well as the number of diavolumes, CS/siRNA polyplexes were purified. Size, PDI, as well as zeta potential (ZP) of polyplexes post-diafiltration were studied by Dynamic Light Scattering (DLS). The morphology of the polyplexes was studied by transmission electron microscopy (TEM). Silencing efficiency of CS/siRNA formulations was measured *in vitro* on $eGFP^+$ H1299 cells. The hemocompatibility of these formulations was evaluated as per ASTM guidelines. Purified polyplexes, were then coated by HA molecules using the in-line mixing system, and further purified using TFF to remove the unbound HA. Size, PDI, as well as ZP of HA-coated polyplexes post filtration were studied by DLS. The morphology of the polyplexes was studied by transmission electron microscopy (TEM). Finally, the *in vitro* silencing efficiency of CS/siRNA formulations was measured on $eGFP^+$ H1299 cells, and finally, the hemocompatibility of these formulations was evaluated.

CHAPTER 4 ARTICLE 1: AUTOMATED IN-LINE MIXING SYSTEM FOR LARGE SCALE PRODUCTION OF CHITOSAN-BASED POLYPLEXES

Journal of Colloid and Interface Science

Ashkan Tavakoli Naeini [a], Ousamah Younoss Soliman [a], Mohamad Gabriel Alameh [a], Marc Lavertu [b], Michael D. Buschmann [a,b,*]

[a] Institute of Biomedical Engineering, Polytechnique Montreal, Montreal, Quebec, Canada

[b] Department of Chemical Engineering, Polytechnique Montreal, Montreal, Quebec, Canada

4.1 Abstract

Chitosan (CS)-based polyplexes are efficient non-viral gene delivery systems that are most commonly prepared by manual mixing. However, manual mixing is not only poorly controlled but also restricted to relatively small preparation volumes, limiting clinical applications. In order to overcome these drawbacks and to produce clinical quantities of CS-based polyplexes, a fully automated in-line mixing platform was developed for production of large batches of small-size and homogeneous CS-based polyplexes. Operational conditions to produce small-sized homogeneous polyplexes were identified. Increasing mixing concentrations of CS and nucleic acid was directly associated with an increase in size and polydispersity of both CS/pDNA and CS/siRNA polyplexes. We also found that although the speed of mixing has a negligible impact on the properties of CS/pDNA polyplexes, the size and polydispersity of CS/siRNA polyplexes are strongly influenced by the mixing speed: the higher the speed, the smaller the size and polydispersity. While in-line and manual CS/pDNA polyplexes had similar size and PDI, CS/siRNA polyplexes were smaller and more homogenous when prepared in-line in the non-laminar flow regime compared to manual method. Finally, we found that in-line mixed CS/siRNA polyplexes have equivalent or higher silencing efficiency of ApoB in HepG2 cells, compared to manually prepared polyplexes.

4.2 Graphical abstract

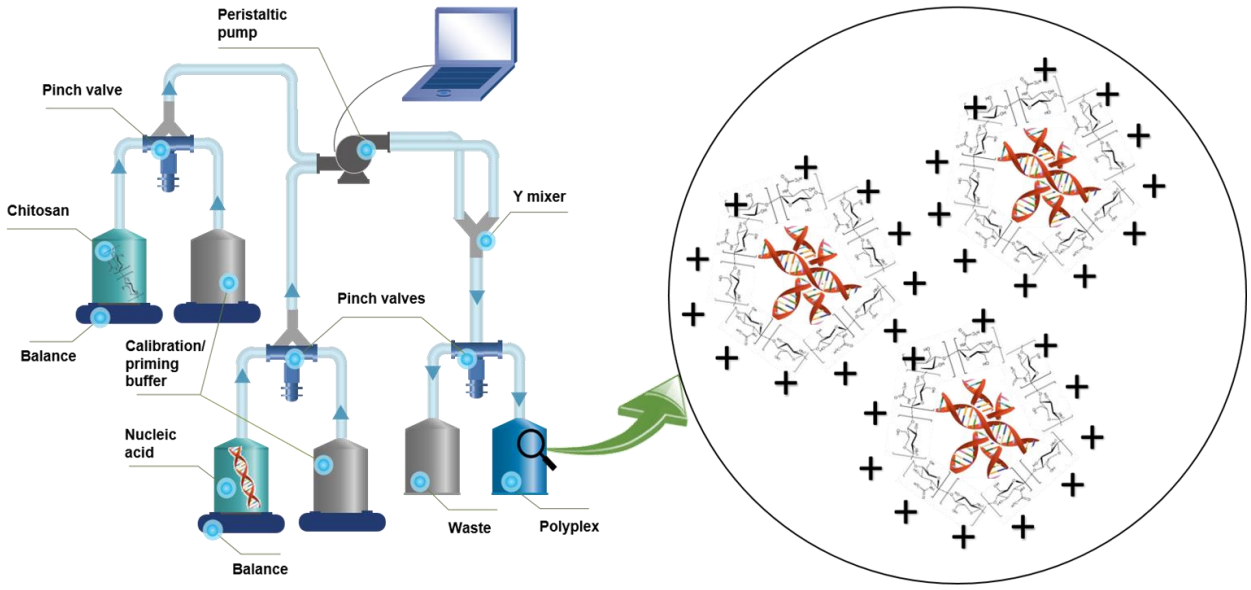

Figure 4.1 Graphical abstract: large scale production of chitosan based polyplexes using the automated in-line mixing system

4.3 Keywords

In-line mixing, Chitosan, siRNA, Plasmid, Polyplex, Non-viral gene delivery, Bioactivity

4.4 Introduction

Non-viral gene delivery mainly relies on the use of cationic lipids and cationic polymers to bind and condense negatively charged nucleic acids (NAs). Complexes formed between a nucleic acid and polymers are referred to as polyplexes. Upon mixing, these oppositely charged species bind to each other by means of attractive electrostatic interactions, a process favored by a concomitant increase in entropy due to the release of low molecular weight counter-ions. In very dilute solutions, complex formation leads to nanoparticle suspensions at the colloidal level, while mixing in a concentrated regime results in macroscopically flocculated systems (Dautzenberg et al., 1996; Muller, 1974; Muller et al., 2011; Thunemann et al., 2004a). Nonetheless, higher mixing concentrations result in higher dose of NA in a given volume of the suspension, hence increasing the deliverable doses.

Chitosan (CS), a naturally derived polycation, is a biocompatible and biodegradable linear polysaccharide that has gained interest for safe delivery of NA. It has been demonstrated that CS-based delivery systems are efficient for delivery of plasmid DNA (pDNA) (Alameh, Jean, Dejesus, Buschmann, & Merzouki, 2010; Buschmann et al., 2013; Jean et al., 2012b; Jean et al., 2009; Lavertu et al., 2006; Mao et al., 2001; Nimesh et al., 2010a; Thibault et al., 2010b), and siRNA (Alameh et al., 2012; Corbet et al., 2016; Gao et al., 2014; Holzerny et al., 2012; Howard et al., 2006a; X. Liu et al., 2007; Malmo et al., 2012a; S. Mao et al., 2010; Ragelle et al., 2014; Ragelle et al., 2013; Raja et al., 2015; Yang et al., 2015), both *in vitro* and *in vivo*. Manual mixing is the most commonly used method to produce CS-based polyplexes. However, this manual method varies in implementation which raises some concerns regarding comparability of the properties of such complexes. Classical pipetting is a frequently reported technique in the literature, where CS is promptly added into NA solution followed by pipetting the mixture up and down for homogenization (Alameh et al., 2012; Alameh et al., 2010; Jean et al., 2011; Jean et al., 2012b; Jean et al., 2009; Lavertu et al., 2006; MacLaughlin et al., 1998a; Nimesh et al., 2010a; Veilleux et al., 2016). One other manual approach is addition of NA into excess CS solution under stirring condition to allow formation of polyplexes (Howard et al., 2006a; X. Liu et al., 2007; Malmo et al., 2012a; Yang et al., 2015). Another technique is drop-wise addition of CS solution into equal volume of NA solution followed by quick mixing (Katas & Alpar, 2006), while similar method was reported with reverse order of addition (Holzerny et al., 2012). Addition of siRNA into CS followed by vortexing of the complex for a short period (30 seconds) is also a reported technique (Corbet et al., 2016; Ragelle et al., 2014). Properties of final polyplexes depend upon the mixing technique, experience of the operator (Lu et al., 2014), and order of addition of the two polyelectrolytes (Zhigaltsev et al., 2012a). Furthermore, independent of the adopted approach, conventional manual mixing is not only a poorly controlled method which may result in irreproducibility (Belliveau et al., 2012; Lu et al., 2014; Valencia, Farokhzad, Karnik, & Langer, 2012), but it is also restricted to relatively small preparation volumes, that seriously limit applicability. Small scale manual preparation of complexes poses risks of batch to batch and inter-user variability (Kasper et al., 2011; Lu et al., 2014; Zelphati et al., 1998), thus, a controlled and repeatable production process of polyplexes in large quantities is a prerequisite for their clinical applications (Valencia et al., 2012). Several mixing techniques and devices have been proposed in the literature to prepare large volumes of complexes. These techniques rely on in-line mixing in Y

or T-shaped connectors (Clement et al., 2005; Davies et al., 2010; Kasper et al., 2011; Zelphati et al., 1998) microfluidics (Balbino, Azzoni, & de la Torre, 2013; Belliveau et al., 2012; Grigsby, Ho, Lin, Engbersen, & Leong, 2013; A. K. Leung et al., 2012; Lu et al., 2014; Stroock et al., 2002; Valencia et al., 2012; Zhigaltsev et al., 2012a), as well as jet mixing (C. Ankerfors et al., 2010a; B. K. Johnson & Prud'homme, 2003). To the best of our knowledge, the very first in-line mixing system for complex production was designed by Zelphati *et al.*, where syringes were used to drive pDNA and cationic lipids into a T-connector (Zelphati et al., 1998). Later, John and Prud'homme invented a Confined Impinging Jet mixing (CIJ) apparatus to generate two opposing high velocity linear jets of polyelectrolyte solutions, where the two streams collide in a chamber for a few milliseconds (rapid mixing takes place in a time less than the nucleation and growth time of complexes) (B. K. Johnson & Prud'homme, 2003). Ankerfors *et al.* applied the CIJ system to investigate the influence of mixing time on the size of produced Polyallylamine hydrochloride (PAH)/polyacrylic acid (PAA) complexes. They reported production of larger particles at reduced speeds of the polyelectrolyte streams (C. Ankerfors et al., 2010a). While establishment of a jet mixer is sophisticated, mixing in a Y or T-shaped connector is a simpler design. In 2005, Clement *et al.* introduced an in-line mixing platform (but not computer controlled) based on two peristaltic pumps and a Y-connector. They showed no difference in transfection efficiencies of manual and in-line mixed complexes (Clement et al., 2005), however, the impact of mixing conditions (*e.g.*, speed and NA concentration) on physico-chemical properties of complexes was not studied. In 2010, Davies *et al.* designed a novel mixing device based on a static mixer and a cylindrical pneumatic actuator connected *via* an adjustable regulator to a compressed air supply (Davies et al., 2010). They were the first to reporting an in-line mixing device for the preparation of polyplexes (PEI/pDNA), however, their device was not easily scalable. In 2011, Kasper *et al.* claimed reproducible production of small and homogeneous PEI/pDNA polyplexes by means of an up-scaled micro-mixer system, consisting of two syringes and a T-connector (Kasper et al., 2011). They reported a reduction in the size of polyplexes by increasing the mixing speed and reducing the concentration of pDNA. Finally, a chaotic mixer specified as "staggered herringbone microfluidic mixing device" was designed based on microfluidic mixing in a laminar regime to produce well-defined lipid nanoparticles (LNPs) (A. K. Leung et al., 2012; Stroock et al., 2002). This staggered herringbone pattern creates transverse flows in the microchannels to induce chaotic mixing at a low speed of the laminar regime. Belliveau *et al.* investigated the ability of SHM to

produce monodisperse LNP-siRNA complexes (Belliveau et al., 2012). While the size of LNPs remained fairly constant over the range of the tested flow rates, the lowest PDI for LNP-siRNA complexes was obtained at the highest tested mixing flow rate. In addition, reducing the concentration of siRNA resulted in a reduction in polydispersity. Although the above-mentioned methods were introduced for up-scaled mixing platforms, there has been no systematic study to date on the operational parameters of a fully automated in-line mixing system that can reproducibly prepare large batches of CS-based polyplexes with defined physico-chemical properties, and transfection efficiency.

The main objective of this study was to develop a computer controlled in-line mixing platform for reproducible production of small sized homogeneous CS-based polyplexes, and examine the influence of mixing parameters on the properties of polyplexes. We hypothesized that reducing the NA concentration and increasing mixing speed would reduce the size and polydispersity of CS-based polyplexes. Another objective was to assess the *in vitro* silencing efficiency of the CS/siRNA polyplexes, where we hypothesized equal or even better bioactivity for in-line CS/siRNA compared to manually prepared polyplexes.

4.5 Material and Methods

4.5.1 Materials

Chitosan was obtained from Marinard. Trehalose dehydrate (Cat #T0167), L-histidine (Cat #H6034) were from Sigma. HepG2 (hepatocellular carcinoma) cells (Cat# HB-8065), and Eagle's Minimum Essential Medium (Cat #30-2003) were from American Type Culture Collection (ATCC). Dulbecco's Modified Eagle Medium, high glucose pyruvate (DMEM-HG, Cat #12800-017) was from Gibco. Fetal bovine serum (FBS, Cat #26140) was from Thermo Fisher Scientific. Plasmid EGFPLuc (Cat #6169-1) was from Clontech Laboratories. siRNA targeting ApoB mRNAs (siRNA ApoB) contains sense sequence of 5’-GUCAUCACACUGAAUACCAAU-3’ and antisense 5’-AUUGGUAUUCAGUGUGAUGACAC-3’ was obtained from GE (Custom synthesis, A4 scale). Double stranded oligodeoxynucleotide (dsODN, 21 bp) encoding the same sequences and mimicking siRNA ApoB physico-chemical properties was obtained from Integrated DNA Technologies Inc, Coralville, IO. The commercially available liposome, DharmaFECT™2

was from Dharmacon RNAi Technologies and Diethyl pyrocarbonate (DEPC) from Sigma Aldrich (Cat #D5758).

4.5.2 Preparation of CS, plasmid DNA and siRNA for mixing

The plasmid eGFPLuc stock solution was prepared and characterized by UV spectrophotometry, as described in Lavertu et al (Lavertu et al., 2006). The plasmid DNA (pDNA) stock solution was diluted to 10, 50, 100, 200, and 300 µg/mL with Milli-Q water as well as sterile filtered trehalose and histidine (pH 6.5) solutions for having final concentration of 0.5% and 3.5mM, respectively (these are optimum concentrations of excipients for freeze-drying and stability of complexes over time that have been previously established) (Veilleux et al., 2016). The siRNA ApoB stock solution was prepared and characterized by UV spectrophotometry, then diluted to 10, 50, 100, 200, 300, and 400 µg/mL with RNase/DNase free water as well as the excipients as described for plasmid DNA. Commercial chitosan was first heterogeneously deacetylated to 92% using concentrated sodium hydroxide and was depolymerized to 10 kDa and 2 kDa using nitrous acid, as established and previously reported by our group (Lavertu et al., 2006). It has been reported that the 10 kDa chitosan with DDA of 92% (CS92-10) form stable complexes when prepared at molar ratio of CS amine to NA phosphate ratio of 5 (N:P=5), and also dissociates effectively upon release from lysosomes, maximizing the level of transfection (Thibault et al., 2010b). Degree of deacetylation (DDA) and number-average molar mass (Mn) of chitosan was confirmed by 1H NMR (Lavertu et al., 2003), and gel permeation chromatography multi-angle light scattering (Nguyen, Winnik, & Buschmann, 2009). A chitosan stock solution at 5 mg/mL was prepared from dry powder dissolved in 28 mM HCl overnight at room temperature (RT). The stock solution was sterile filtered, then diluted with Milli-Q or RNase free water (for siRNA applications), as well as excipients as described before for N:P=5, based on the concentration of nucleic acid (either pDNA or siRNA).

4.5.3 Preparation of CS/NA polyplexes by Manual Mixing (classical pipetteing)

CS/NA polyplexes were prepared by manual addition of CS (100 µL) to equal volume of NA (diluted to maintain N:P=5), following by immediate pipetting up and down repeated 10 times. Samples were then incubated for 30 minutes at RT before analyses or transfections.

4.5.4 Preparation of CS/NA polyplexes by In-line Mixing

In addition to the manual mixing, both types of polyplexes (CS/pDNA and CS/siRNA) were produced *via* AIMS in the exact same formulation as for the manual mixing. Both initial and advanced versions of AIMS (configuration a and b of Figure 4.2) were tested. Prepared samples were incubated in the original collecting vessel for 30 minutes at RT before analyses or transfections.

4.5.5 Polyplex Size, Polydispersity, and Surface Charge Analysis

Hydrodynamic size and polydispersity index of the produced polyplexes were measured using dynamic light scattering (Zetasizer Nano ZSP- ZEN5600, Malvern Instruments, Worcestershire, UK). Samples were diluted by 4-5 fold by adding Milli-Q or RNase free water, then analyzed for three consecutive runs at 25°C. Zeta potential (ZP) measurements were made with the Malvern Zetasizer Nano ZSP using folded capillary cells. ZP value was calculated from the measured electrophoretic mobility u_E by applying the Henry equation: $ZP = \frac{3\eta u_E}{2\varepsilon f(\kappa a)}$, where U_E is the velocity of the particle in the applied electric field (referred to as the electrophoretic mobility), ε and η are the dielectric constant and the viscosity of the medium, respectively. $f(\kappa a)$ is the Henry's function, where a is the particles radius, and $1/\kappa$ is the Debye length, thus κa is the ratio of particle radius to Debye length. For calculation of the ZP from electrophoretic mobility, a value of 3/2 for the Henry function was used so that $ZP = \frac{\eta u_E}{\varepsilon}$ was used. This limiting case is referred to as the Smoluchowski equation, an approximation that is valid when the size of the particle is much larger than the Debye length ($\kappa a \gg 1$), a condition generally satisfied in an aqueous media with moderate to high electrolyte concentration. For ZP measurements, each sample was diluted 8 fold to a final volume of 800 µL by adding 700 µL of buffer (trehalose 0.5%, and 3.5mM histidine) for a final ionic strength of about 1 mM. Each sample was analyzed for three consecutive runs at 25°C.

4.5.6 Transmission Electron Microscopy Imaging

Morphology of both in-line and manually produced polyplexes was studied using Transmission Electron Microscopy (TEM). On a carbon coated copper grid (200 mesh, Electron microscopy sciences), 5 µL drop of polyplex suspension was pipetted and allowed to evaporate for 30 minutes. To avoid drying artifacts, remaining solvent was removed by blotting using a filter paper. 5 µL of

2% phosphotungstic acid was placed on the grid. After 10 minutes the stain was removed as described above. The grid was washed two times with deionized water to avoid any salt contamination from the sample and air dried. TEM images were obtained using a Tecnai T12 electron microscope operating at 120 keV. For each sample four random areas on the grid were imaged at different magnifications.

4.5.7 Sterile and RNase free production *via* AIMS

The AIMS system including the upstream vessels, collecting containers, as well as the tubing set were autoclaved for sterility. In order to maintain the sterility of AIMS, the entire tubing network is isolated from the environment where each vessel is open to atmosphere *via* a 0.22 µm syringe filter in order to maintain pressure during pumping and mixing. When working with siRNA, the closed system was treated with diethylpyrocarbonate (DEPC) in order to inactivate contaminant nucleases.

4.5.8 Cell culture and transfection

HepG2 cells were cultured in EMEM supplemented with 8% fetal bovine serum (FBS). One day prior to transfection, cells were seeded in a 24 well plate at 300,000 cells per well to reach ~80% confluence on the day of transfection. Prior to transfection, media over cells was aspirated and replenished with serum free DMEM-HG media (pH 6.5) supplemented with 0.976g/L MES and 0.84g/L $NaHCO_3$. In-line and manually mixed polyplexes were prepared as described above and a specific volume was pipetted into each well to reach a target siRNA concentration of 100nM/well (~0.66µg/500µL). FBS was added 5 hours post-transfection to reach a final concentration of 8%. Transfection media was aspirated 24 hours post transfection, replenished with complete EMEM and incubated for an extra 24 hours. DharmaFECT®2/siRNA lipoplexes were used as positive control and were prepared as per manufacturer recommendation. Lipoplex and naked siRNA transfection were performed at a final concentration of 100nM/well. Chitosan only and untreated cells were used as negative controls.

4.5.9 Assessment of silencing efficiency

Polyplex bioactivity was assessed using MIQE compliant quantitative real time PCR (qPCR) (Bustin et al., 2009). All primers and probes were intron spanning to avoid amplification of

potential genomic DNA contamination and *in silico* validated using the NCBI blast tool for specificity (Supp info). Total RNA extraction was performed 48 hours post transfection using the EZ-10 Spin column Animal total RNA extraction kit (BioBasic). Total RNA was extracted as per manufacturer protocol and subjected to in-column DNase digestion (Qiagen, Cat#79254). The purity of the eluate was assessed using UV/VIS spectrometry at 260, 280, 230 and 340 (Nanodrop 8000). The integrity of extracted RNA was determined using the Agilent 2100 Bioanalyzer (Agilent technologies). Total RNA concentration was determined using the Qubit reagent (Life technologies, Cat# Q10210) as per the manufacturer's protocol. For each condition tested, a total RNA quantity of 200ng/20µL reaction was reverse transcribed using the SuperScript VILO cDNA synthesis kit (Life technologies, Cat#11754250). Primer and probe efficiency was experimentally determined using the standard curve method on the same plate where target gene knockdown is being assessed (Supp info). Reference gene stability was validated using the GeNorm statistical package (Biogazelle NV) (Supp info) cDNA was amplified using TaqMan Fast Advanced Master Mix (Life technologies, Cat# 4444557) on a QuantStudio 12K flex system (ThermoFisher Scientific). All reactions were performed in a 384 well plate (ThermoFisher Scientific, Cat# 4309849) using a final volume of 10µL (10ng of cDNA) and the following cycling conditions: 2 minutes hold at 55°C, then 10 minutes hold at 95°C followed by 40 cycles at 95°C for 15 seconds and 60°C for 1 minute. Data was exported in RDML and analyzed using the Biogazelle qBase+ software package.

4.5.10 Statistical analyses

All experiments were repeated once with technical replicates within each for the transfections. Values are given as average ± standard deviation. For statistics and plotting, SigmaPlot 13.0 package was used. One way ANOVA (at a significance level of 0.05) was applied and normality and other assumptions were validated.

4.6 Results and Discussion

4.6.1 Design and Establishment of the Up-scaled Automated In-line Mixing System (AIMS)

The in-line mixing setup uses peristaltic pumps to drive fluids based on pulsatile motion, where the natural oscillation of the fluids provides a wavy and stretched interface between the two streams, thus enhancing the mixing (Jackson et al., 2002; Truesdell, Vorobieff, Sklar, & Mammoli, 2003). A schematic of the in-line mixing is shown in Figure 4.2

Figure 4.2 Schematic of Automated In-line Mixing System (AIMS): initial version (configuration a), and advanced version (configuration b).

. Digital peristaltic pumps are programmed *via* LabVIEW^{TM} to drive CS and NA solutions through either silicon or PharmaPure tubings that were connected to each other with a connector (Y, T or cross connector). The mixing system also comprises digital balances that record the masses of buffers (*e.g.*, water) for calibration of the pump(s), and to monitor the volume/mass of payloads during mixing process. The whole closed tubing network was designed to be primed in order to remove air pockets trapped in streams as well as to pre-wet the inner walls of the tubings prior to the actual mixing. Pinch valves were programmed to switch from one stream to the other (*i.e.*, in the downstream: from waste line to the collecting vessel, as well as in the upstream: from buffer line to the payloads after priming, and vice versa). Calibration of the pump(s) was done automatically *via* a sub-program developed in house by LabVIEW^{TM}. Configuration (a) of Figure 4.2 displays an overview of the initial version of AIMS which features: 1) two separate but inter-connected peristaltic pumps where one drives NA and the other dispenses the CS solution, simultaneously, at the same flow rate; 2) priming of the tubings is done using the NA and CS solutions; 3) mixing takes place both during and after the acceleration phase of the pumps (acceleration phase refers to the period of time during which the pump head starts from stationary and reaches the target speed). Configuration (b) of Figure 4.2 displays the advanced version of the mixing system that features some technical, hardware and software improvements: 1) only one peristaltic pump with a dual channel head drives both CS and NA, simultaneously; 2) priming of the tubings is done with the buffer solution rather than the NA and CS solutions in order to minimize consumption of NA; 3) mixing takes place after the acceleration phase of the pump,

hence, polyplexes are mixed only at the target speed by switching the pinch valve from waste to the collection vessel once the final target speed was reached.

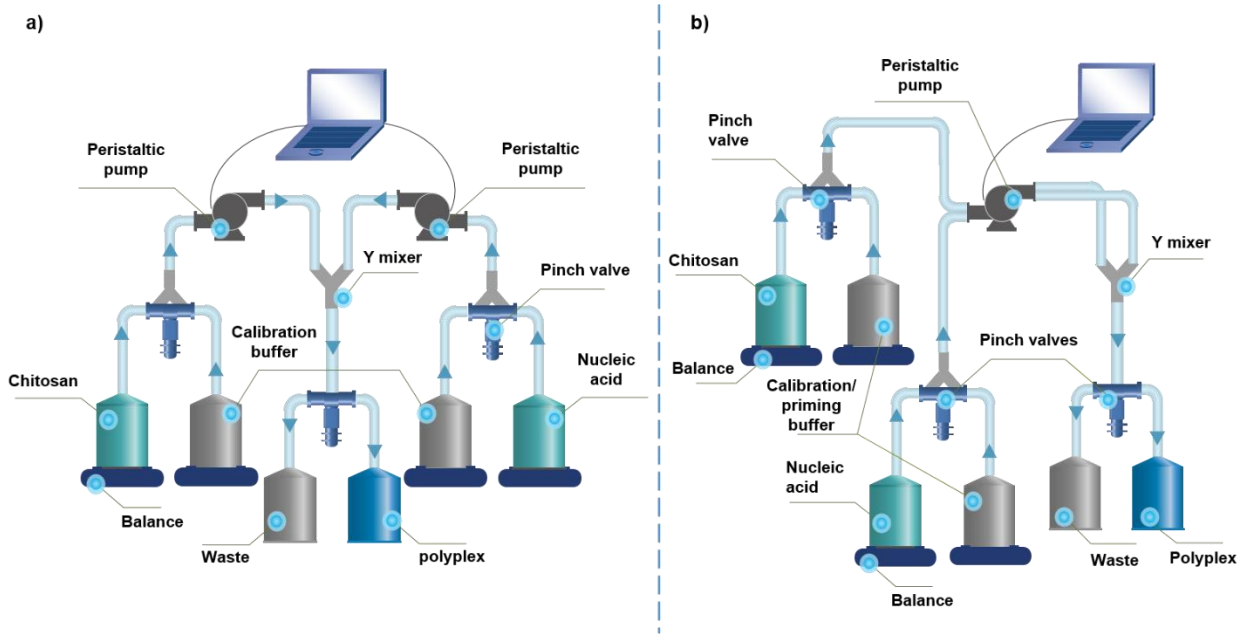

Figure 4.2 Schematic of Automated In-line Mixing System (AIMS): initial version (configuration a), and advanced version (configuration b).

4.6.2 Influence of mixing speed on the properties of CS/NA polyplexes

In order to examine the impact of mixing speed on the size and polydispersity of final complexes, CS/NA polyplexes were mixed *via* AIMS using flow rates ranging from 2 to 300 mL/min (1.7 to 253 cm/s given 1/16” as the tube inner diameter, ID). 300 mL/min is the maximum flow rate achievable using tubing ID=1/16”. Equal volumetric flow rates between the inlets was used in all mixing experiments. Production of polyplexes was done in duplicates for every mixing flow rate tested. The dimensionless Reynolds number (Re) was calculated in the outlet as $Re = UD/\nu$, where U is fluid velocity, D is the tube inner diameter and ν represents the fluid kinematic viscosity. The Re range covered in this study was 26-4,000. In a cylindrical/tubular geometry with smooth walls, Re ~<2,000 and Re ~>4,000 are indicative of laminar, and turbulent flow regime, respectively (Green & Perry, 2007). 2,000<Re<4,000 corresponds to transitional flow regime, which has characteristics of both laminar and turbulent regime. However, these values may not accurately translate the flow regimes in our system, due to the presence of peristaltic motions.

Literature reveals that the size and polydispersity of manually mixed CS/pDNA and CS/siRNA polyplexes both increase significantly at NA concentrations higher than about 0.1 mg/mL, and 0.2 mg/mL, respectively (Lavertu et al., 2006; Thunemann, 2004; Veilleux et al., 2016; Xu & Anchordoquy, 2011a), hence, these concentrations were taken to optimize the speed of mixing in AIMS. Both initial and advanced versions of AIMS were used for producing polyplexes by mixing 2 mL of CS and 2 mL of NA with either LS14 (ID=1/16”) or LS13 (ID=1/32”) tubing. For comparison purposes, manual mixing was performed through classical pipetting by addition of 100µL of CS into 100µL of NA followed by pipetting up and down ten times.

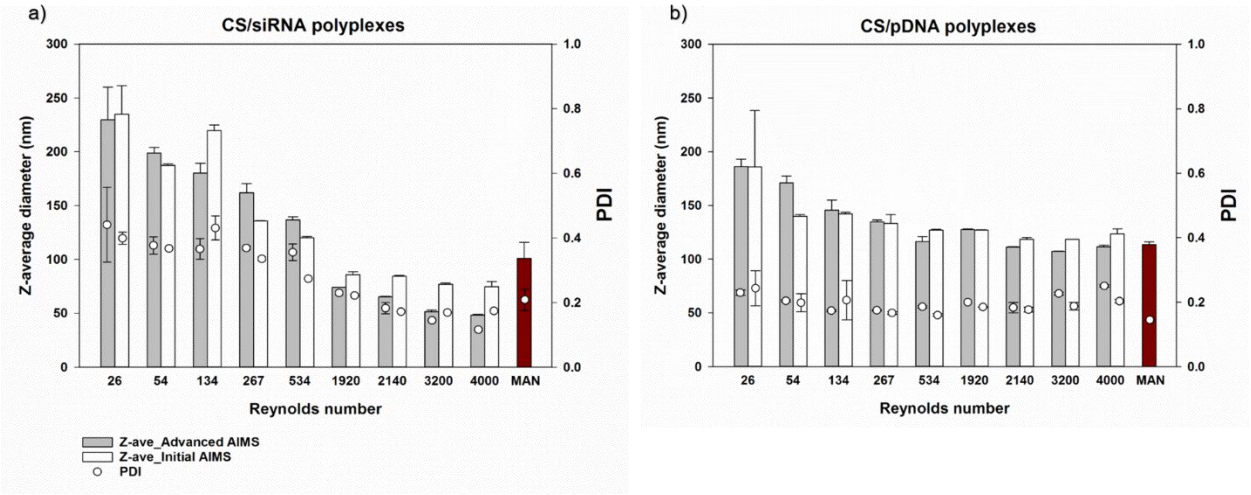

Figure 4.3 Influence of mixing speed on size and polydispersity of CS/siRNA polyplexes (a) and CS/pDNA polyplexes (b) produced by initial and advanced versions of AIMS. pDNA and siRNA concentration prior to mixing were 0.1 mg/mL, and 0.2 mg/mL, respectively, at molar ratio of CS amine to NA phosphate ratio of 5 (N:P=5). In-line mixing was done using 2 mL of CS and 2 mL of NA. Manual mixing was done by addition of 100µL of CS into 100µL of NA, followed by pipetting up and down ten times. Error bars represent standard deviation between the duplicates.

4.6.2.1 Faster mixing results in smaller and more homogenous CS/siRNA polyplexes

As shown in Figure 4.3a, a marked reduction in size and polydispersity of CS/siRNA polyplexes was observed when Re increased. Z-average diameter and PDI dropped from 235 to 75nm, and from 0.40 to 0.17, respectively, using the initial version of AIMS in the Re range from 26 to 4,000. Similar trend was observed using the advanced version of AIMS in the same range of Re where Z-average diameter and PDI were reduced further from 230 to 47nm, and from 0.44 to 0.12, respectively.

In a purely laminar flow regime with smooth walls (*e.g.*, using syringe pumps), where the streams move in parallel with no transverse movements or vortex, mixing relies solely on diffusion (Jackson et al., 2002; Stroock et al., 2002). The speed of molecular diffusion is a constant and intrinsically slow process; hence relying on diffusion results in incomplete mixing before fluid enters the collecting vessel, and non-homogenous complexes due to concentration gradient. As mentioned previously, the natural peristaltic actions of the pump(s) promote(s) diffusion by stretching the interfacial area (Jackson et al., 2002; Truesdell et al., 2003). The stretched contact area is associated with shorter diffusion path so that at each snapshot of the mixture throughout the outlet tubing, the two polyelectrolytes are brought closer to each other to bind quickly and form the complex (B. K. Johnson & Prud'homme, 2003). Increasing the frequency of rotation of the peristaltic pump (faster mixing), augments the intensity of pulsatile effect which enhances the overall mixing process by further stretching the interface area which favors production of smaller and more homogenous polyplexes. Reduction in size and PDI of CS/siRNA polyplexes could be also due to introduction of chaotic advection (irregular/random transport of matter by flow) in the mixing process at high mixing flow rates. Chaotic advection can be introduced to a system by either implementing obstacles in the flow channel (Stroock et al., 2002), or non-aligned inputs that generates vertical flow in the mixer (Ansari, Kim, Anwar, & Kim, 2012), or turbulence and vortex by high speed streams (C. Ankerfors et al., 2010a; B. K. Johnson & Prud'homme, 2003). By folding the streams, chaotic advection offers enhanced mixing performance due to transverse components of flow. Not only intertwinement of the two streams by chaotic advection generates additional contact area, but also quickly alters and refreshes the interfacial area that accelerates diffusion. Here, it was revealed that by increasing the speed (Re>2,140), mixing efficiency increases and translates into smaller and more homogenous CS/siRNA polyplexes in non-laminar regime (Figure 4.3a).

AIMS led to better reproducibility in production of CS/siRNA polyplexes *versus* the manual method except for the very low Re of 26. AIMS produced much smaller and more homogenous CS/siRNA polyplexes in the non-laminar regime (Re between 2,140 and 4,000) compared to manual polyplexes, with Z-average diameter and PDI from 84nm to 75nm and, 0.18 to 0.17 in the initial version of AIMS, and 65nm to 47nm and, 0.18 to 0.12 using the advanced version of AIMS, *versus* 101nm and 0.2, respectively for manual mixing. The largest improvement was at the highest Re=4,000 with the advanced version of AIMS to produce CS/siRNA polyplexes with Z-average of 47nm, and PDI of 0.12, while manual mixing led to Z-average of 101nm, and PDI of 0.2. This

suggests that in-line mixing in a non-laminar regime is more efficient than manual mixing, which is likely due to the role of chaotic advection which offers enhanced mixing performance due to transverse components of flow.

Moreover, as shown in Figure 4.3a, smaller and more homogenous CS/siRNA polyplexes were obtained using the advanced version of AIMS. In order to better understand the source of this reduction in size and polydispersity of polyplexes, each of the three modifications of the advanced version of AIMS (as described above) was isolated and studied separately, where oligonucleotide (ODN) was used to mimic siRNA as a lower-cost alternative. It was found that mixing during the acceleration phase of the pump was the source of increase in size and PDI of CS/ODN polyplexes (see supplementary material, Figure S1). This can be attributed to the fact that CS/siRNA polyplexes are sensitive to the speed Figure 4.3a, and mixing in the acceleration phase of the pump, where the mixing takes place at different speeds results in the formation CS/siRNA polyplexes with various sizes.

4.6.2.2 CS/pDNA polyplexes properties are not very sensitive to mixing flow rate

For 26<Re<4,000, Z-average diameter and PDI of CS/pDNA polyplexes varied only slightly between 186 and 112nm, and between 0.25 and 0.23, respectively. As shown in Figure 4.3b, size and PDI of CS/pDNA polyplexes change very smoothly throughout the tested range of Re. Davies *et al.* reported the same behavior for PEI/pDNA polyplexes in the moderate range of 568<Re<2,840 when a static mixer was applied in the downstream (Davies et al., 2010). This suggests that the pulsatile action of the peristaltic pumps produces sufficient perturbation and interface stretching for efficient mixing and production of homogeneous small sized pDNA/CS polyplexes, even at very low speeds. Due to its high MW (~4MDa, with 6.4kbp), pDNA has a low diffusivity, hence, while pDNA has limited mobility, mostly CS molecules diffuse to contribute to complex formation. Once association starts on a pDNA supercoil, the chance of collision with subsequent CS is much higher than colliding with another pDNA molecule, which limits random bridging of polyplexes and heterogeneity. Rapid saturation of pDNA binding sites by CS molecules limits the heterogeneity of the CS/pDNA polyplexes, even when advection is limited as pDNA does not diffuse quickly.

On the other hand, the stronger dependence of CS/siRNA polyplexes size upon the mixing speed is likely due to high diffusivity of siRNA molecules. siRNA as a much smaller molecule

(MW~14kDa with only 21 bp duplex) has a characteristic diffusion time scale much shorter than that of pDNA. Hence, in addition to CS, siRNA diffusion significantly contributes to the complex formation. Thus, in order to achieve efficient mixing, stronger advection is required to eventually saturate siRNA with excess CS molecules rather than colliding with another siRNA.

It was also observed that in-line CS/pDNA polyplexes (regardless of the AIMS configuration) have similar properties and similar reproducibility to the manually prepared polyplexes (Figure 4.3b). This could be again explained by low diffusivity of pDNA and limited sensitivity of CS/pDNA polyplexes to the mixing speed, suggesting that even the low advection provided by manual mixing is sufficient for having an efficient mixing.

4.6.3 Mixing patterns and tube length have no impact on the properties of CS/NA polyplexes

Two other mixers were tested at relatively low speed (Re=266), as well as in the highest mixing speed (Re=4,000): Y-connector was replaced by either a T-connector or a cross connector. Moreover, five mixing lengths with the output downstream after the connector, were tested (25, 35, 45, 55, and 65cm) at the highest speed, Re=4,000. We found that the mixing pattern and mixing length have no effect or a very slight effect on polyplex properties (data not shown), suggesting that pulsatile actions and transverse advection are sufficient for mixing over 25cm.

4.6.4 Influence of NA concentration on the properties of CS/NA polyplexes

Based on the results of Figure 4.3, the highest Re (4,000) was chosen for further mixings and investigation of the impact of NA concentration on properties of polyplexes. Here, NA concentration was varied from 0.01 to 0.4 mg/mL. Equal flow rate between the inlets was maintained. Both configurations of AIMS were tested. For comparison purposes, manual mixing was done at every concentration by pipetting, as described in the method section. Polyplexes were prepared in duplicate for each mixing condition.

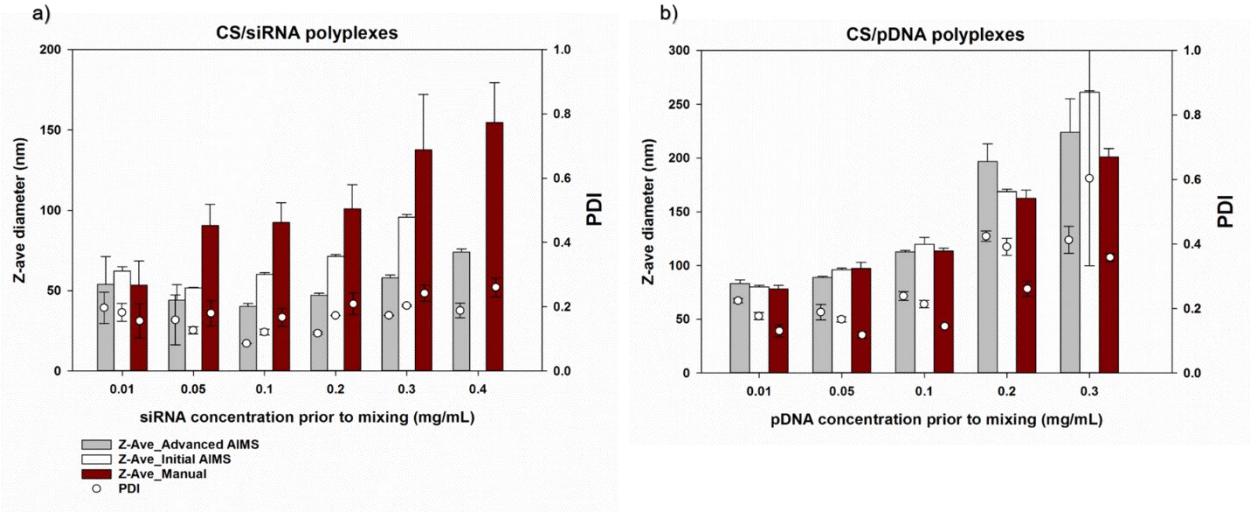

Figure 4.4 Influence of NA mixing concentration on size and polydispersity of CS/siRNA polyplexes (a) and CS/pDNA polyplexes (b) produced manually and by AIMS (using both initial and advanced versions), at molar ratio of CS amine to NA phosphate ratio of 5 (N:P=5). In-line mixing was done using 2 mL of CS and 2 mL of NA at Re=4,000. Manual mixing was done by addition of 100µL of CS into 100µL of NA, followed by pipetting up and down for ten times. CS/pDNA polyplexes severely aggregate at ≥0.4 mg/mL. Error bars represent standard deviation between the duplicates.

4.6.4.1 Mixing in dilute regime results in small and homogeneous polyplexes

As shown in Figure 4.4, regardless of the type of NA (siRNA or pDNA), mixing method (manual or in-line), and configuration of AIMS (initial or advanced), concentration of NA prior to mixing increases the size and PDI of polyplexes. The increase in polyplex size and PDI with increasing NA concentration has been reported in the literature (Belliveau et al., 2012; Kasper et al., 2011; Zelphati et al., 1998), Z-average diameter for CS/siRNA polyplexes produced with AIMS varied from 53 to 95nm in the concentration range of 0.01 to 0.4 mg/mL (Figure 4.4a), while for CS/pDNA Z-average diameter increased from 80 to 261nm in the concentration range of 0.01 to 0.3 mg/mL (Figure 4.4b), respectively. The small increase in Z-average and PDI of polyplexes prepared at the very lowest NA concentration (0.01 mg/mL) compared to 0.05 mg/mL can be explained by the low intensity of the scattering signal. When the number of particles is very low, the particle count (particles recognized by the DLS instrument) is too low for the instrument to derive a precise size distribution. Independent of the mixing method, macroscopic flocculation in CS/pDNA polyplexes

was observed at 0.4 mg/mL, however, such behavior was not found for CS/siRNA polyplexes up to the highest concentration tested (0.4 mg/mL). It is already reported in the literature that for production of stable and small size homogenous complexes, the mixing of two polyelectrolytes has to be done in dilute regime (Klausner et al., 2010; Lavertu et al., 2006; Malmo et al., 2012a; Mao et al., 2001). In fact, there is a significant difference between the characteristics of a dilute polymer solution (where polymer chains are completely separated) and a semi-dilute to concentrated solution (where polymer chains are overlapped). Generally, the transition concentration of polyelectrolyte solutions from dilute to semi-dilute regimes is defined as the overlap concentration (C*) (de Gennes, 1979). The closer the starting concentration of polyelectrolytes to their C*, the bigger the size and increased polydispersity of the final complexes.

The maximum concentration of pDNA for the preparation of small size uniform polyplexes is reported as ~0.1 mg/mL (Xu & Anchordoquy, 2011a), while production of small sized lipoplexes using relatively high concentration of siRNA (0.59 mg/mL) was reported by Belliveau *et al.* (Belliveau et al., 2012). As shown in Figure 4.4b, regardless of the mixing method (manual vs in-line) and configuration of AIMS (initial vs advanced), the onset pDNA concentration for increasing size and PDI of CS/pDNA polyplexes is clearly 0.1 mg/mL. However, with siRNA AIMS allowed production of relatively small and homogeneous CS/siRNA polyplexes at increased concentrations of 0.3 mg/mL and even 0.4 mg/mL. The possibility of producing CS/siRNA polyplexes at higher concentrations could be attributed to the smaller size of siRNA (higher C*) as compared to pDNA. Several techniques are used to measure the overlap concentration C* of polymeric solutions, such as small angle light scattering, osmometry, viscometry, light scattering and nuclear magnetic resonance (Wandrey, 1999; Zhu & Choo, 2008). According to our calculations, while C* for CS 92-10 and pDNA are close to each other and fairly low (C* ~3.6 mg/mL and ~1.36 mg/mL for chitosan 92-10 and pDNA, respectively), C* for siRNA is relatively high at ~790 mg/mL, which permits increased siRNA mixing concentration before reaching flocculation (see supplementary material for C* calculations).

In order to further investigate the impact of C* on the highest possible mixing concentrations, a smaller CS molecule (Mn= 2 kDa) was used to prepare CS/siRNA polyplexes. Being a smaller chain, CS92-2 has a smaller radius of gyration (Rg), hence, has a higher C*. It was shown that CS92-2 allows for production of small size homogeneous polyplexes at increased concentrations of siRNA, up to 0.6 mg/mL (see supplementary material, Figure 4.10), confirming the direct impact

of chain length on the mixing concentrations. Using manual method, the maximum siRNA concentration for producing relatively small size polyplexes is clearly 0.2 mg/mL, where a sharp increase in size of polyplexes was observed at higher concentrations. However, using the advanced version of AIMS small and monodisperse polyplexes were successfully prepared at elevated concentration of 0.4 mg/mL.

4.6.4.2 CS/siRNA polyplexes are smaller than CS/pDNA polyplexes

At a given concentration, CS/siRNA polyplexes were generally smaller than CS/pDNA polyplexes. For example, at an NA mixing concentration of 0.1 mg/mL, CS/siRNA and CS/pDNA polyplexes have Z-average of 40nm and 112nm, respectively. This is most probably due to the fact that pDNA is a larger molecule compared to siRNA, which naturally leads to larger complexes. Yet, the larger size of CS/pDNA polyplexes could be attributed to the slower diffusion of pDNA molecules that leads to broader distribution of pre-complexes which therefore induces formation of polyplexes with more than one pre-complex (C. Ankerfors et al., 2010a). As shown in Figure 4.4b, the configuration of AIMS has no significant influence on the properties of CS/pDNA polyplexes. This was also observed previously in Figure 4.3b where the properties of CS/pDNA polyplexes are independent of the AIMS configuration. However, in the case of CS/siRNA polyplexes (Figure 4.4a), the advanced version of AIMS produced smaller and more monodisperse CS/siRNA polyplexes at the given concentrations, which again confirms their sensitivity to mixing speed as described in Figure 4.3a. Compared to manual mixing, production of CS/siRNA polyplexes with AIMS at Re=4,000 (regardless of the AIMS configurations) provided better reproducibility, smaller size, lower PDI, and production of small size homogeneous polyplexes at elevated concentrations.

4.6.5 Surface charge density of CS/NA polyplexes increases with NA mixing concentration

Independent of the type of NA, concentration of polyelectrolytes prior to mixing also influenced the zeta potential (ZP) of polyplexes: the higher the NA concentration prior to mixing, the higher the electrophoretic mobility/calculated ZP of final complexes (Figure 4.5). In-line CS/siRNA had ZP varying between +10.5 and +21 mV in the concentration range of 0.01 to 0.4 mg/mL Figure 4.5a), whereas for in-line CS/pDNA the recorded ZP was from +5 to +16.5mV in the concentration range of 0.01 to 0.3 mg/mL (Figure 4.5a). As shown previously in Figure 4.4, polyplex size

increases with increasing NA concentration, so both ZP and size increase with mixing concentration. It is worth mentioning that for the polyplexes tested and analysis conditions used in this study, the ratio of the particle size to the Debye length changes with particle size and in all conditions, does not strictly meet the criteria for Smoluchowski model to apply precisely (*i.e.* $\kappa a \gg 1$, and the Henry function is not exactly 1.5 as explained in the methods). In order to examine if size variations could account, at least partially, for the observed ZP variations, calculations using the complete Henry function were also performed (data not shown). These calculations reveal that even if the calculated ZP changes slightly *versus* that obtained with the Smoluchowski equation, the general trend observed is unchanged, namely, ZP increases as mixing concentration increases. Therefore, although ZP is not a direct measurement of surface charge (Doane, Chuang, Hill, & Burda, 2012), our results indicate that the surface charge density of the polyplexes increases with mixing concentration, suggesting that more chitosan is incorporated in polyplexes when mixing concentration is higher. This could be the result of faster association kinetics at higher mixing concentrations.

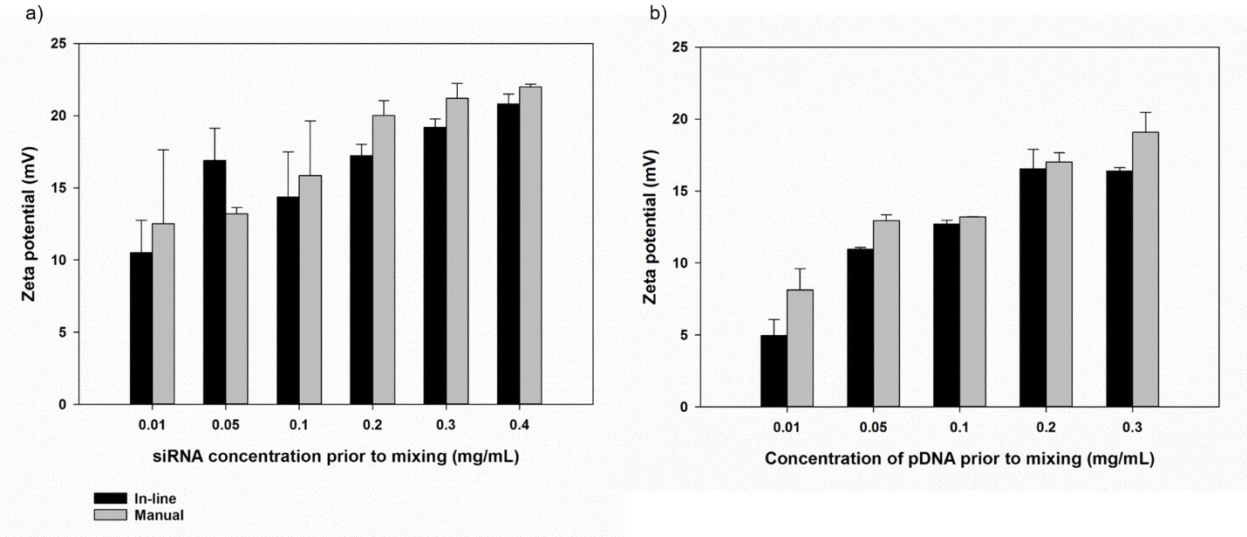

Figure 4.5 Influence of NA mixing concentration on zeta potential of CS/pDNA polyplexes (a) and CS/siRNA polyplexes (b). In-line mixing was done using the advanced version of AIMS: 2 mL of CS and 2 mL of NA at Re=4,000. Manual mixing: pipetting 100µL of CS into 100µL of NA. Zeta potential measurements were done in 0.5% trehalose and 3.5mM histidine (Ionic strength =1mM). Error bars represent standard deviation between the duplicates.

4.6.6 Morphology of the CS/pDNA and CS/siRNA polyplexes

Morphology of polyplexes was assessed by Transmission Electron Microscopy (TEM). CS/pDNA, and CS/siRNA polyplexes were prepared both manually and in-line using the advanced version of AIMS at NA starting concentrations of 0.1 mg/mL and 0.2 mg/mL, respectively. TEM images show CS/pDNA polyplexes with mixed morphology (spherical, toroidal and rod like) when produced both manually and using the AIMS (Figure 4.6a and b). This morphology of CS/pDNA polyplexes was reported in literature (Danielsen, Varum, & Stokke, 2004; Strand et al., 2005). On the other hand, CS/siRNA polyplexes were generally spherical regardless of the method of preparation (Figure 4.6c and d). The spherical shape of CS/siRNA polyplexes was also reported previously (Holzerny et al., 2012; Howard et al., 2006a; X. Liu et al., 2007). However, CS/siRNA polyplexes produced using AIMS (Figure 4.6d) were smaller and more uniform than those prepared manually (Figure 4.6c), in agreement with DLS results.

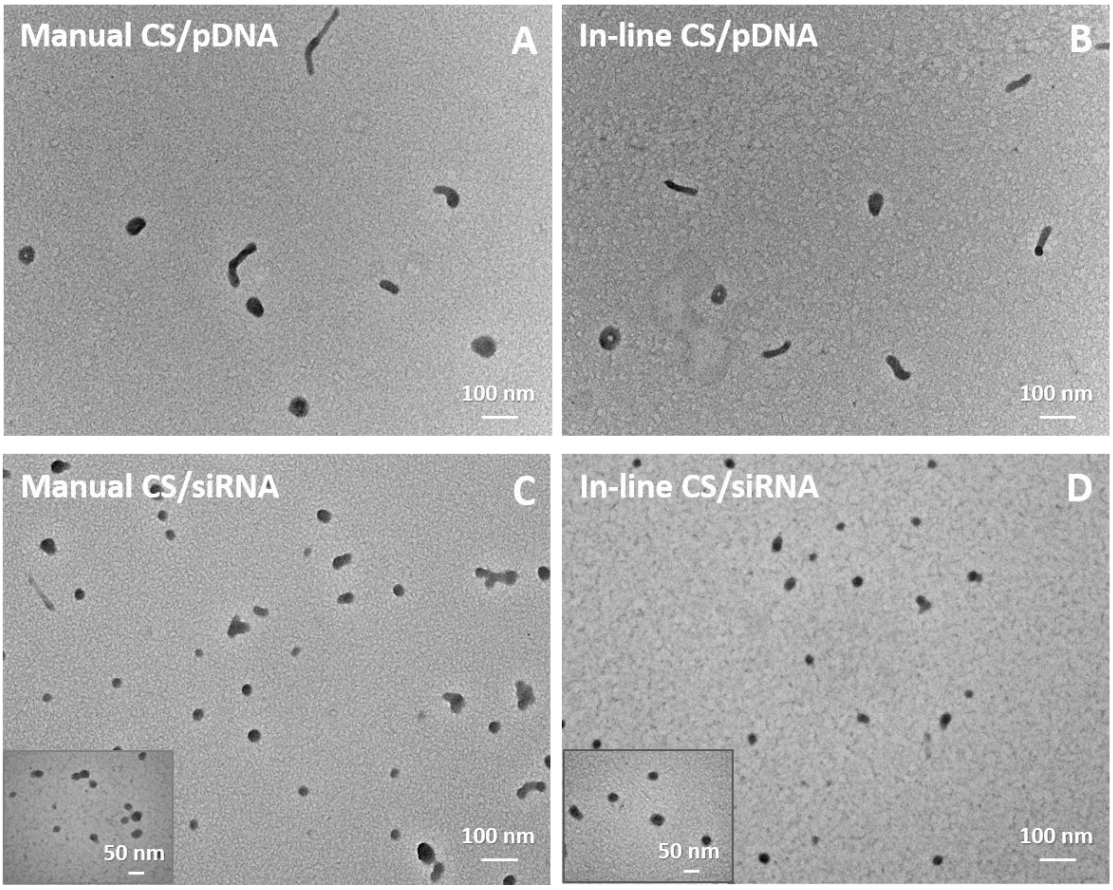

Figure 4.6 Transmission Electron Microscopy (TEM) images of CS/pDNA polyplexes (a and b) and CS/siRNA polyplexes (c and d), produced both manually (a and c) and using the advanced

version of AIMS (b and d). pDNA and siRNA concentration prior to mixing were 0.1 mg/mL and 0.2 mg/mL, respectively. In-line mixing was done by mixing 2 mL of CS and 2 mL of NA at 150 mL/min. Manual mixing was done by pipetting 100µL of CS into 100µL of NA.

4.6.7 CS/siRNA polyplexes produced in-line are as bioactive as manual polyplexes

In order to test the suitability of AIMS to produce bioactive CS/siRNA polyplexes, the hepatocellular carcinoma cell line HepG2 was transfected *in vitro* and Apolipoprotein B (*ApoB*) mRNA knockdown assessed using quantitative real time polymerase chain reaction (qPCR). Cells were transfected with polyplexes prepared using the advanced version of AIMS at Re=4,000, and different siRNA mixing concentration (0.05-0.4 mg/mL). Manually prepared polyplexes were also transfected for comparison purposes. DharmaFECT®2, a commercially available lipoplex, was used as positive control. Naked siRNA, mock chitosan and non-treated cells were used as negative controls.

ApoB mRNA knockdown reached 40-55% when produced *via* AIMS (Figure 4.7). Statistical analysis revealed no significant effect of mixing siRNA concentrations on gene knockdown. Compared to the in-line mixed polyplexes, manually prepared polyplexes resulted in slightly lower ApoB mRNA knockdown (~30-45%). These results are consistent with a previous study where CS/siRNA polyplexes achieved ApoB mRNA knockdown of ~50% in HepG2 when prepared manually at N:P 5 and siRNA concentration of 0.05 mg/mL (Alameh et al., 2010). Although manually prepared polyplexes at siRNA concentration of 0.2 mg/mL showed the lowest transfection efficiency (~30%), analysis of variance did not show statistical significance compared to other siRNA mixing concentrations. CS-based polyplexes achieved comparable knockdown efficiency to DharmaFECT®2 (Figure 4.7), independent of the mixing method. We have previously shown that manually prepared polyplexes achieve comparable knockdown efficiencies to DharmaFECT®2 but with lower toxicity (Alameh et al., 2012; Alameh et al., 2017; Jean et al., 2012b). Nanoparticle size and surface charge are cited in the literature to be important parameters for nanoparticle uptake and bioactivity (Nel et al., 2009; Son, Tkach, & Patel, 2000).

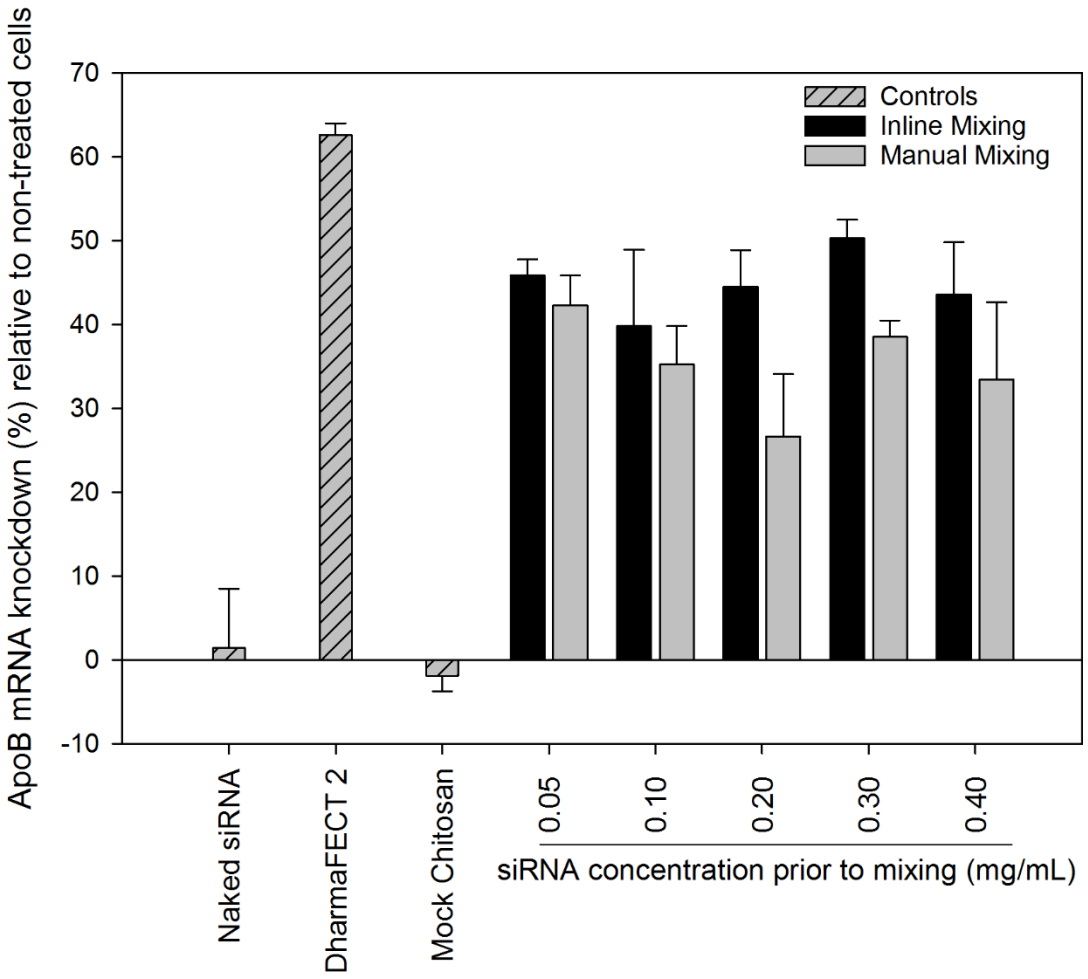

Figure 4.7 Bioactivity of In-line and manually mixed CS/siRNA polyplexes. HepG2 cells were transfected with either inline or manually mixed anti-ApoB CS/siRNA polyplexes at a final siRNA concentration of 100 nM/well. Apob mRNA knockdown was assessed by qPCR using geometric averaging of the most stable reference genes (GAPDH and B2M) and expressed relative to non-treated cells. Data represent the mean of two independent experiments (N=2) with two technical replicate per experiment (n=2). Analysis of Variance (ANOVA) was performed using the SigmaPlot 13.0 statistical package.

In our study, polyplex size correlated moderately (r^2= 0.376) with knockdown efficiency (Figure 4.8a), with smaller sized polyplexes inducing higher knockdown efficiency. This trend can be seen from results presented in Figure 4.4a and Figure 4.7 where in-line mixed polyplexes demonstrate a smooth reduction in size with decreasing siRNA concentration and a generally better efficiency

at knocking down ApoB mRNA *in vitro*. The slight correlation suggests that uptake of smaller polyplexes could be higher, but determining if it is really the case would require further investigation and is beyond the scope of this study. Interestingly, our results also indicate that ZP does not correlate (r^2= 0.060) with improved bioactivity (Figure 4.8b). The slight correlation between size and knock-down as well as the lack of correlation between ZP and knock-down could be explained by serum dependent size stabilization of polyplexes occurring through rapid protein corona formation, which will also rapidly alter their surface charge and ZP (Albanese & Chan, 2011; Nimesh et al., 2010a). The aggregation due to protein binding upon transfection, might either inhibit, or facilitate the cellular uptake (Saptarshi, Duschl, & Lopata, 2013). It is worth mentioning that ZP was measured in low ionic strength (1mM) buffer and not at ~ 150 mM as in culture medium, and it could contribute to the lack of correlation between ZP and knock-down. Additionally, the somewhat limited range of both size and ZP values tested could also explain the limited correlations observed.

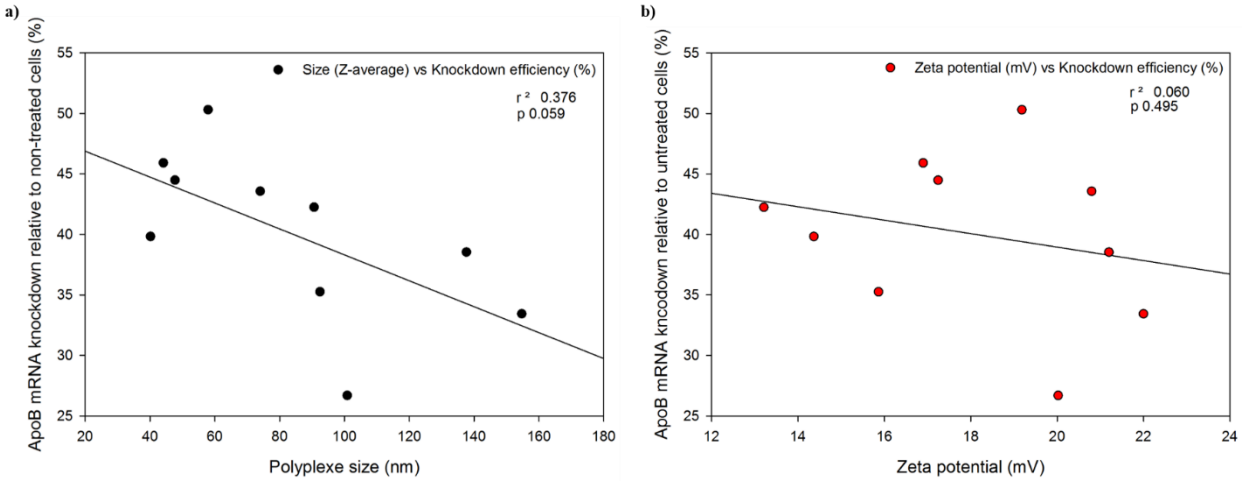

Figure 4.8 Correlation between bioactivity and physico-chemical parameters of in-line and manually prepared polyplexes. a) correlation between ApoB mRNA knockdown (average) and polyplexe size (average). b) correlation between ApoB mRNA kncockdown (average) and polyplexe zeta potential (average). Regression and pearson correlation analysis was performed with SigmaPlot 13.0 statistical package.

Altogether our data show that AIMS is able to produce small sized polyplexes that retain their physico-chemical integrity and bioactivity as demonstrated by equal or superior performance to manually prepared polyplexes.

4.7 Conclusion

A fully automated in-line mixing platform was developed for production of large batches of CS-based polyplexes to overcome the drawbacks of conventional manual mixing methods that are not only poorly controlled but also restricted to small volumes. This scaled-up platform addresses the risk of batch to batch inter-user and intra-user variability, resulting in a controlled quality of large quantities of polyplexes. While manual mixing cannot practically deliver more than 2 mL of product, polyplexes prepared *via* AIMS are expected to have similar physico-chemical properties and bioactivity when produced in batch sizes up to a litre, 10 L, and 100 L. Size and polydispersity of CS/siRNA polyplexes can be simply controlled *via* the mixing flow rate and mixing concentrations. We found that by increasing NA concentration, Z-average diameter and the PDI of the polyplexes increase. Moreover, AIMS is capable of production of smaller and more homogeneous CS/siRNA polyplexes using a non-laminar flow regime compared to manual polyplexes. The established AIMS allowed production of well-defined CS/siRNA polyplexes with maintained bioactivity at every siRNA mixing concentration tested, demonstrating the suitability of this system for large scale production of polyplexes intended for pre-clinical and clinical applications.

4.8 Acknowledgements

The authors thank Dr. R. K. Panicker for help with Transmission Electron Microscopy, and M. Bail for assistance in qPCR experiments. This research was supported by the Natural Sciences and Engineering Research Council (NSERC) and ANRis Pharmaceuticals Inc.

4.9 Supplementary material

4.9.1 Investigation of the impact of mixing in the acceleration phase of the peristaltic pump

Mixing CS and NA solutions using AIMS can take place in two different scenarios: either 1- during and after the acceleration phase of the peristaltic pump, or 2- only after the acceleration phase of the pump. In order to better examine the differences between the properties of polyplexes produced in these two scenarios, ODN/CS polyplexes were prepared at the target flow rate of 150 mL/min

in both scenarios, at four different starting concentrations of ODN solution (0.1 mg/mL, 0.2 mg/mL, 0.3 mg/mL, 0.4 mg/mL). Z-average diameter and PDI of the polyplexes were recorded using DLS and shown in Figure 4.9. According to our calculations, for the type of peristaltic pump we used (Masterflex L/S Digital Drive), the acceleration period (the time it takes from stationary to reach the maximum flow rate, 150 mL/min = 2.5 mL/s) is 610ms. During the acceleration phase of the pump, mixing takes place in different speeds. On the other hand, mixing after the acceleration period takes place only at the target speed. In order to avoid collecting the polyplexes during the acceleration phase, water was first pumped to the waste container, before switching (using a pinch valve) to the collection vessel once the final target speed was reached.It was shown that at a given concentration, mixing of CS and ODN solutions only after completion of the acceleration phase of the pump produced smaller and more homogenous polyplexes compared to polyplexes produced both during and after the acceleration phase (Figure 4.9). This is consistent with the influence of speed on polyplex size (as shown in Figure 4.3), since mixing in the acceleration phase of the pump involves a range of uncontrolled speeds with direct impact on the size and PDI of these polyplexes.

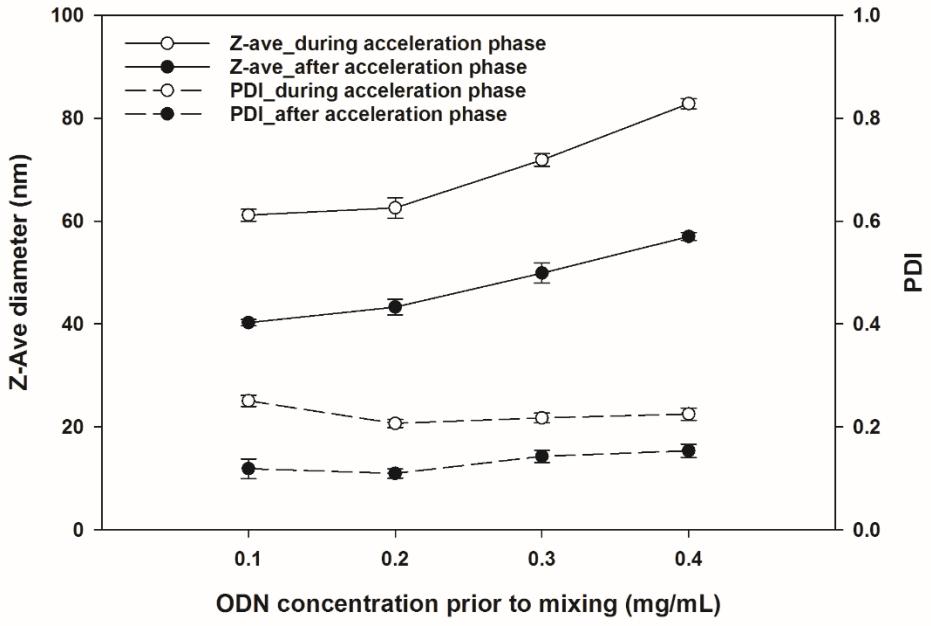

Figure 4.9 Influence of mixing during and after (white circles), and only after (black circles) the acceleration phase of the peristaltic pump on size and PDI of ODN/CS polyplexes produced using AIMS. In-line mixing was done using 2 mL of CS and 2 mL of NA at 150 mL/min. Error bars represent standard deviation between the duplicates.

4.9.2 Calculation of overlap concentration (C*) for pDNA, siRNA, CS solutions

The overlap concentration of a polymer is expressed as shown in the equation below:

$$C^* = \frac{3M}{4\pi N_A \times R_g^3} \qquad \text{Eq. 4.1}$$

where M is the Molar Mass of polymer, N_A stands for Avogadro's number, and Rg is the radius of gyration of the polymer. While the molecular weights for different polymers (pDNA, siRNA, and CS) are known, the challenge is to estimate the Rg value of each polymer in order to calculate the C*.

4.9.2.1 pDNA overlap concentration

The plasmid pEGFPLuc used in this study comprises 6.4 kbp, with a corresponding molar mass of 3.94 MDa. Latulippe et al. reported the Rg values of plasmid DNA of various sizes, some with molar masses close to that of pEGFPLuc used in this study (Latulippe & Zydney, 2010). More specifically, they reported Rg values of 102 ± 2 and 117±3 nm for plasmids of 5.76 and 9.80 kbp, respectively. From a simple linear interpolation between the Rg values of these two plasmid DNA we estimated the Rg value of pEGFPLuc (6.4kbp) to 105nm. C* was calculated accordingly: 1.3 mg/mL.

4.9.2.2 siRNA overlap concentration

In this study, siRNA with 21bp, and molar mass of 13,974 Da was used. Pavan et al. reported a Rg value 1.91nm for a 21bp siRNA (Pavan et al., 2010). C* was calculated accordingly: 790 mg/mL.

4.9.2.3 Chitosan overlap concentration

Rg of chitosan depends on its DDA and Mw. Relatively few studies have derived relations to estimate the Rg value of chitosan molecules for given DDA and Mw (Brugnerotto, Desbrieres, Roberts, & Rinaudo, 2001; Rinaudo, 2006). Brugrenotto et. al. correlated Rg values (obtained by Static Light Scattering) for different chitosan molecules (different DDA and Mw) in a Mark–Houwink equation, Rg=kMw^a (Brugnerotto et al., 2001). The chitosan used in this study had a Mn=10,000 Da, Mw=15,000Da, DDA= 92%. Mark–Houwink parameters (k and a) for the exact DDA of 92% were applied to estimate the Rg of a 15,000Da chitosan. Rg (nm) = 0.062 $(15000)^{0.546}$= 11.8 nm. C* was calculated accordingly: 3.6 mg/mL.

4.9.3 Verification of the effect of overlap concentration (C*) on the maximum NA starting concentration to produce homogeneous small sized polyplexes

The data obtained for manually mixed CS92-10-based polyplexes indicate that the maximum mixing concentration for siRNA and pDNA to produce homogeneous small sized polyplexes is 0.2, and 0.1 mg/mL, respectively. As discussed, since the C* value for pDNA and chitosan 92-10 are relatively low and close to each other, the maximum concentration of pDNA to prepare homogeneous small sized polyplexes is limited. However, C* for siRNA is significantly higher, thus we hypothesized that if a CS with a higher overlap concentration C* is used, it would be possible to mix with siRNA at higher concentrations before a sharp increase in size and PDI of polyplexes occurs. In other words, a lower molecular weight chitosan should favor production of homogeneous small sized polyplexes at higher siRNA starting concentrations. In order to further investigate the impact of C* on the highest possible mixing concentrations, a smaller CS but with the same DDA (Mn= 2 kDa, DDA=92%) was chosen to be mixed with siRNA at elevated concentrations.

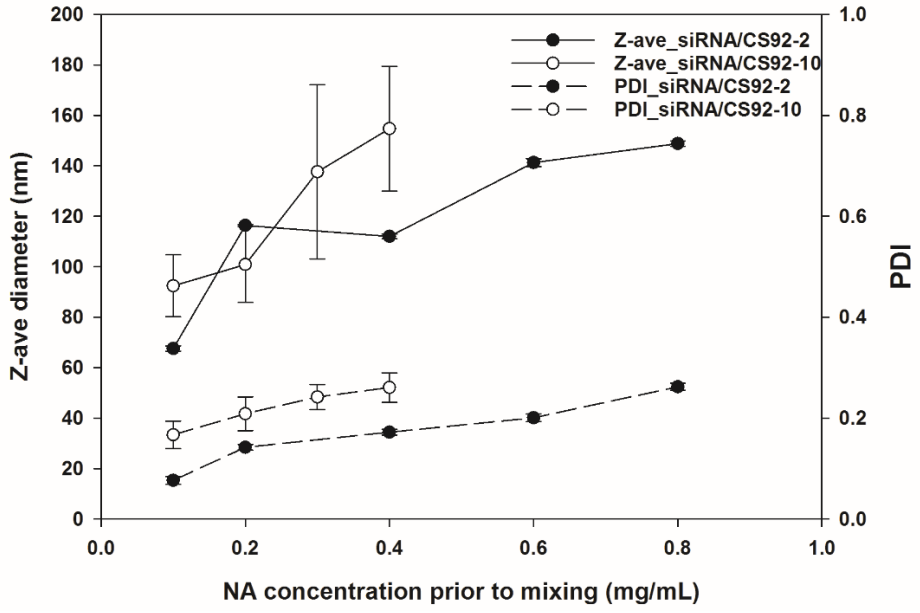

Figure 4.10 Influence of chitosan C* on size and PDI of siRNA/CS polyplexes produced manually. Two CS with the same DDA (92%), but different molecular weights (10 kDa and 2 kDa) were tested

As shown in Figure 4.10, while the maximum siRNA concentration for preparation of homogeneous small sized CS/siRNA polyplexes is 0.2 mg/mL using CS92-10, this concentration for CS2-10 is 0.6 mg/mL. This suggests that the molecular weight and consequently C* of CS solution have a direct influence on the maximum possible starting concentration of nucleic acid for production of homogeneous small sized polyplexes. Note that manual mixing of CS92-10 at siRNA starting concentration of 0.3 mg/mL results in irreproducible size records with PDI>0.2. Also, mixing CS92-2 at siRNA starting concentration of 0.8 mg/mL is associated with limited macroscopic flocculation.

4.9.4 MIQE compliant qPCR

4.9.4.1 Transcript structure analysis

The analysis of the region containing the amplicon was performed using m-fold (version 2.3). The default setting of 60ºC was selected to mimic the temperature at which qPCR is performed and only the most stable structure was analyzed. No secondary structures hindering the amplicon were detected.

4.9.4.2 Details of the qPCR assay

The sequence of the forward, reverse and the probe for each assay used in this manuscript is listed in Table 4.1. The NCBI ref_sequence ID and the position of the forward, reverse, the probe and the anti-ApoB siRNA relative to the ref_sequence is also given.

4.9.4.3 Efficiency of the assays

Assay efficiency was determined using the standard curve method. In each experiment, a 6 log 10-fold dilution curve was constructed by plotting the quantification cycle (Cq) *versus* Log complementary DNA (cDNA) concentration and linearly regressed to fit the data. PCR reaction efficiency was estimated by using $E = 10^{\left(-\frac{1}{\text{slope}}\right)} - 1$. The efficiency of all assays for the two experiments (shown in

Table 4.2) was within the acceptable range of 95-105%. The inter-experiment variability or difference in efficiency was ≤ 3% indicating reproducibility and robustness of the assays.

Table 4.1. The sequence of the forward, reverse and the probe for each assay used

Assay name		Sequence (5' to 3')	Position	Ref_Seq
IDT_ApoB	Forward	GAC ACA CCA AAG ATC AGC	996-1016	NM_000384.2
	Reverse	GAG AGT CTT CAA AAC AGC TTC G	1115-1094	
	Probe	/5'6-FAM/CAC CAA ATC/ZEN/CAC ATC ACC TCC AAA GC/3'IABkFq	1064-1089	
UPL_ApoB	Forward	GAC GAC TTT TCT AAA TGG AAC TTC TAC	12177-12203	
	Reverse	CTC AGT TTT GAA TAT GGT GAG TTT TT	12254-12229	
	Probe	TCCTCTCC (UPL probe #55, Cat #04688520001)		
IDT_GAPDH	Forward	ACA TCG CTC AGA CAC CAT G	173-191	NM_002046.5
	Reverse	TGT AGT TGA GGT CAA TGA AGG G	315-294	
	Probe	5'6-FAM/AAG GTC GGA/ZEN/GTC AAC GGA TTT GGT C /3'IABkFq	201-225	
ABI_B2M	Forward	Information not publically available. TaqMan Assay ID: Hs00984230_m1		NM_004048.2
	Reverse			
	Probe			
ApoB siRNA	Sense	GUC AUC ACA CUG AAU ACC AAU	10167-10187	NM_000384.2
	Anti-sense	AUU GGU AUU VAG UGU GAU GAC AC	10187-10165	

Table 4.2 Assay efficiency for the two experiments

Assay name	Experiment 1					Experiment 2					Difference (%) in E between experiments
	E (%)	Standard Error E	R^{sqrt}	Slope (error)	Intercept (error)	E (%)	Standard Error E	R^{sqrt}	Slope (error)	Intercept (error)	
IDT_ ApoB	95.2	0.024	0.997	-3.4413 (0.0633)	17.318 (0.1205)	95	0.0228	0.996	-3.458 (0.0610)	19.779 (0.1044)	0.2
UPL_ ApoB	96%	0.0178	0.998	-3.4214 (0.0461)	17.985 (0.0789)	95	0.0111	0.999	-3.455 (0.0296)	19.651 (0.0506)	1
IDT_ GAP DH	102.2	0.0255	0.996	-3.2685 (0.0585)	22.291 (0.1001)	99.5	0.0205	0.997	-3.332 -0.0495	22.341 (0.0848)	3
ABI_ β2M	96.4	0.0135	0.999	-3.4112 (0.0348)	19.997 (0.059)	96.4	0.012	0.999	-3.412 (0.0310)	20.439 (0.0531)	0

4.9.4.4 Reference gene stability

The reference genes used in this study viz. human glyceraldehyde-3-phosphate (GAPDH) and human β-2 microglobulin (β2M) were selected from a pilot study where the stability of references genes was assessed using a panel of 10 reference genes and 8 treatment conditions including DharmaFECT®2- lipoplexes, chitosan based polyplexes prepared at different DDA and N:P ratios, concentration of chitosan/well and cell lines (Alameh et al., 2017). In this study, the stability of GAPDH and β2M was re-validated using the geNorm statistical package. The M score for both reference genes, computed from all treatment conditions viz. in-line (0.05 to 0.4 mg/mL), manual (0.05 to 0.4 mg/mL), DharmaFECT®2, Mock chitosan, naked siRNA and non-treated, was ≤ 0.25. As a consequence, these two reference genes were deemed stable. The suitability of these reference genes was not only decided based on their stability *vis-a-vis* treatment conditions but also to the fact that they are on two different cellular pathways and cannot be co-regulated.

4.9.4.5 RNA quality, integrity, and quantity

Total RNA quality, integrity, and quantity was assessed using the UV-Vis (Nanodrop 8000), Agilent Bioanalyzer 2100 and Qubit assay, respectively.

The results of one technical replicate from each experiment is shown in Table 4.3. The UV 260/280, 260/230 and 340 ratios were above 2, 1.8 and equal to 0 respectively indicating high purity and absence of contamination with guanidium salts and/or other compounds *i.e.* silica. RNA integrity of all extracted samples was above 9, indicative of intact RNA.

Table 4.3 Total RNA quality, integrity, and quantity for the two experiments

Sample/parameter	Experiment 1					Experiment 2				
	[RNA] (ng/µL)	UV 260/280	UV 260/230	UV 340	**RIN**	[RNA] (ng/µL)	UV 260/280	UV 260/230	UV 340	**RIN**
InL 0.05 mg/mL	121.5	2.1	1.9	-0.007	**9.6**	183.8	2.13	1.97	-0.061	**9.8**
InL 0.10 mg/mL	114.7	2.1	1.9	-0.012	**9.6**	149.8	2.12	1.97	-0.027	**9.7**
InL 0.20 mg/mL	134	2.1	2	0.006	**9.8**	195.2	2.09	1.91	-0.042	**9.8**
InL 0.30 mg/mL	150.1	2.1	1.4	-0.029	**9.8**	192	2.11	1.97	0.011	**9.8**
InL 0.40 mg/mL	123.9	2.1	1.9	-0.011	**9.7**	168.4	2.12	1.99	0.003	**9.8**
Man 0.05 mg/mL	60.2	2.1	1.9	-0.083	**9.8**	142.8	2.13	2	-0.004	**9.7**
Man 0.10 mg/mL	109.1	2.1	1.9	-0.043	**10**	160.2	2.12	2.02	0.016	**9.7**
Man 0.20 mg/mL	129.3	2.1	1.9	-0.004	**9.9**	159	2.12	1.86	-0.06	**9.7**
Man 0.30 mg/mL	124.7	2.1	1.9	0.023	**9.9**	169.6	2.12	1.94	-0.039	**9.8**
Man 0.40 mg/mL	134.1	2.1	2	-0.013	**9.9**	214	2.1	1.97	-0.049	**9.8**
DharmaFECT® 2	113.9	2.1	2	0.032	**10**	127	2.11	1.96	-0.055	**10**
Naked siRNA	133	2.12	2.01	0.01	**10**	163	2.08	1.9	0.02	**9.5**
Mock chitosan	127.2	2.12	1.88	-0.097	**9.9**	120.8	2.12	1.94	-0.006	**9.9**
Non-treated cells	138.9	2.1	2.1	0.03	**9.9**	176.6	2.12	1.95	-0.006	**9.8**

4.9.4.6 Controls

No reverse transcription control (NRTC) and no template control (NTC) were used as controls. There was no amplification in controls.

4.9.4.7 Comparison between the two assays used

The two probes used in this study detect the ApoB mRNA at two different regions. The Integrated DNA (IDT) and Universal Library (UPL) probes detect and amplify sequences on the ApoB cDNA that are around 10kbp apart. The IDT and UPL assays are located at the 5’ and 3’ sides of the ApoB mRNA respectively. The data in Figure 4.11 show that the two assays were in agreement indicating a true knockdown of the target gene, demonstrating that the knockdown assay is not dependent on the probe position.

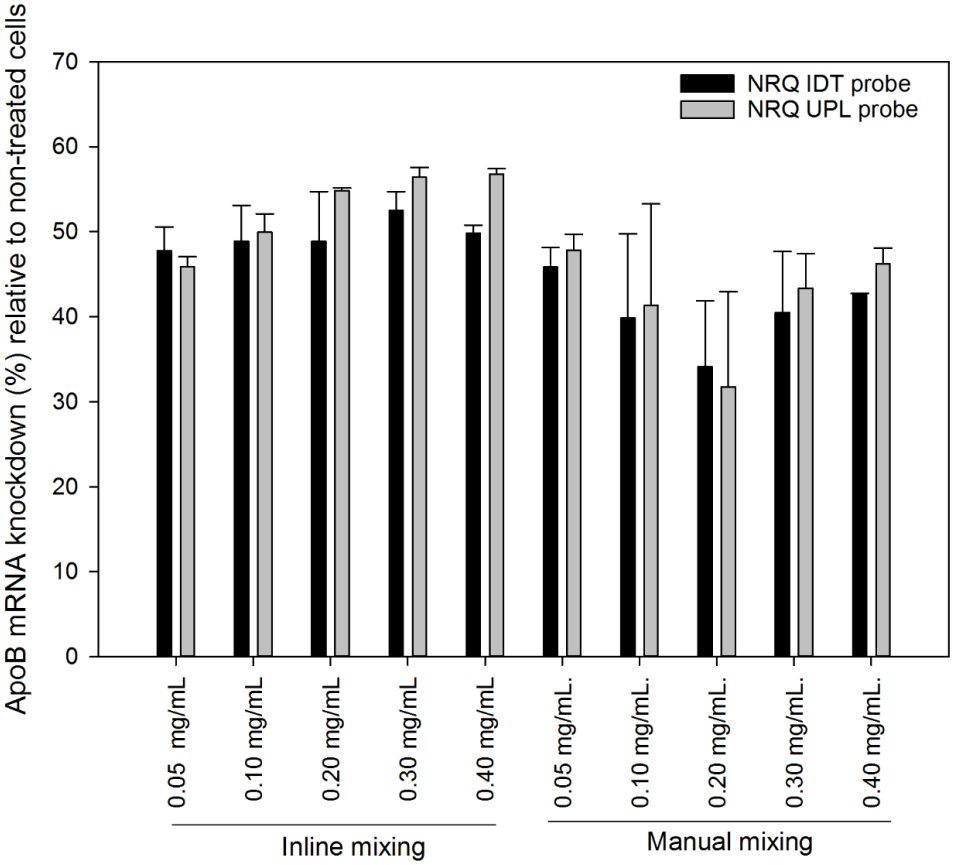

Figure 4.11 Comparison of knockdown detected by two different primer-probe pairs targeting the ApoB mRNA. The IDT primer-probe pair detect the ApoB mRNA at 996-1115 (amplicon 120 bp). The UPL primer-probe pair (#55) detect the ApoB mRNA at 12177-12254 (amplicon 78 bp).

CHAPTER 5 PURIFICATION AND MODIFICATION OF CHITOSAN-BASED POLYPLEXES USING TANGENTIAL FLOW FILTRATION

5.1 Objective

The first objective of this chapter is to establish TFF technique and optimize its operational conditions for purification and concentration of CS-based polyplexes. The second objective is to develop HA-coated complexes, upon purification of polyplexes, to enhance their hemocompatibility for intravenous clinical applications.

5.2 Summary

Chitosan(CS)-based polyplexes are produced by electrostatic association of positively charged CS and nucleic acids (NAs) upon mixing, while CS is in excess *versus* NA. The final solution includes polyplexes with positive surface charge as well as unbound CS molecules. However, due to interactions with negatively charged blood components, the unbound CS as well as the positive surface of polyplexes limit the applicable dosage of these therapeutics for intravenous (IV) administrations. Hence, clinical application of this technology requires the development of hemocompatible formulations for IV delivery systems. One approach to tackle such drawbacks is to purify (remove the unbound CS), then coat the polyplexes with hyaluronic acid (HA) through electrostatic interactions between the anionic groups of HA and the cationic groups of CS on the surface of the polyplexes. Here, we introduced tangential flow filtration (TFF) for purification of CS-based polyplexes. Using 100 kDa mPES hollow fibers, TFF operational conditions were established at trans-membrane pressure (TMP) of 0.9-1.0 psid, and relatively low shear rates of 7000-11000 s^{-1}. Thereafter, the optimal number of diafiltration volumes (DV) for purification of polyplexes was established at 5 DV. We demonstrated that at shear rate of 7000 s^{-1} (TMP=0.9 psid), 98% of the unbound CS was removed, while 81% of the polyplexes were recovered. No marked change in physico-chemical properties and morphology of polyplexes was observed post-diafiltration. Purified CS/siRNA eGFP polyplexes were then coated by a library of HA molecules with different molecular weights and degrees of sulfation, at different phosphate to carboxyl ratios (C:P). Our data revealed that C:P$\geq$ 2 is needed to effectively coat the polyplexes and sign reversal of the surface of complexes. It was also demonstrated that regardless of C:P ratio, addition of a high molecular weight HA (866 kDa) results in macroscopic flocculations. Furthermore, we

showed that low molecular weight (10 kDa and 12 kDa) HA-coated CS/siRNA complexes have equivalent or increased silencing efficiency of eGFP in H1299 cells, with improved hemocompatibility as compared to uncoated polyplexes. Finally, it was shown that although both sulfated and non-sulfated HAs resulted in small sized, homogenous, and bioactive coated complexes, sulfated HA molecules presented higher stability during filtration process, indicating their stronger binding affinity to polyplexes. Development of these modified formulations represent an important step forward to the clinical use of CS-based complexes for IV applications.

5.3 Introduction

In the past decade, chitosan (CS)-based formulations have gained increasing interest for safe delivery of nucleic acids (NAs). We have already demonstrated reproducible production of CS/pDNA and CS/siRNA polyplexes using an Automated In-line Mixing System, AIMS (Tavakoli Naeini, Soliman, Alameh, Lavertu, & Buschmann, 2017). CS/NA polyplexes are produced by electrostatic-mediated association of CS and NA solutions upon mixing, while CS is used in excess *versus* NA, typically, 5X higher in molar charge concentration (Alameh et al., 2017; Jean et al., 2012b; Jean et al., 2009; Lavertu et al., 2006; Tavakoli Naeini et al., 2017; Thibault et al., 2010b; Veilleux et al., 2016). Since CS is in excess, a significant portion of this molecule remains free (unbound to polyplexes) in the solution. Despite the potential of these polyplexes *in vivo* (Alameh et al., 2017; Corbet et al., 2016; Gao et al., 2014; Howard et al., 2006a; Nielsen et al., 2010; Yang et al., 2015), intravenous (IV) administration remains problematic due to hemolysis and haemagglutination of erythrocytes in contact with both bound and unbound CS (Carreno-Gomez & Duncan, 1997). CS binds to the red blood cells (RBCs) and causes haemagglutination, even at very low concentrations (Rao & Sharma, 1997). The interactions between CS molecules and the anionic charges on the surface of the erythrocytes induces stresses to the cell membranes which eventually leads to their rupture (Carreno-Gomez & Duncan, 1997; Rao & Sharma, 1997). Thus, CS-based formulations need to be modified before transferring for IV administrations of especially higher doses. Modification of polyplexes involves neutralization or coating the polyplexes with another molecule in order to eliminate the interactions with blood cells, and finally enhance the pharmacokinetics of polyplexes (Buschmann et al., 2013). Several surface modification approaches have been suggested in literature (Buschmann et al., 2013). One approach pursued here is to coat the CS/NA polyplexes using hyaluronic acid (HA) through electrostatic interactions between the

cationic groups of CS and the anionic groups of HA. HA is a highly hydrophilic, non-toxic and hemocompatible glycosaminoglycan which is widely distributed throughout extracellular matrices. Another important feature of HA which nominates this molecule as a great therapeutic targeting agent is that it binds to the CD44 receptor, which is overexpressed in a wide variety of cancer cells (Dosio et al., 2016; Karbownik & Nowak, 2013; Platt & Szoka, 2008). HA is available in a wide range of molecular weight (Karbownik & Nowak, 2013; Tripodo et al., 2015). The carboxyl groups on the D-glucuronic acid residues have pKa value ~3-4, hence, these functional groups are ionized at physiological pHs (Dosio et al., 2016). HA can also be modified by the insertion of ionic sulfate ($SO3^-$) groups in the polysaccharide chain. Sulfated HAs have been reported with different degrees of sulfation, ranging from 1 to 4 sulfate groups per disaccharide (Magnani et al., 1999). Stronger binding affinity, and slower degradation of sulfated HA by hyaluronidase was reported in the literature (Feng et al., 2017; Magnani et al., 1999). HA chains (either non-sulfated or sulfated) can simply form electrostatic bonds with CS molecules on the surface of the polyplexes to improve their pharmacokinetics and hemocompatibility. However, before CS-based polyplexes can be used for further surface modifications, they must be purified. Purification of CS-based polyplexes relies on elimination of the unbound chitosan molecules from the polyplex solution. Appropriate purification techniques are required to effectively purify the polyplexes post-mixing. Conventional techniques used for purification of nanoparticles (NPs) such as ultrafiltration, dialysis and gel filtration are associated with several drawbacks when it comes to their application in purification of gene loaded NPs. These methods are mainly used for “hard” NPs such as gold NPs, and cannot be easily applied to “soft” NPs (Robertson et al., 2016). The conventional techniques are either invasive, expensive, time-consuming, relatively inefficient, and more importantly difficult to scale-up. Ultracentrifugation is associated with irreversible aggregation of NPs due to centrifugal forces (Dalwadi et al., 2005), and becomes much more problematic when transitioning from small scale to large scale purifications (Correa et al., 2016). Dialysis involves the risk of product loss during manual manipulations, requires a large amount of exchange buffer which produces large volumes of aqueous waste, and can take up to several days (Sweeney et al., 2006). Moreover, due to the lengthy process, dialysis can result in release of NP’s payload (Dalwadi et al., 2005). Gel filtration is relatively a faster process; however, a small volume of NP solution can be processed at a time. Moreover, irreversible adsorption of molecules onto the column and not a perfect selectivity of small and bigger NPs can restrict the application of this approach for purification of drug or gene-

loaded particulates (Dalwadi et al., 2005). Tangential Flow Filtration (TFF), on the other hand, overcomes the main limitations of the conventional techniques. By re-circulation of the fluid parallel to the surface of the filter, TFF inhibits built-up cake on the surface of the membrane. During TFF, molecules smaller than membrane pores pass through the membrane (generating the permeate) and larger molecules are retained and re-circulated in the system (generating the retentate) until the desired concentration is reached. Diafiltration is a TFF process that involves washing out the original buffer by continuously adding a new buffer to the sample at the same rate as permeate is being removed from the system (L. Schwartz, 2003). As a membrane-based method, pore size dictates the retention of particles of interest in the sample during re-circulation, thus, diafiltration offers to combine purification and size separation into a single process. Due to simple equipment requirements and the scalability of the technique, diafiltration can be performed quickly and conveniently (Sweeney et al., 2006). Another important advantage of diafiltration is that the sample could be concentrated in the same system, minimizing the risk of sample loss or contamination (Limayem et al., 2004). Diafiltration has been used in separation of proteins that differ by only a single charged amino acid residue (Ebersold & Zydney, 2004), purification of polymeric nanocapsule suspensions (Limayem et al., 2004), gold NPs (Sweeney et al., 2006), silver NPs (Anders et al., 2012), NP suspension (Dalwadi et al., 2005), PEGylated NPs (Dalwadi & Sunderland, 2007), and drug loaded layer by layer complexes (Correa et al., 2016). However, the application of diafiltration for CS-based polyplexes has not been reported yet. Here, we specifically describe, for the first time, the approach to adopt and optimize the TFF technique for processing CS-based polyplexes. Optimization of a TFF process was executed by examination of the interdependence of TMP, shear rate and permeate flux, which is known as TMP scouting (Cross flow filtration Method Handbook, 2014; Millipore, 2013). Afterwards, the capability of TFF for concentration and diafiltration of these polyplexes in the established operational conditions is demonstrated. Thereafter, diafiltered polyplexes were coated by different HA molecules to deliver a layer by layer complex. Finally, to highlight the compatibility of TFF technique to safely process CS-based polyplexes, bioactivity and hemocompatibility of the purified CS/siRNA polyplexes, as well as HA-coated complexes were examined.

5.4 Materials and Methods

5.4.1 Materials

Chitosan was obtained from Marinard. Custom synthesized siRNA targeting EGFP (siRNA EGFP) contains sense sequence of 5' GAC GUA AAC GGC CAC AAG UUC 3' and antisense 5' ACU UGU GGC CGU UUA CGU CGC 3' (Howard et al., 2006a) was obtained from GE. Custom made double stranded oligodeoxynucleotide (dsODN, 21 bp) encoding the same sequences and mimicking siRNA EGFP physic-chemical properties was obtained from Integrated DNA Technologies Inc, Coralville, IO. The commercially available liposome, DharmaFECT 2 was from Dharmacon RNAi Technologies. A human non-small lung carcinoma (H1299) cell line stably expressing enhance green fluorescence protein (eGFP+ H1299) was donated by Dr Jorgen Kjems (AARHUS University, Denmark) upon approval of Dr Anne Chauchereau. Stanbio hemoglobin standards (Cat #SB 0325 006) was from Fisher Scientific. RPMI 1640 (Cat #31800-022), Fetal Bovine Serum (FBS, Cat #26140), GlutaMAX 100X (Cat #35050-061) were from ThermoFisher Scientific. Trehalose dihydrate (Cat #T0167), L-histidine (Cat #H6034), triton X-100 (Cat #T8532), poly-L-Lysine hydrobromide (PLL, Cat #P1399), polyethylene glycol (PEG 8 kDa, Cat #P1458), orange II sodium salt (Cat #195235), 1N hydrochloric acid solution (Cat #318949), glacial acetic acid (Cat #338826), sodium acetate trihydrate (Cat #S7670), 1N sodium hydroxide solution (Cat #319511) were from Sigma Aldrich (Cat #D5758). DC protein assay kit (5000111), and fetal bovine serum (FBS, Cat #26140) were from LifeTechnologies. Modified polyethersulfone (mPES) MWCO of 100 kDa (part #C02-E100-05-N) and 300 kDa (C02-E300-05-N) were obtained from Spectrum Labs, MicroKros Class. Non-sulfated sodium hyaluronate (MW=866 kDa, Cat #HA1M-1), Non-sulfated sodium hyaluronate (MW=10 kDa, Cat #HA10K-1), Non-sulfated sodium hyaluronate (MW= 40 kDa, Cat #HA40K-1), was from Lifecore Biomedical. Sulfated sodium hyaluronate (MW=184 kDa with degree of sulfation=2.0, Cat # FP-RD009-26), Sulfated sodium hyaluronate (MW=154 kDa with degree of sulfation=1.0, Cat # FP-RD009-27), Sulfated sodium hyaluronate (MW=148 kDa with degree of sulfation=0.6, Cat # FP-RD009-29), and Sulfated sodium hyaluronate (MW=12 kDa with degree of sulfation=1.4, Cat # FP-RD009-33) were from HTL Biotechnology.

5.4.2 Preparation of CS, ODN, and siRNA formulations for mixings

ODN ApoB, and siRNA ApoB stock solutions were prepared and characterized by UV spectrophotometry, then diluted to 200 µg/mL with RNase/DNase free water, as well as sterile filtered trehalose and histidine (pH 6.5) solutions for having final concentration of 0.5% w/v and 3.5mM, respectively (these are optimum concentrations of excipients for freeze-drying and stability of complexes over time that have been established within our group (Veilleux et al., 2016)). Commercial chitosan was first deacetylated to 92% using concentrated sodium hydroxide and was depolymerized to Mn=10 kDa using nitrous acid, as previously described (Lavertu et al., 2006). It has been repeatedly shown that the 10 kDa chitosan with DDA of 92% (CS92-10) form stable polyplexes with bigh transfection efficiency, when prepared at molar ratio of CS amine to NA phosphate ratio of 5 (N:P=5). Number-average molecular mass (Mn) as well as degree of deacetylation (DDA) of CS were confirmed by gel permeation chromatography multi-angle light scattering (Nguyen et al., 2009), and 1H NMR (Lavertu et al., 2003), respectively. CS stock solution was prepared at 5 mg/mL from dry powder dissolved in 28 mM HCl overnight at room temperature (RT). Dry HA was dissolved in DNase/RNase free water at RT, to a stock solution concentration of 1 mg/mL. CS and HA stock solutions were then sterile filtered, and diluted with DNase/RNase free water, as well as excipients (trehalose and histidine) for the target N:P and C:P ratios, respectively.

5.4.3 Preparation of polyplexes by in-line mixing

CS/ODN and CS/siRNA polyplex solution were produced at N:P=5 *via* the advanced version of Automated In-line Mixing System (AIMS) with Re=4000 (300 mL/min), tubing size=1/16” (LS14) as described by Tavakoli *et al.* (Tavakoli Naeini et al., 2017).

5.4.4 Preparation of HA-coated polyplexes by manual mixing

HA-coated polyplexes were formed by adding HA to diafiltered polyplexes at carboxyl to phosphate ratio (C:P) of 1.0, or 1.5, or 2.0, or 3.0. HA was added to the uncoated diafiltered polyplexes in a HA:polyplex volumetric ratio of 1:2. Manual mixing was done by pipetting up and down of the final solution for approximately 10 times.

5.4.5 Preparation of HA-coated polyplexes by in-line mixing

HA-coated polyplexes were formed by adding HA to diafiltered polyplexes at carboxyl to phosphate ratio (C:P) of 3 using the Automated In-line Mixing System, AIMS (Tavakoli Naeini et al., 2017). PharmaPure tubing, size=1/16” (LS-14) was used. In order to maintain the HA:polyplex volumetric ratio of 1:2, polyplexe solution was pumped at Re=2000 (150 mL/min), while the HA solution was dispensed at Re=1000 (75 mL/min).

5.4.6 Tangential flow filtration

Polyplex solution was transferred to a three-port cap 50 mL or 250 mL conical vessel (Corning), and connected to the TFF system (KrosFlo Research II*i*; Spectrum Labs). All connections were made using MasterFlex PharmaPure tubing, LS-14, size=1/8”. Filer modules composed of modified polyethersulfone (mPES), either 100 kDa or 300 kDa (MicroKros class by Spectrum Labs) were used. The digital TFF pump was programmed using LabView^{TM} software. Feed, permeate, and retentate pressure values were monitored and recorded by the transducers. The mass of permeate was also monitored using a programmed digital balance. The permeate flow rate (Qp) was being calculated in real time *via* the software (mass of permeate collected in every 20 seconds and converted to mL/min). Knowing the feed flow rate (Qf, set by the user), the retentate flow rate (Qr) was calculated by simple subtraction of Qp from Qf.

5.4.6.1 Normalized water permeability

Normalized water permeability measures the flow rate of water through the membrane under an applied trans-membrane pressure (TMP). Water flow rate gives an indication of the performance of a filter. By tracking the water permeability before and after filtration, it is possible to determine if a filter is clogged. Water permeability is usually carried out when the filter is new and after each use. Water permeability test was done by placing the permeate and retentate tubings into two separate waste containers. Permeate containers was placed on a digital balance that was programmed and recorded the mass every 20 seconds. The pump was first adjusted at 10 mL/min. Feed, retentate, and permeate pressures (Pf, Pr, Pp) were recorded by the transducers while all of the streamlines were open. TMP was then calculated in real time by the software; TMP=[(Pf+Pr)/2]-Pp . Upon stablization of the pressures, permeate flow rate was calculated by the the permeate mass collected in two minutes. The permeate flow rate was then translated in flux,

permeate flow rate in litre per hour per m^2 of the membrane, represented as litre/m^2/h (LMH). The calculated permeate flux corresponded to the recorded TMP. This was the first point of the normalized water permeability curve. The same procedure was done for four extra feed flow rates (20, 30, 40, and 50 mL/min). The slope of the generated curve defined the permeability of the membrane.

5.4.6.2 Equilibration of the hollow fibers prior filtration

Before use, every hollow fiber was equilibrated by passing 200 mL of diafiltration buffer through the membrane. Following steps were taken: both retentate and permeate streams were directed to a waste container, then the feed flux was adjusted at 200 to 300 LMH. Ratio of permeate to retentate flow rate was adjusted at 40%-50%. When half the buffer mixture has been flushed, the system was put in total recirculation mode (TRM) where the permeate and retentate lines were put back in the feed vessel, for 15 minutes.

5.4.7 Polyplex size, polydispersity, and surface charge analysis

Hydrodynamic size and polydispersity index of the produced polyplexes were measured using dynamic light scattering (Zetasizer Nano ZSP- ZEN5600, Malvern Instruments, Worcestershire, UK). Samples were diluted 4 folds by adding Milli-Q or RNase free water, then analyzed for three consecutive runs at 25°C. Zeta potential (ZP) measurements were made *via* laser Doppler velocimetry with the Malvern Zetasizer Nano ZS using folded capillary cells. For ZP measurements, samples were diluted by 8 fold to a total volume of 800 µL using RNase free water. Each sample was analyzed for three consecutive runs at 25°C. Electrophoretic mobility was calculated based on the Smoluchowski model.

5.4.8 Orange II assay

The concentration of free (unbound) CS in permeate and retentate solutions was determined by Orange II assay, established by Drogoz *et al.* (Drogoz, David, Rochas, Domard, & Delair, 2007). Polyplex samples were first ultracentrifuged (Optima MAX-E, TLA-110 fixed rotor, Beckman Coulter, Brea, CA, USA) for 45 min at 60000 rpm to spin down polyplexes. A supernatant aliquot of 20 µL was collected for each sample. Supernatants were diluted 20 fold with 50 mM acetic acid/sodium acetate buffer at pH 4.0. Supernatants from the permeate samples were not diluted as

they were already very dilute for CS. Orange II dye was prepared at a concentration of 1 mM in the acetic acid/sodium acetate buffer, and was added to supernatants, at a volumetric ratio of 1:32 (ensuring Orange II sulfonic acid groups are in excess relative to fully protonated CS amine groups during the assay), and mixed by vortexing. Samples were incubated 5 min to allow formation of CS/Orange II complexes, which were then precipitated by centrifugation (IEC Miromax, 891 rotor, Thermo Fisher Scientific, Waltham, MA, USA) at 15000 rpm for 45 min. 200 µL of the final supernatant (containing the unbound Orange II) was transferred to each well of a 96-well microplate and the absorbance was measured at 484 nm by Infinite M200 microplate reader (Tecan, Mannedorf, Switzerland). The free CS content was calculated using a calibration curve obtained from CS standard dilutions (in the range of 2-20 µg/mL) prepared in the same procedure as the samples.

5.4.9 Transmission electron microscopy imaging

Morphology of both uncoated, and HA-coated polyplexes (pre- and post-diafiltration) was studied using Transmission Electron Microscopy (TEM). On a carbon coated copper grid (200 mesh, Electron microscopy sciences), 5 µL drop of polyplex suspension was pipetted and allowed to evaporate for 30 minutes. Remaining solvent was removed by blotting using a filter paper. 5 µL of 2% phosphotungstic acid was placed on the grid. After 10 minutes the stain was removed as described above. The grid was washed two times with deionized water to avoid any salt contamination from the sample and air dried. TEM images were obtained using a Tecnai T12 electron microscope (FEI, Hillsboro, OR, USA) operating at 120 keV. For each sample four random areas on the grid were imaged at different magnifications.

5.4.10 Cell culture and transfection

eGFP^{+} H1299 cells were cultured in RPMI-1640 media supplemented 10% FBS, 1% GlutaMAX® and 500 µL/ mL of G418 antibiotic at 37°C in 5% CO2. For target gene knockdown cells were seeded in 96 well plates at a density of 7500 cells per well to reach 75-85 % confluence on the day of transfection. Prior to transfection, cells were washed once with 500 µL of warm Ca^{2+}/Mg^{2+} free PBS and replenished with complete RPMI-1640 adjusted at pH of 6.5 (5mM MES, 10 mM sodium bicarbonate, pH 6.5).

2.7µL of uncoated polyplexes, or 4 µL of HA-coated complexes were added to each well prefilled with 197.3 µL and 196 µL of transfection medium (pH 6.5), respectively, to reach a final siRNA concentration of 100 nM (0.268 µg of siRNA per well). In the case of purified CS/siRNA (uncoated polyplexes post-diafiltration), after 15 minutes, 2.7 µL of pure CS solution at 0.2 mg/mL was added to the designated wells for CS rescue (note that the addition of chitosan is to compensate the diafiltered free chitosan as it was previously shown to be necessary for endosomal release of the payload) (Thibault et al., 2010b). Cells were incubated for 24h, then medium was aspirated and replenished with 200 µL of culture medium. Cells were incubated again for extra 24 hours before analysis.

DharmaFect® 2/siRNA nanoparticles were prepared by diluting siRNA stock solution to 0.025 mg/mL (4 µM) in Opti-MEM® serum free media and complexed to the lipid component as per manufacturer recommendation; a volume of 6.4 µL of DharmaFect® 2 in 153.6 µL Opti-MEM® was used for complexation. Untreated and naked siRNA at a final concentration of 100nM were used as negative controls.

5.4.11 Assessment of *in vitro* silencing efficiency

Before analysis, eGFP^{+} H1299 cells were washed twice with 200µL ice cold Ca^{2+}/Mg^{2+} free PBS, lysed by addition of 200 µL of PBS containing 1% NP-40 and incubated at room temperature for 10 minutes to allow complete membrane disintegration. Lysates were homogenized by pipetting, a volume of 100 µL transferred in a black 96 well assay plate, and EGFP fluorescence measured at 510 nm using a TECAN Infinite® F-500 microplate system (Tecan, Mannedorf, Switzerland). Total protein content of the lysate was assessed using the BioRad DC Protein assay as per manufacturer recommendation. For assessment of gene knockdown, EGFP fluorescence was background subtracted and normalized to total protein content and expressed relative to non-treated cells. The assay was performed in duplicate.

5.4.12 Hemocompatibility assays

Hemolytic and hemagglutinative properties of both uncoated and HA-coated polyplexes were tested according to ASTM E2524 ("Standard Test Method for Analysis of Hemolytic Properties of Nanoparticles," 2013) and the method described by Evani and Ramasubramanian (Evani & Ramasubramanian, 2001), respectively. CS/siRNA polyplexes both pre- and post-diafiltration were

diluted to final siRNA concentrations of 0.1, 0.05, and 0.025 mg/mL. Also, the HA-coated polyplexes pre- and post-diafiltration were diluted to final siRNA concentration of 0.0667, 0.0335, and 0.0167 mg/mL. Negative controls included 40% w/v polyethylene glycol (PEG, 8 kDa), 20% w/v trehalose, 1 mg/mL HA, 0.1 mg/mL siRNA, and PBS pH 7.0. Positive controls included 10 mg/mL poly-L-lysine (PLL), and 10% v/v Triton X-100. Sodium citrate anti-coagulated whole blood (collected from a subject who had responded positively to an Informed Consent Form) was diluted with PBS pH=7.0 to adjust total blood hemoglobin concentration to 10 mg/mL. 100 µL of each test sample, positive or negative control was mixed with 700 µL of PBS pH 7.0, and 100 µL of diluted blood. The mixture was then incubated for 3 hours in a water bath at 37ºC. Supernatant was collected following centrifugation for 15 min at 800 g and used for colorimetric measurement of hemoglobin content (absorbance read at 540 nm) using Stanbio™ hemoglobin (Fisher, Product No SB 0325). A calibration (standard) curve was generated to calculate the hemoglobin concentration in the supernatant of each sample. The percentage of hemolysis for each sample was calculated as: $\%\,\text{Hemolysis} = \frac{\text{Hemoglobin conc.in the sample}}{\text{Hemoglobin conc.in diluted blood}} \times 100$. %Hemolysis above 5% indicates the test material causes damage to red blood cells. Hemagglutination was assessed qualitatively by incubation of 200 µL of each sample-PBS-diluted blood mixture for 3 hours at 37ºC in a round-bottomed (U-shaped) 96-well plate. Hemagglutination occurs if a granular or irregular ring of erythrocytes covered more than half of the well bottom.

5.4.13 Statistical analysis

Unless otherwise indicated, data were expressed as mean value ± standard deviation (n = 2). Sigma Plot 13.0 was used to generate curves and standard deviation calculations. Also, for hemocompatibility results, Sigma Plot 13.0 was used to generate the four parameter logistic (4PL) regression curves and calculate values.

5.5 Results and discussion

5.5.1 Establishment of TFF operational parameters

Choosing a membrane with appropriate retention characteristics is an important and integral part of the establishment of a membrane filtration to ensure high product yield. Here, we picked mPES membrane due to its advanced hydrophilic chemistry, almost neutral charge, and low binding

properties which yields higher product recovery. Working with nanoparticles, hollow fiber geometry was chosen as it has been demonstrated that the tubular geometry of hollow fibers is more beneficial than the cassette geometry for filtration of particles, which is attributed to migration of particles to the center of the hollow fiber where the flow velocity is the highest (tubular pinch effect) (Serway & Tamashiro, 2010). To assure complete retention of NPs, the molecular weight cut-off (MWCO) of the membrane should be 1/6th to 1/3rd of the molecular weight of the molecule to be retained: 3-6X rule (L. Schwartz, 2003). The closer the size of the particles to that of the membrane pores, the greater the risk for loss of some small particles (L. Schwartz, 2003). For retention of ODN/CS and siRNA/CS NPs (with a hydrodynamic size of 45-60 nm), and permeation of CS molecules (<5 nm), mPES membranes with MWCO of 300 kDa and 100 kDa were deemed to be suitable (according to the manufacturer, 100 kDa and 300 kDa have pores nominally in the range of 5-7 nm and 13-15 nm, respectively). Identical operational conditions were applied for both membranes (shear rate of 11000 s^{-1}, and TMP of 1.0 psid). CS/ODN polyplexes were diafiltered up to 5DV. Optical density at 260 nm for each solution (initial polyplex sample, retentate, permeate, and cleaning solutions after diafiltration) was recorded then translated to concentration. Based on the volumes, the mass of polyplexes present in each solution was calculated. Loss on membrane was then computed by simple subtraction. It was found that while using 100 kDa membrane it is possible to recover up to 85% of the polyplexes, 300 kDa membrane retains only 57% of polyplexes (Figure 5.1). It should be noted that in the applied conditions, 13% of the polyplexes were permeated using 300 kDa. Interestingly, this value was reduced to only ~1% when 100 kDa membrane was used. This suggest that due to bigger pore sizes, polyplexes can partially cross the 300 kDa membrane. Moreover, higher risk of deposition of polyplexes on the 300 kDa membrane surface was observed (25% of initial polyplexes). The significant drop in the normalized water permeability of 300 kDa membrane post filtration (to 62% of its original value) also advocats the high risk of penetration of polyplexes into the pores of the membrane. Normalized water permeability of 100 kDa membrane changed slightly to 89% of its original value, confirming very lower risk of clogging the membrane. Altogether of data, 100 kDa membrane is a better pick for filtration of CS-based polyplexes with the size range of 45-50 nm.

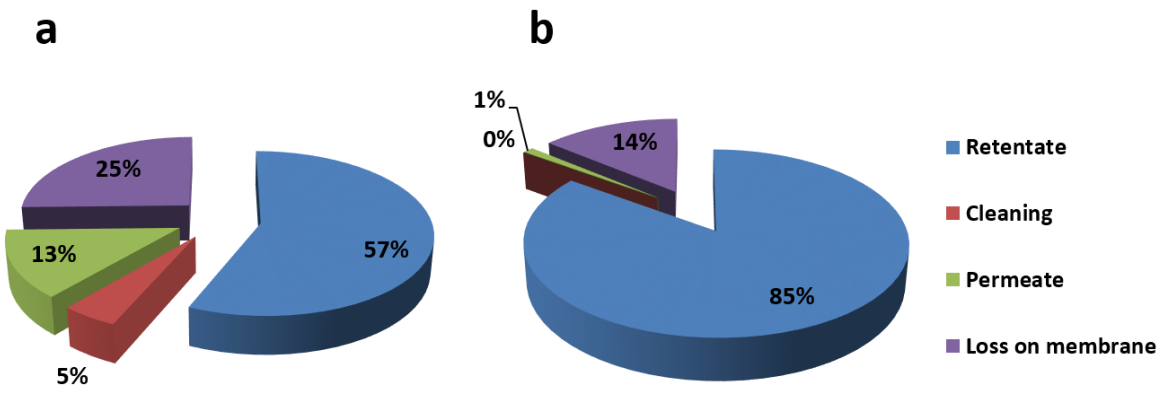

Figure 5.1 Distribution of CS/ODN polyplexes post-diafiltration by 300 kDa mPES (A), and 100 kDa mPES (B) membranes. Diafiltration was done at shear rate of 11000 s^{-1}, and TMP of 1.0 psid at 5DV.

Therefore, 100 kDa mPES membrane was picked for further optimizations. TFF operational parameters include TMP, permeate flux, as well as cross flow rate (CFR), which is expressed as shear rate in the case of hollow fibers. Shear rate produces the force required to sweep away the molecules which tend to accumulate on the filter. Optimization of a TFF process involves the examination of the interdependence of these parameters, which is known as TMP scouting (Cross flow filtration Method Handbook, 2014; Millipore, 2013). In a safe operational condition, there is no risk of forming a gel layer on the membrane, hence, the permeate flux varies linearly by TMP (Cross flow filtration Method Handbook, 2014; Millipore, 2013). Despite its high importance, a systematic optimization approach for TFF operational parameters prior to its application is not often found in literature and not available for CS-based NPs. This may result in lack of consistency, significant drop in permeate flux during the process, and finally low product yield. For instance, Limayem et.al., reported 85% drop in the permeate flux after 170 minutes of both concentration and diafiltration of indomethacin loaded NPs. This flux drop is due to the continuous fouling of the membrane which is likely due to running the system in a suboptimal condition. Other studies just reported the applied conditions with no clear justification (Anders et al., 2012; Correa et al., 2016; Dalwadi et al., 2005; Dalwadi & Sunderland, 2007; Limayem et al., 2004; Robertson et al., 2016; Trefry et al., 2010). For the determination of the safe operational

conditions for filtration of CS-based polyplexes, TMP scouting was executed for five shear rates: 7000 s^{-1}, 11000 s^{-1}, 16500 s^{-1}, 22000 s^{-1}, 30000 s^{-1}. Since for the TFF optimization study large volumes of polyplexes were needed, ODN encoding the same sequences and mimicking siRNA eGFP physico-chemical properties was used as a lower-cost alternative. 60 mL CS/ODN polyplexe solution was prepared at ODN concentration of 0.2 mg/mL and N:P=5 *via* AIMS. 10mL of CS/ODN polyplex sample was loaded into the feed vessel. In order to maintain the concentration and total volume of the CS/ODN starting solution during TMP scouting, the system was kept in total recirculation mode (TRM). TMP was increased very gradually from very low values (as low as 0.2 psid). In order to control the permeate and retentate flow rates, a needle valve was used in each stream. For each shear rate tested (each curve), a fresh polyplex solution (10 mL) was loaded and a brand new 100 kDa hollow fiber was used.

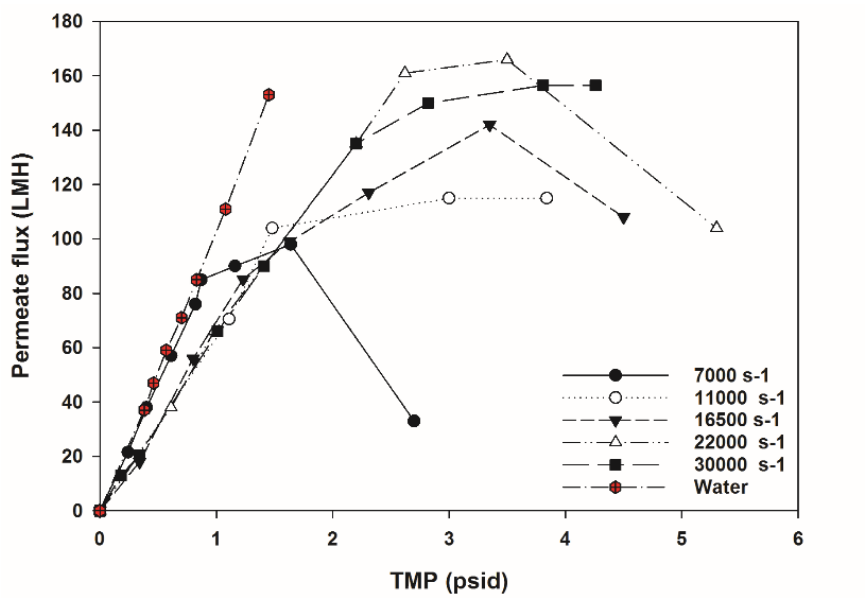

Figure 5.2 Relationship between permeate flux and TMP at five different shear rates using 100 kDa mPES hollow fibers. CS/ODN polyplexe solution prepared at ODN concentration of 0.2 mg/mL and N:P=5 *via* AIMS. Filtration of polyplexes was kept in total recirculation mode (TRM). For each curve, a fresh polyplex solution (10 mL) was loaded and a brand new 100 kDa hollow fiber was used.

As shown in Figure 5.2, there is a general trend in the curves for all of the shear rates tested. The curves started with a linear behavior confirming the proportional increase in permeate flux by TMP up to a threshold (knee point). The linearity of permeate flux and TMP shows that the polyplex

solution represents the same behavior as pure water which ensures low concentration gradient of polyplexes on the membrane (indicating the safe operational zone). However, when TMP passes the knee point, permeate flux is no longer proportional to TMP, as it reaches a plateau, confirming high concentration gradient on the membrane. This is due to accumulation of polyplexes on the surface of membrane which limits generating of permeate. At higher TMPs the flux even drops, confirming blockage of filter pores which is due to formation of a gel layer on the surface that prevents liquid passage across the membrane. Furthermore, as shown in Figure 5.2, the higher the applied shear rate, the broader the linear zone. TMP values at the knee points were 0.9 psid, 1.4 psid, 1.6 psid, 2.3 psid, and 2.6 psid for 7000 s^{-1}, 11000 s^{-1}, 16500 s^{-1}, 22000 s^{-1}, 30000 s^{-1} shear rates, respectively. This expected behavior can be simply explained by the increased sweeping actions at higher shear rates which reduce the concentration gradient on the membrane, and lower the chances of gel layer formation on the membrane. Generally, the linear part of the curves is considered as the safe operational zone for filtration of particles. Among the five shear rates tested, the lowest, 7000 s^{-1} shear rate, demonstrated closest behavior to the linear trend of water (red points). Moreover, working with shear sensitive materials (*i.e.* soft polyplexes with not a very high surface charge), it is always recomended to apply lower shear rates, when possible. Hence, the two lowest shear rates were picked for diafiltration optimization.

5.5.2 Diafiltration of CS-based polyplexes is optimized at 5 diavolume

When the volume of permeate collected equals the starting feed volume, one diafiltration volume (also refered to as diavolume, DV) has been processed. The number of DV needed for a complete buffer exchange is a key parameter in a diafiltration process which directly depends on the permeability of the molecules of the buffer through the chosen membrane. In order to establish the optimum DV for purification of CS-based polyplexes (removal of unbound CS), diafiltration of 20 mL of ODN/CS polyplexes was done using 100 kDa mPES hollow fibers in ten different DVs (from 1DV to 10DV). Diafiltration process was performed against the buffer mixture (trehalose 0.5% and 3.5mM histidine: the mixture in which the polyplexes were prepared) at the two lowest shear rates (at a TMP close to the knee point): 7000 s^{-1} (at TMP=0.9 psid), and 11000 s^{-1} (at TMP=1.0 psid). Although, it is also possible to run the system in lower TMPs (in the linear part of the TMP scouting curves), performing filtration in a TMP close to the knee point ensures higher

permeate flux, and shorter filtration time (Cross flow filtration Method Handbook, 2014; Millipore, 2013).

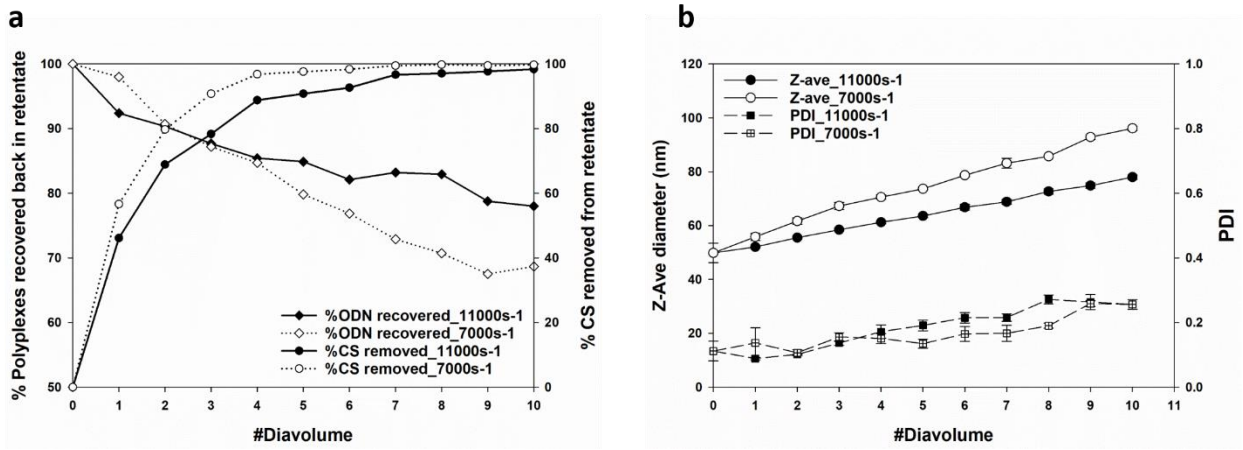

Figure 5.3 Mass percentage of chitosan removed, and mass percentage of polyplexes recovered (a), as well as the size and PDI of polyplexes (b) at each diavolume. Diafiltration was performed using 100 kDa mPES hollow fibers at shear rates of 7000 s^{-1} (TMP=0.9 psid) and 11000 s^{-1} (TMP=1.0 psid). CS/ODN polyplexe solution prepared at ODN concentration of 0.2 mg/mL and N:P=5 *via* AIMS.

In order to evaluate the recovery of polyplexes, and the amount of free CS remained in the polyplex solution, UV absorbance and Orange II measurements were performed on the retentate solution at each DV. As shown in Figure 5.3a, by increasing the DV, more CS was removed from the polyplex solution. However, increased DV was associated with a reduction in recovery yield (Figure 5.3a), and an increase in the size and PDI of polyplexes (Figure 5.3b). The increase in size and PDI of polyplexes by increasing the DV is likely due to the increased processing time, during which the polyplexes are pushed toward each other under pressure on the membrane during re-circulation. Figure 5.3a suggest removal of CS up to 98% and 92% at 5DV diafiltration, for shear rates of 7000 s^{-1} and 11000 s^{-1}, respectively. Diafiltration at 11000 s^{-1} reaches 98% only after 9DV. These results indicate that CS removal at lower shear rate (7000 s^{-1}) is more efficient, which is due to lower re-circulation rate that lets CS molecules pass across the filter more quickly. While there is not a significant difference in recovery yield of polyplexes at 5DV at the shear rates of 7000 s^{-1} and 11000 s^{-1} (81%, and 85% respectively), diafiltration at lower shear rate is faster. Higher recovery at higher shear rate can again be explained by stronger sweeping actions on the membrane surface. Normalized water permeability of hollow fibers was reduced to 86%, and 89% of the original value

post-diafiltration for 5DV at shear rates of 7000 s^{-1} and 11000 s^{-1}, respectively. The small change in the permeability of membrane post-diafiltration is an indication that filtration was done with very low risk of clogging of the membrane.

5.5.3 TFF is capable in concentration of CS-based polyplexes

In order to examine the capability of TFF in concentration of CS-based polyplexes in the established operational zone, CS/ODN polyplexes were concentrated using 100 kDa mPES hollow fibers in shear rate=7000 s^{-1}, TMP=0.9 psid. 60 mL of polyplexes were loaded into the TFF system. The volume of the polyplex was reduced to 30 mL, 20 mL, 15 mL, 12 mL, 10 mL, and 8.5 mL to achieve volume concentration factors (VCF) of 2, 3, 4, 5, 6, and 7, respectively. Since the system hold-up volume (including tubings and the module) was 7.6 mL, the concentration process was stopped at seven-fold before introduction of air into the TFF closed loop. VCF only mirrors the concertation of the sample at each stage when no loss of material during the concentration process. In order to confirm the actual concentration factor (CF), optical density (OD) of the samples at each VCF was recorded using UV spectroscopy at 260 nm. CF was then calculated as following:

$$CF = \frac{OD\ of\ the\ sample\ at\ each\ VCF}{OD\ of\ the\ initial\ sample}$$

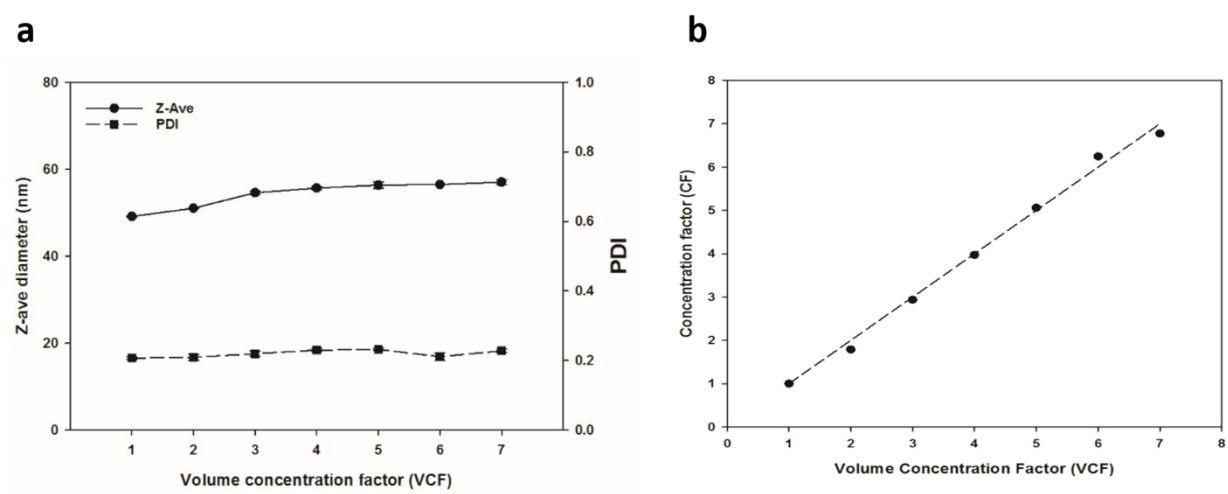

Figure 5.4 Z-average and PDI of uncoated CS/ODN polyplexes at each VCF (a), Deviation between volume concentration factor (VCF) and the real concentration factor (CF) (b). Concentration of 60 mL of CS/ODN polyplexes was done up to sevenfold using 100 kDa mPES hollow fibers in shear rate=7000 s^{-1}, TMP=0.9 psid.

As shown in Figure 5.4a, physico-chemical properties of polyplexes (Z-average and PDI) was maintained during the concentration process, since there was no marked change is the size and PDI of polyplexes (Figure 5.4a). Moreover, during the concentration process, VCF was equal to CF indicating the capability of the TFF system to concentrate the polyplexes, in the applied operational conditions, with no loss of up to seven-fold (Figure 5.4b). Normalized water permeability of hollow fiber was reduced to 81% of the original value after this concentration process which confirms that concentration was done in conditions with very low risk of clogging of the membrane.

5.5.4 Influence of molecular weight and degree of sulfation of HA, as well as the mixing C:P ratio on the physico-chemical properties of complexes

Upon establishment of the TFF process for filtration of CS/ODN polyplexes, ODN was replaced with siRNA for further HA-coatings. 15 mL of CS/siRNA polyplexes were prepared at N:P=5, using AIMS, then diafiltered at shear rate of 7000 s^{-1} (TMP=0.9) against HCl at pH=4 (low pH was chosen to ensure that the CS molecules are fully ionized for maximum repulsion during filtration, and fully charged for further HA-coating). TMP was stable during diafiltration, indicating no gel layer creation of the membrane. UV abs showed >95% recovery of CS/siRNA polyplexes. Diafiltered CS/siRNA polyplexes were then transferred for HA-coating. In order to examine the influence of HA molecular weight (MW), degree of sulfation (DS), as well as the C:P ratios of carboxyl of HA (C) to the phosphate of NA (P) on the properties of final complexes, seven HAs with different MW and DS including three non-sulfated (10 kDa, 40 kDa, and 866 kDa), as well as four sulfated (12 kDa with DS=1.4, 148 kDa with DS=0.6, 154 kDa with DS=1.0, and 184 kDa with DS=2.0) were tested.

Before addition of HAs to the purified CS/siRNA polyplexes, the amount of bound CS on the surface of the polyplexes was investigated. In order to dissociate the CS and siRNA, the diafiltered polyplexes were first treated with 10X Tris-Acetate-EDTA (TAE) buffer, which contains 400 mM Tris, 200 mM acetic acid, and 10 mM EDTA. TAE 10X buffer was added polyplex solution in equal volumes for a final TAE concentration of 5X. Final sample was then centrifuged at 21 kg for 20 minutes to pellet down the precipitated CS. The supernatant was pipetted out very slowly, and the precipitated CS was dissolved back in acetic acid pH=4. Orange II assay was then performed to quantify the bound CS. Our data showed that the bound N:P ratio in the diafiltered CS/siRNA polyplexes is 1.7. Also, no CS and no siRNA was detected in the supernatant and precipitate,

respectively. Thus, it is assumed that the diafiltered polyplexes have a net positive charge of 0.7. Therefore, HA could be added at C:P ≥ 0.7 to the purified polyplexes. Accordingly, HA solutions were added at four different C:P ratios of 1.0, 1.5, 2.0, and 3.0. In order to save on polyplexes, HA-coating was done by manual addition of small volumes (200 µL of HA into 400 µL of diafiltered polyplexes). Preparation of HA-coated complexes was done in duplicates for each condition.

5.5.4.1 HA-coating of polyplexes requires C:P ≥ 2.0

Our data showed that regardless of MW and DS, addition of HA at C:P of 1 and 1.5 resulted in either macroscopic flocculations or complexes with sizes similar to CS/siRNA polyplexes, with no change in their ZP (data not shown). This suggests that although theoretically addition of HA at C:P>0.7 should neutralize and reverse the charge sign of the surface (from positive to negative), use of HA in excess is required to fully condense and coat the polyplexes. At higher C:P ratios (2 and 3) a size increase (Figure 5.5a), and a clear switch in ZP (Figure 5.5b) was observed, suggesting availability of enough HA molecules to effectively coat the polyplexes.

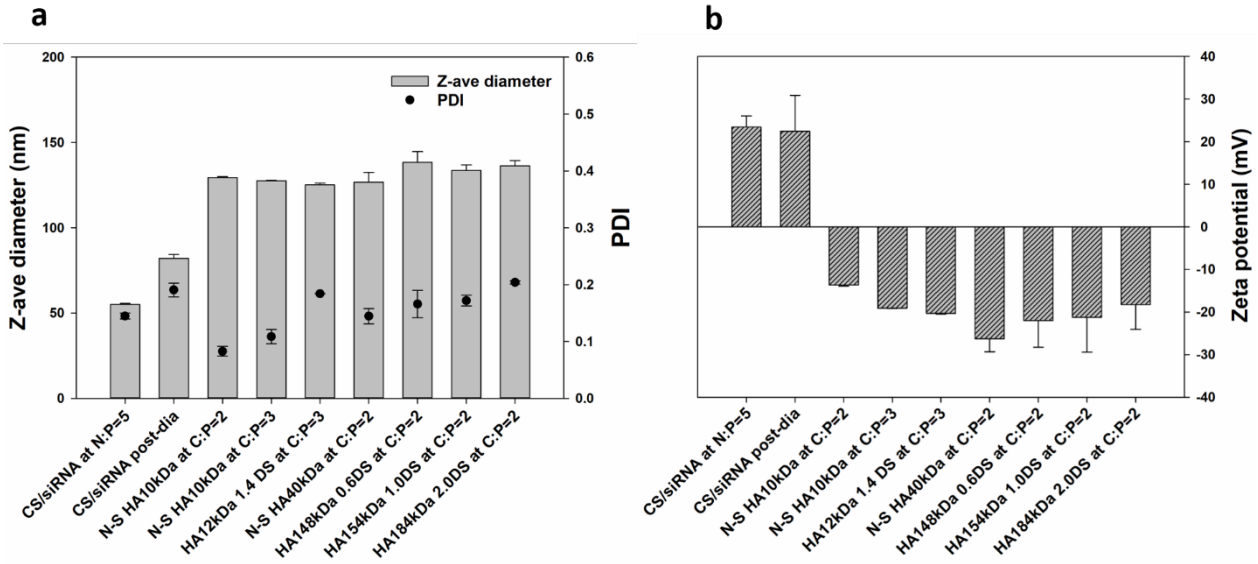

Figure 5.5 Effect of HA molecular weight, HA degree of sufation, and C:P ratio on the size and PDI (a), as well as zeta potential (b) of polyplexes post HA-coating. Uncoated CS/siRNA polyplexes were prepared at N:P=5, then diafiltered against HCl at pH=4 to remove the unbound CS. Diafiltered polyplexes were then coated by different HAs. HA was added manually to the polyplex solutions (200 µL of HA into 400 µL of diafiltered polyplexes). Error bars represent standard deviation between the duplicates.

5.5.4.2 Low and moderate MW HA result in small sized and homogeneous coated complexes

Addition of the high MW HA (866 kDa) to the purified CS/siRNA polyplexes resulted in macroscopic flocculations, which occurred at all of the tested C:P ratios. However, when mixing was done at C:P of 2 or 3 with relatively moderate MWs (148 kDa, 154 kDa, and 184 kDa) and low MWs (10 kDa, 12 kDa and 40 kDa) of HAs, this parameter (C:P ratio) had no marked influence on the size of the HA-coated complexes with z-average between 125 and 133 nm (Figure 5.5a). Nonetheless, the lowest MW HA 10 kDa resulted in the most homogenous coated complexes (PDI of 0.08-0.1). Upon addition of different HAs at C:P of 2 or 3, the ZP of the polyplexes reversed from +22mV to negative values ranging from -13mV to -26mV. There is not a clear correlation between the ZP of the coated complexes and the MW and DS of the HAs, nevertheless, the non-sulfated HA10 kDa and the non-sulfated HA40 kDa resulted in complexes with the lowest ZP (-13mV) and the highest ZP (-26mV), respectively (Figure 5.5b).

5.5.4.3 DS has no or negligible influence on the size, PDI and ZP of coated complexes

As shown in Figure 5.5, there is no marked difference in the size, PDI and ZP of the HA-coated complexes prepared with three HAs having similar MWs of 148 kDa, 154 kDa, and 184 kDa but different DS of 0.6, 1.0, and 2.0. They all were added at the fixed C:P of 2. Z-average, PDI, and ZP of the HA-coated polyplexes were in the small ranges of 133 to 138 nm, 0.17 to 0.2, and -18 to -21mV, respectively. The data suggests that the charge density (represented by DS) has no effect on the size, PDI and ZP of the coated complexes (when C:P ratio is high enough (≥2) for an effective binding of HA molecules to the surface of polyplexes), however, their stability and circulation time in physiological conditions might be different.

5.5.4.4 Only complexes coated with sulfated HA remained stable post diafiltration

The two low MW HAs (non-sulfated 10 kDa, and sulfated 12 kDa with 1.4 DS) were chosen for large scale production of HA-coated complexes. 10 mL of diafiltered polyplexes were mixed with 5 mL of HA at C:P=3 using AIMS as described in methods. The HA-coated polyplexes produced *via* AIMS were smaller and more homogenous than manually prepared complexes: 119 nm (PDI of 0.07) *versus* 127 nm (PDI of 0.10) for non-sulfated HA10 kDa, and 100 nm (PDI of 0.18) *versus* 125 nm (PDI of 0.19) for sulfated HA12 kDa 1.4 DS. The smaller size and PDI of polyplexes produced *via* AIMS *versus* manual method was also reported by Tavakoli Naeini *et al.* for

CS/siRNA production (Tavakoli Naeini et al., 2017). Due to similar conditions of HA-coated complex solution to the uncoated polyplexes (both have unbound excess materials, at ~10-12 kDa), same operational conditions were applied for diafiltration of HA-coated complexes upon mixing: shear rate=7000 s^{-1}, and TMP=0.9 psid. In order to keep the HA molecules fully ionized, diafiltration of HA-coated complexes was done against HCl at a pH=5 (well above their pKa, but low enough to still keep the CS molecules charged).

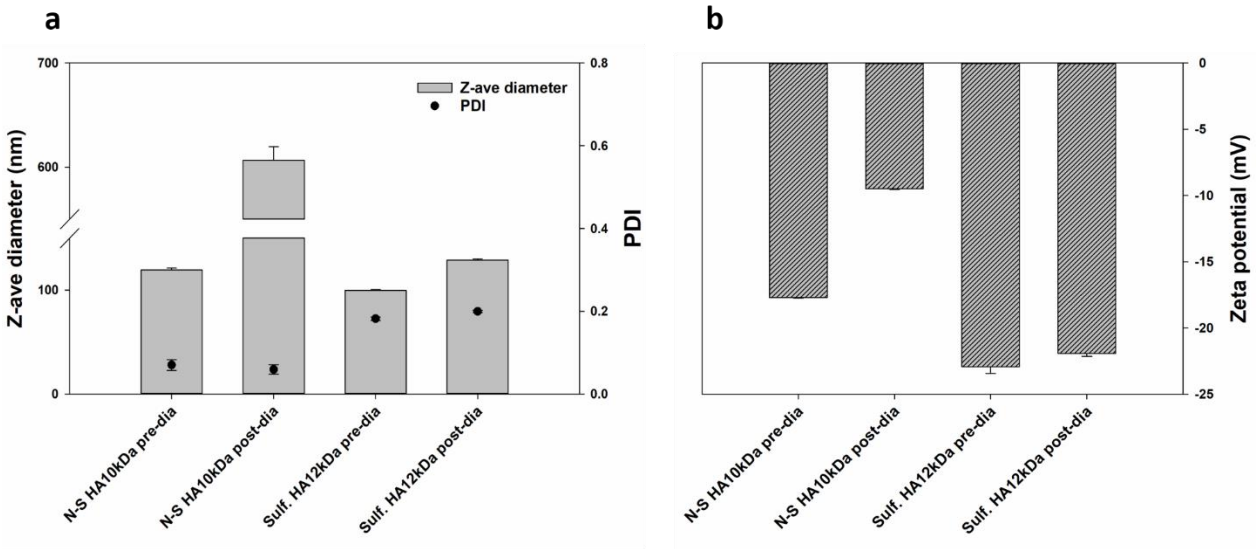

Figure 5.6 Effect of diafiltration on the size and PDI (a), and zeta potential (b) of HA-coated complexes prepared at C:P=3. Both non-sulfated 10 kDa and sulfated 12 kDa HAs were tested. Diafiltration of HA-coated complexes was done at 5DV against HCl at pH=5 using 100 kDa mPES hollow fibers at shear rate=7000 s^{-1}, and TMP=0.9 psid. Error bars represent standard deviation between the duplicates.

As shown in Figure 5.6, diafiltration of complexes coated with non-sulfated HA 10 kDa was associated with a drastic increase in size, Z-average from 119 nm to ~600 nm (Figure 5.6a), and a ZP closer to neutral, from -18mV to -9mV (Figure 5.6b) indicating aggregation of complexes. In contrast, the size, PDI, and ZP of complexes coated with the sulfated HA 12 kDa was maintained over the course of diafiltration: small increase in size from 100 nm to 128 nm, and PDI from 0.18 to 0.20 (Figure 5.6a). Moreover, as shown in Figure 5.6b, ZP of sulfated HA-coated complexes was almost unchanged after diafiltration (-22mV *versus* -23mV pre-diafiltration). Higher stability of complexes coated with sulfated HA could be explained by the increased charge density of the sulfated HA, and its enhanced binding affinity to polyplexes, which protects complexes from

dissociation by external shear (due to recirculation and filtration pressure), and pH change (during diafiltration). Stronger binding affinity of the sulfated HA compared to non-sulfated HA was also reported previously (Feng et al., 2017; Magnani et al., 1999).

5.5.5 Morphology of the uncoated and HA-coated CS/siRNA polyplexes

Morphology of uncoated CS/siRNA polyplexes as well as HA-coated complexes was assessed by Transmission Electron Microscopy (TEM). TEM images show similar spherical morphology of CS/siRNA polyplexes pre- and post-diafiltration (Figure 5.7a and Figure 5.7b). The spherical shape of CS/siRNA polyplexes was reported previously (Holzerny et al., 2012; Howard et al., 2006a; X. Liu et al., 2007; Tavakoli Naeini et al., 2017). Figure 5.7c, and Figure 5.7e show the HA-coated complexes produced by non-sulfated 10 kDa HA and sulfated 12 kDa 1.4DS, respectively. Generally, HA-coated complexes are noticeably larger than uncoated polyplexes, due to the presence of HA. However, HA corona is more evident when non-sulfated HA was used. Stronger binding of sulfated HA molecules to the surface of polyplexes results in more compact complexes (Figure 5.7e). Morphology of the complexes post-diafiltration is shown in Figure 5.7d (non-sulfated) and Figure 5.7f (sulfated). As can be clearly seen, the size of non-sulfated HA-coated complexes increased post-diafiltration. In contrast, sulfated HA-coated complexes maintained their morphology and size during diafiltration which could be attributed to their initial compact morphology. This is in agreement with DLS results, which again suggests higher stability of complexes produced by sulfated HA.

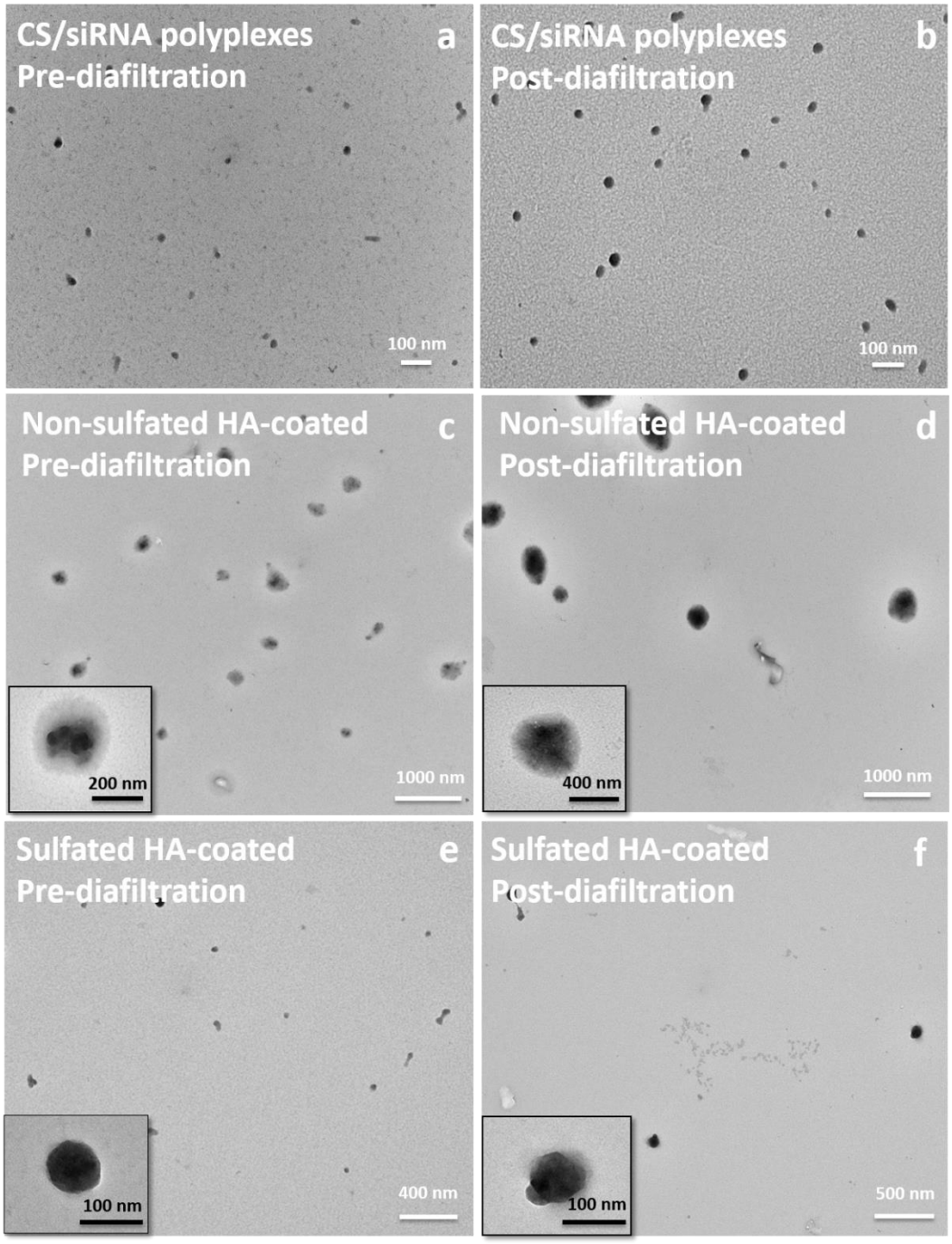

Figure 5.7 TEM images of uncoated polyplexes (prepared at N:P=5), pre-diaifltration (a) and post-diafiltration agiast HCl at pH=4 (b). HA-coated complexes were prepared using the diafiltered polyplexes *via* AIMS at C:P=3 (c is non-sulfated 10 kDa HA, and e is sulfated 12 kDa HA with 1.4DS). HA-coated complexes were diafiltered against HCl at pH=5 (d is non-sulfated 10 kDa HA, and f is sulfated 12 kDa HA with 1.4DS). Diafiltration of HA-coated complexes was done at 5DV using 100 kDa mPES hollow fibers at shear rate=7000 s^{-1}, and TMP=0.9 psid.

5.5.6 HA-coated complexes are as bioactive as uncoated CS/siRNA polyplexes

In order to test the suitability of TFF to maintain the bioactivity of CS/siRNA polyplexes, the eGFP$^+$ H1299 cells were transfected *in vitro* and eGFP$^+$ knockdown was assessed by fluorescence measurement at 510 nm, and normalized to total protein content and expressed relative to non-treated cell. Cells were transfected with uncotaed CS/siRNA polyplexes prepared at N:P=5, both pre-diafiltration and post-diafiltration. HA-coated complexes (prepared by either non-sulfated or sulfated HAs) were also transfected, both pre- and post-diafiltration. DharmaFECT®2, a commercially available lipoplex, was used as positive control. Naked siRNA, and non-treated cells were used as negative controls.

eGFP knockdown reached ~55% and 60% when uncoated polyplexes were transfected pre-diaifltration and post-diafiltration, respectively (Figure 5.8). Compared to the uncoated polyplexes, HA-coated complexes, resulted in slightly higher eGFP knockdown (~75% with non-sulfated 10 kDa HA, and 81% with sulfated 12 kDa HA 1.4 DS). Higher eGFP knockdown with HA-coated complexes could be possibly explained by protection of polyplexes from interactions with negatively charged molecules in the serum. Moreover, since HA binds to the CD44 receptor, which is overexpressed on the surface of H1299 cells, it can act as the addressing molecule of polyplexes, and increases receptor mediated endocytosis.

As shown in Figure 5.8, bioactivity of non-sulftaed HA-coated complexes reduced significantly post-diafiltration (to ~30%). In contrast, complexes prepared using sulfated HA preserved their bioactivity at the same level upon filtration (82-84%). Consistant bioactivity of sulfated HA-coated complexes upon filtration confirm high stability of these formulations, which is aligned with the DLS data (Figure 5.6), and morphology of complexes (Figure 5.7).

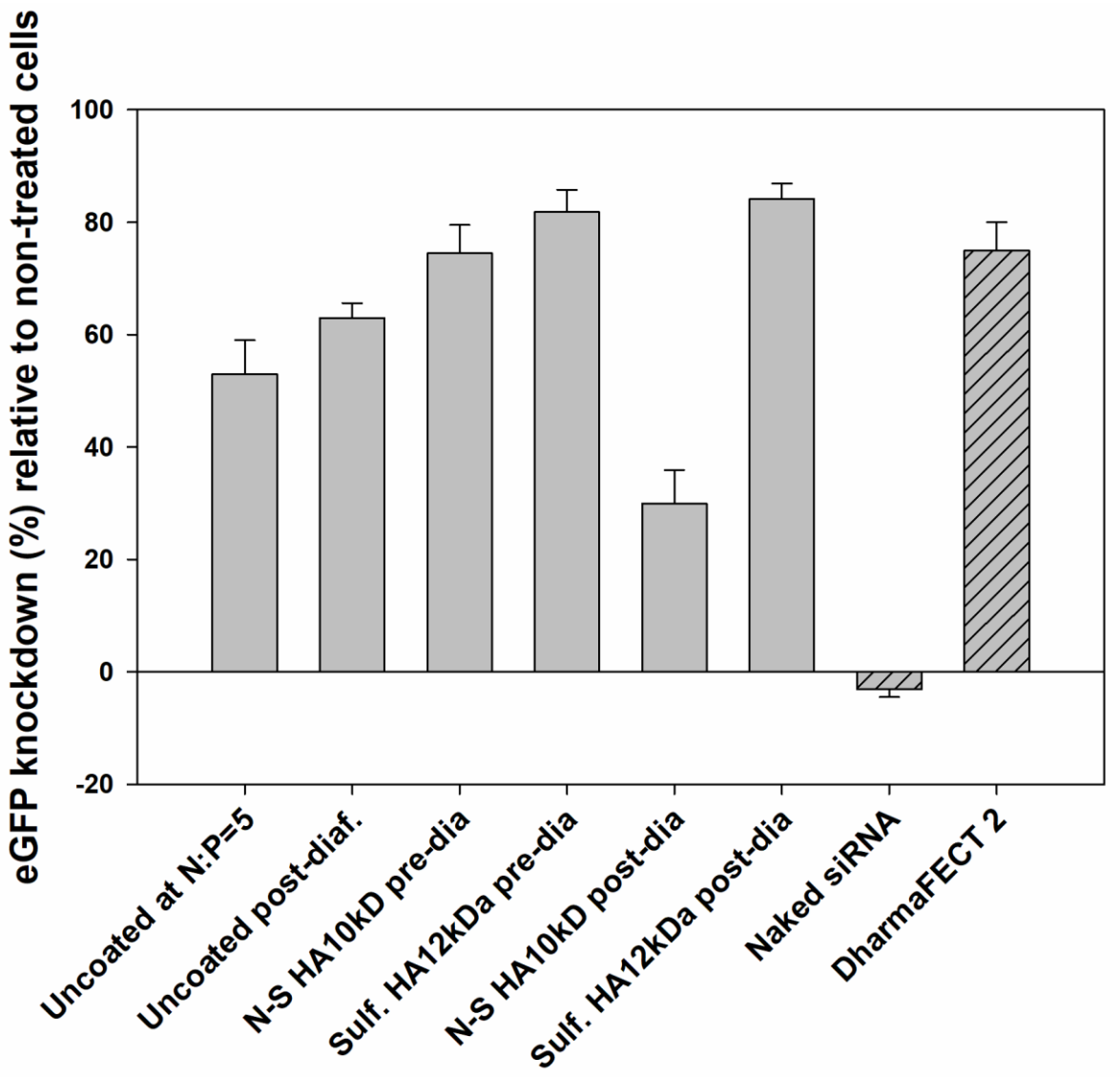

Figure 5.8 Bioactivity of CS/siRNA polyplexes as well as HA-coated complexes both pre-diafiltration and post-diafiltration. eGFP^{+} H1299 cells were transfected with either uncoated or HA-coated anti-eGFP CS/siRNA polyplexes at a final siRNA concentration of 100 nM/well. eGFP silencing was assessed by fluorescence measurement at 410 nm, and normalized to total protein content and expressed relative to non-treated cell. Data represent the mean of two independent experiments (N=2) with three technical replicates per experiment (n=3).

5.5.7 HA-coated complexes have increased hemocompatibilty

None of the formulations induced hemolysis (see Table 5.1).

Table 5.1 Hemolysis (%) and hemagglutination of RBCs following incubation with serial dilutions of uncoated CS/siRNA polyplexes (N:P=5), and HA-coated (sulfated or non-sulfated) both pre- and post-diafiltration. Maximum final siRNA concentration was of 0.1 mg/mL and 0.066 mg/mL for uncoated and HA-coated complexes, respectively. siRNA (0.1 mg/mL), HAs (1 mg/mL), and PEG (40% w/v) were used as negative controls. PLL (10mg/mL) and TX-100 (10% v/v) were used as positive controls. Uncoated polyplexes at N:P=5 and HA-coated polyplexes were all nonhemolytic (< 2% hemolysis) for all the concentrations. Mean ± standard deviation (n = 2).

Formulation	Max concentration	Hemolysis %	Hemagglutination
Uncoated CS/siRNA pre-dia	0.1 mg siRNA/mL	1.5	+
Uncoated CS/siRNA pre-dia	0.1 mg siRNA/mL	<1	+
Non-sulfated 10kD HA-coated pre-dia	0.066 mg siRNA/mL	<1	-
Non-sulfated 10kD HA-coated post-dia	0.066 mg siRNA/mL	<1	-
Sulfated 12kD HA-coated pre-dia	0.066 mg siRNA/mL	<1	-
Sulfated 12kD HA-coated post-dia	0.066 mg siRNA/mL	1.1	-
PLL	10 mg/mL	16.5	+
TX-100	10% v/v	100	+
PEG	40% w/v	1.5	-
siRNA alone	0.1 mg/mL	<1	-
Non-sulfated 10kD HA	1 mg/mL	<1	-
Sulfated 12kD HA, DS=1.4	1 mg/mL	<1	-

However, uncoated polyplexes induced hemagglutination at the highest concentration tested, 0.1 mg siRNA/mL (see Figure 5.9), whether pre-diafiltration (with unbound CS) or post-diafiltration (without unbound CS). It suggests that although the unbound CS is removed upon diafiltration, this is not sufficient to prevent hemagglutination in these formulations due to their positive surface charge. Hemagglutination of CS-based polyplexes at elevated concentrations (1 mg siRNA/mL) was previously reported (Veilleux, 2016). On the other hand, HA-coated complexes (weather with sulfated or non-sulfated) did not cause hemagglutination up to the highest

concentration tested, 0.0667 mg siRNA/mL (see Figure 5.10 and Figure 5.11), which suggest that HA corona reduces the interactions of polyplexes with red blood cells.

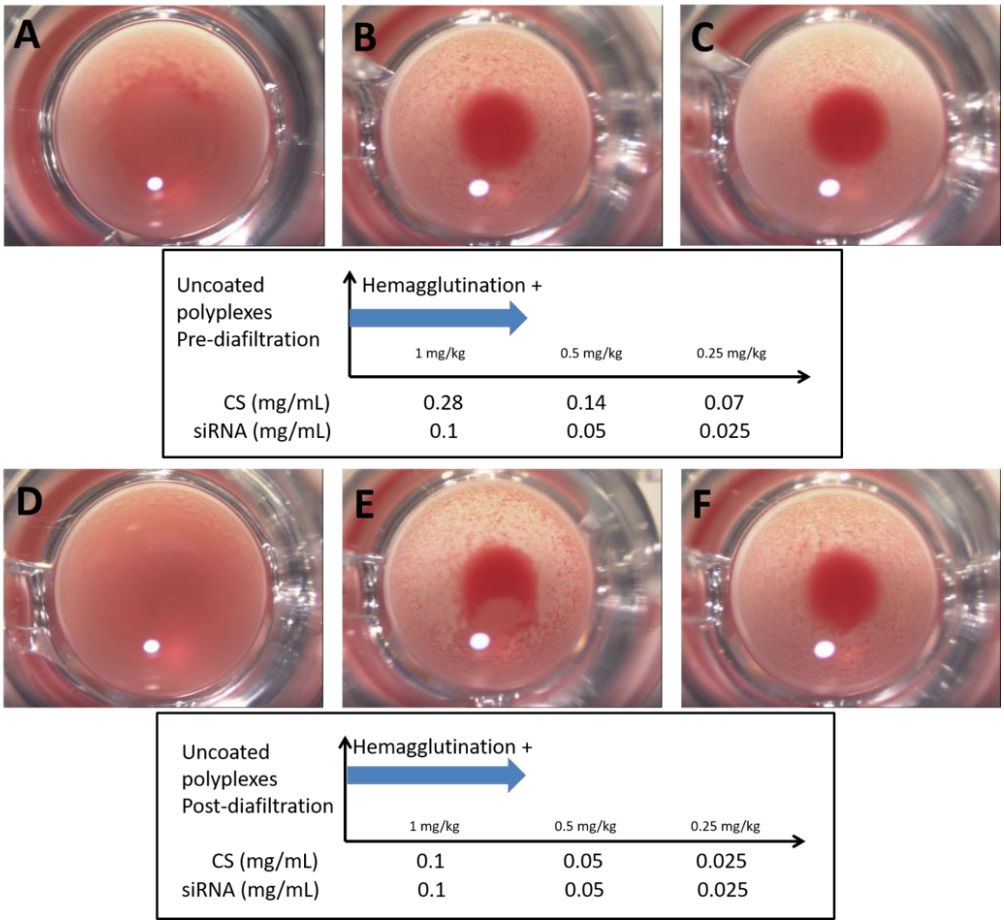

Figure 5.9 Hemagglutination assay of uncoated CS/siRNA polyplexes prepared at N:P=5 at 0.1, 0.05, and 0.025 mg siRNA/mL pre-diafiltration (A, B, C), and post-diafiltration (D, E, F). Note that 1 mg siRNA/mL equals to 1 mg/kg injectable dose for a mouse of 10g (for an injection of 10 µL/g). Highest dose of uncoated polyplexes cuased hemagglutination both pre- (A) and post-diafiltration (D).

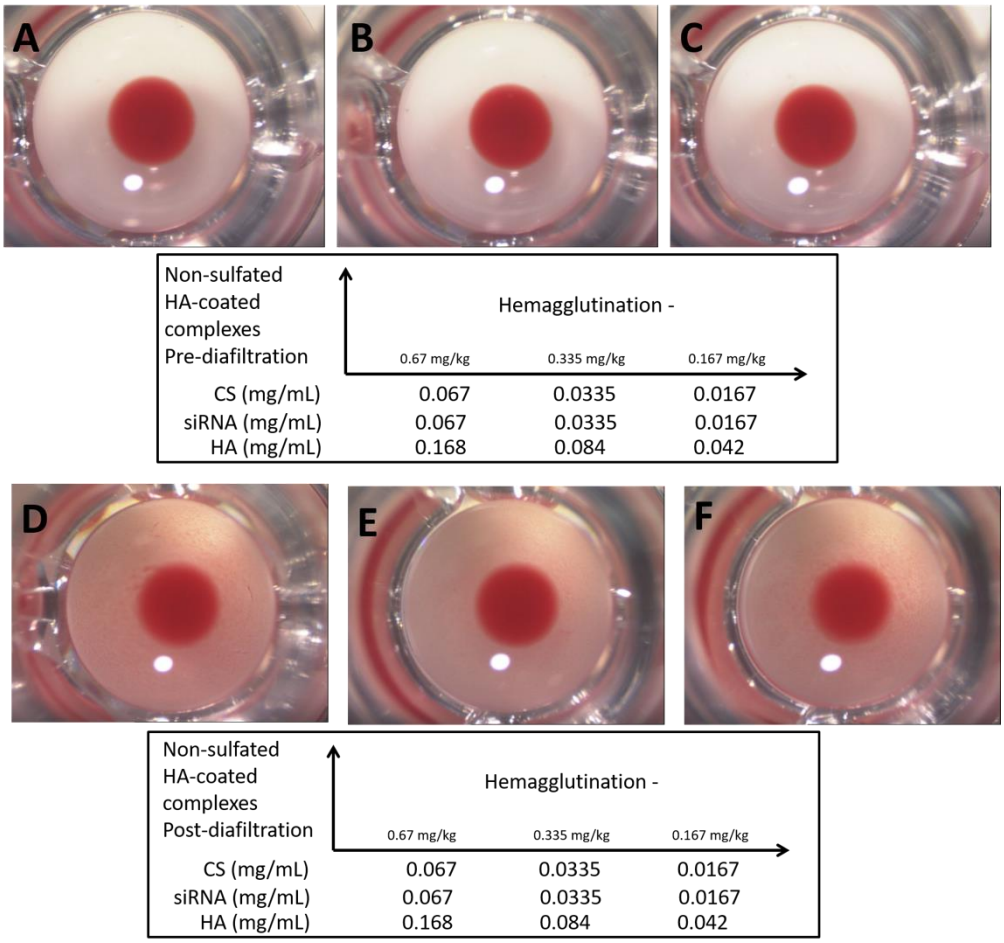

Figure 5.10 Hemagglutination assay of non-sulfated HA-coated complexes prepared at P:C=3 at 0.067, 0.0335, and 0.0167 mg siRNA/mL pre-diafiltration (A, B, C), and post-diafiltration (D, E, F). Note that 1 mg siRNA/mL equals to 1 mg/kg injectable dose for a mouse of 10g (for an injection of 10 µL/g). None of the samples caused hemagglutination.

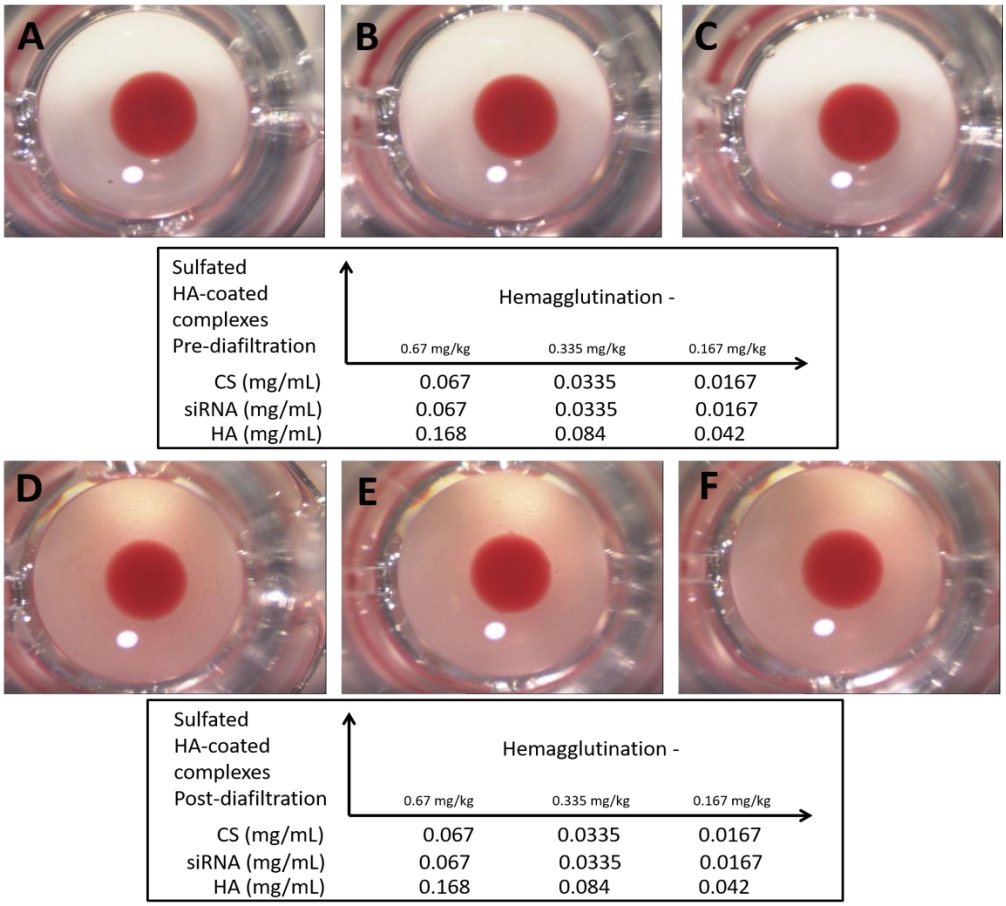

Figure 5.11 Hemagglutination assay of sulfated HA-coated complexes prepared at P:C=3 at 0.067, 0.0335, and 0.0167 mg siRNA/mL pre-diafiltration (A, B, C), and post-diafiltration (D, E, F). Note that 1 mg siRNA/mL equals to 1 mg/kg injectable dose for a mouse of 10g (for an injection of 10 µL/g). None of the samples caused hemagglutination.

5.6 Conclusion

To tackle the limitations of CS-based polyplexes for intravenous delivery, TFF was applied, for the first time, to purify CS-based polyplexes from the unbound CS. Through TMP scouting analysis, safe TFF operational conditions were established. It was shown that polyplexes preserved their physico-chemical properties, morphology, and bioactivity after the TFF process. Purified CS/siRNA eGFP polyplexes were then coated by different HA molecules. Our study examined the impact of HA molecular weight and degree of sulfation, as well as C:P ratio on the physicochemical properties of coated complexes. We found that regardless of the degree of sulfation, low molecular weight HA at C:P ratios above 2 is needed to effectively coat the polyplexes and surface charge reversal. Additionally, it was shown that the HA-coated CS/siRNA complexes have even higher knockdown efficiency of eGFP in H1299 cells (75-82%), compared to uncoated polyplexes (53-63%), which is likely due to 1) improved protection of polyplexes by HA corona, and 2) increased receptor mediated endocytosis by the HA-coating through the CD44 receptor on the surface of the cells. Our data indicated that although both sulfated and non-sulfated HAs result in small sized and homogenous coated complexes, only complexes prepared with sulfated HA preserved their physico-chemical properties and bioactivity post filtration, indicating their stronger binding affinity to polyplexes. Finally, we showed that the HA-coated complexes eliminated hemagglutination and hemolysis. Improved bioactivity and hemocompatibility of these modified formulations are promising for the clinical use of CS-based complexes for IV applications.

CHAPTER 6 GENERAL DISCUSSION

The published study (Chapter 4) aimed to develop a fully automated in-line mixing system (AIMS) that is capable in reproducible production of large batches of CS/NA polyplexes. We started the work by designing a mixing platform based on two peristaltic pumps. The choice of peristaltic pumps was to drive fluids based on pulsatile motion, where the natural oscillation of the fluids provides a wavy and stretched interface between the two streams, thus enhancing the mixing. In order to have an automated system, digital peristaltic pumps were programmed via LabView software, to simultaneously drive CS and NA solutions (at a flow rate set by the user), and mix them in a Y, or T, or cross connector. For maxium precision on dispensed volumes, a sub-program was desgined to calibrate the pumps using digital balances before actual mixing. Balances were also used to monitor the volume/mass of payloads during mixing process. The whole system was closed to maintain sterility. The primary design (named "initial version" throughout the text) was further improved, aiming to enhance the quality of products (smaller size and more homogeneous), and to reduce the capital cost, and save space. The new design (named "advanced version" throughout the text) features (1) only one peristaltic pump with a dual channel head that drives both CS and NA, simultaneously; (2) priming of the tubings with water rather than the NA and CS solutions in order to minimize consumption of payloads; (3) mixing after the acceleration phase of the pump to produe the polyplexes only at the target speed set by the user.

In order to optimize the mixing process for production of small size and uniform polyplexes, the influence of mixing parameters (*i.e.* mixing speed, mixing concentrations, mixing pattern and length) on physico-chemical properties of CS/pDNA and CS/siRNA were studied for both initial and advanced versions of AIMS. Increasing mixing concentrations was directly associated with an increase in size and polydispersity of both CS/pDNA and CS/siRNA polyplexes. We found that regardless of the mixing method (manual *versus* in-line) and configuration of AIMS (initial *versus* advanced), the maxium concetration for reproducible production of small and homogeneous CS/pDNA is 0.1 mg/mL. However, AIMS allowed production of relatively small and homogeneous CS/siRNA polyplexes at increased concentrations of 0.3 mg/mL and even 0.4 mg/mL (using the advanced version). The possibility of producing CS/siRNA polyplexes at higher concentrations could be attributed to the higher C* of siRNA as compared to pDNA. While C* for CS and pDNA are close to each other and relatively low (3.6 mg/mL and 1.36 mg/mL for chitosan 92-10 and pDNA, respectively), this value is 790 mg/mL for siRNA which gives a lattitude in siRNA mixing

concentration before reaching flocculation (up to the tested concentraion of 0.4 mg/mL), nevertheless, the increased siRNA mixing concentration is associated with an increase in size and PDI of final polyplexes. Additionally, we found that ZP increases as mixing concentration increases. This behavior was found for the both type of NAs. This result suggests that when mixing concentration is higher, more chitosan is incorporated in polyplexes which could be the result of faster association kinetics at higher mixing concentrations.

The speed of mixing found to have a negligible impact on the properties of CS/pDNA polyplexes: for $26 < Re < 4000$, z-average diameter and PDI of CS/pDNA polyplexes varied only slightly between 186 and 112 nm, and between 0.25 and 0.23, respectively. It seems that even at very low speeds, the pulsatile action of the peristaltic pumps generates sufficient perturbation and interface stretching for efficient mixing and production of homogeneous small sized pDNA/CS polyplexes. pDNA is a relatively big molecule with a low diffusivity, thus, at the time of mixing, mostly CS molecules diffuse to contribute to complex formation. Once association of CS molecules starts on a pDNA supercoil, the chance of collision with another pDNA molecule is much lower than colliding with a subsequent CS. This limits bridging of polyplexes and potential heterogeneity, even at low mixing speeds. Similar physico-chemical properties of manual and in-line CS/pDNA polyplexes (regardless of AIMS version), in a given concentration, could be explained by low diffusivity of pDNA and limited sensitivity of these polyplexes to the mixing speed, suggesting that even the low advection provided by manual mixing is sufficient for having an efficient mixing. However, interestingly, the size and polydispersity of CS/siRNA polyplexes are influenced by the mixing speed: the higher the speed, the smaller the size and polydispersity. This is likely due to high diffusivity of siRNA molecules. As a very small molecule, in addition to CS, siRNA significantly contributes to the complex formation. Thus, in order to achieve homogeneous polyplexes, stronger advection is required to eventually saturate siRNA with excess CS molecules rather than colliding with another siRNA. Accordingly, it is not surprising that compared to manual method, AIMS (both initial and advanced versions) provided with smaller and more homogenous CS/siRNA polyplexes when mixing was done at a high speed ($Re \geq 2140$, non-laminar flow regime). Compared to manual CS/siRNA polyplexes (z-average diameter and PDI of 101 nm and 0.2), for Re between 2140 and 4000, the initial version of AIMS produced polyplexes with z-average diameter and PDI from 84 nm to 75 nm and, 0.18 to 0.17; and the advanced version produced polyplexes with z-average diameter and PDI from 65 nm to 47 nm and, 0.18 to 0.12,

respectively. Knowing the fact that CS/siRNA polyplexes are sensitive to mixing speed, and since in the advanced version of AIMS mixing only takes place in the target speed, it was expected that this version provides with smaller CS/siRNA polyplexes with lower PDI, as compared to the initial version (where mixing starts at a low speed and ends at the target speed). We also found that the mixing pattern (Y, T, or a cross connector), and mixing length (from 25cm to 65cm) had no effect or a very small effect on polyplex properties. This suggests that no matter what mixing pattern is chosen, the pulsatile actions and transverse advection inside the 25cm outlet is sufficient for a complete mixing.

TEM images show that regardless of the mixing method (AIMS *versus* manual), CS/pDNA polyplexes have a mixed morphology (spherical, toroidal and rod like). This was expcted as was previously reported in literature. CS/siRNA polyplexes, on the other hand, were generally spherical. In agreement with DLS data, TEM images revealed smaller and more uniform CS/siRNA polyplexes when produced *via* AIMS *versus* manual method. Finally, it was demonstrated that CS/siRNA polyplexes produced *via* AIMS had equivalent or higher silencing efficiency of ApoB in HepG2 cells: 40-55% ApoB mRNA knockdown as compared to manual polyplexes (30-45%).

Chapter 5 aimed to establish TFF technique for concentration and purification of CS-based polyplexes. Hollow fiber geometry was taken as it has been demonstrated that the tubular geometry of hollow fibers is more beneficial than the cassette geometry for filtration of particles, which is attributed to migration of particles to the center of the hollow fiber where the flow velocity is the highest (tubular pinch effect). Moreover, hollow fibers are less expensive than cassette geometry and are available as pre-sterilized single use modules, which reduces the risk of cross contamination, cleaning labour, and time needed for system overhaul. mPES membranes are extremely hydrophilic, and almost all of the commercially available hollow fibers for ultrafiltration purposes are made form modified Polyethersulfone (mPES). According to the size range of polyplexes (45-60 nm aimed to retentate), and the chitosan molecules (~5 nm aimed to permeate), and based on the data obtained from manufacturer on the pore size of different cut-offs, mPES hollow fibers at 100 kDa and 300 kDa were selected for filtration of CS-based polyplexes. Our results showed that filtration of polyplexes using a 300 kDa membrane was associated with a very low recovery (57%) *versus* the 100 kDa membrane with 85% recovery (both tested at the shear rate of 11000 s^{-1}, and TMP=1.0 psid). This was due to partial penetration of polyplexes into bigger pores of 300 kDa membrane (data showed higher deposition of polyplexes on the 300 kDa

membrane surface (25% of the initial polyplexes). Altogether, 100 kDa membrane was found as a better pick for filtration of CS-based polyplexes. Thereafter, optimal TFF operational conditions were established using 100 kDa mPES hollow fibers. TMP scouting revealed that for filtration of CS-based based polyplexes, TMP had to be generally maintained lower than 1.0 psid. Among the shear rates tested (between 7000 s^{-1} and 30000 s^{-1}), the lowest shear rate (7000 s^{-1}) demonstrated closest behavior to the linear trend of water, suggesting a very low concetration gradient on the surface of the membrane (no excessive pressure and enough shear rate to sweep the polyplexes away). In order to reduce the processing time at a given feed flow rate, TMP should increase, which requires higher shear rate to sweep away the polyplexes more efficiently to keep the concentration gradient on the membrane surface as low as possible. However, higher TMP is always associated with the risk of membrane fouling as it is the pressure that pushes the polyplexes on the membrane. Moreover, working with shear sensitive materials (*i.e.* soft polyplexes with not a very high surface charge), it is always recomended to apply lower shear rates, when possible. Hence, the two lowest shear rates were picked for further diafiltration optimizations. We found that by increasing the DV, more chitosan was removed from the system, at the cost of recovery yield, and a gradual increase in the size and PDI of polyplexes. The increase in size and PDI of polyplexes by increasing the DV is likely due to the increased recirculation of polyplexes in the system where they were pushed toward each other under pressure on the membrane. Our data suggest that at 5DV up to 98% and 92% of CS was removed, when shear rate was set at 7000 s^{-1} and 11000 s^{-1}, respectively. Removal of CS at 11000 s^{-1} reached 98% only after 9DV. These results indicate that CS removal at lower shear rate (7000 s^{-1}) is more efficient, which is due to lower re-circulation rate that lets CS molecules pass across the filter more quickly. Recovery yield of polyplexes at 5DV was 81%, and 85%, for shear rates of 7000 s^{-1} and 11000 s^{-1} respectively. The slight higher recovery at higher shear rate (11000 s^{-1}) can be explained by stronger sweeping actions on the membrane surface. However, achieving a certain purity is faster and less expensive (less buffer usage) at lower shear rate. Upon establishment of the TFF operational conditions, polyplexes were concentrated up to sevenfold while preserving their physico-chemical properties (shear rate=7000 s^{-1} at TMP=0.9 psid).

The final objective of the thesis was to modify the surface of the polyplexes upon purification. A library of HA molecules was used to coat the polyplexes to enhance their hemocompatibility for IV administration. HAs with different molecular weights (from 10kDa to 866 kDa) and degrees of

sulfation (from 0.6 to 2.0), at different carboxyl to phosphate ratios (C:P from 1.0 to 3.0) were tested. We initially found that high molecular weight HA (866 kDa) results in macroscopic flocculations at every C:P ratio tested. Moreover, it was demonstrated that C:P≥ 2.0 is needed to effectively coat the polyplexes and switch the surface charge of complexes. It was shown that polyplexes coated with lower molecular weight HAs, non-sulfated 10kDa and sulfated 12kDa (z-average of 125-129nm, PDI of 0.09-0.18, and average zeta potential of −17 mV) have have even higher knockdown efficiency of eGFP in H1299 cells (75-82%), compared to uncoated polyplexes (53-63%). This is likely due to the improved protection of polyplexes by HA corona in serum, and the increased receptor mediated endocytosis by the HA-coating through the CD44 receptor on the surface of the cells. Our data indicated that although both sulfated and non-sulfated HAs result in small sized and homogenous coated complexes, only complexes prepared with sulfated HA preserved their physico-chemical properties and bioactivity post filtration, indicating their stronger binding affinity to polyplexes. We finally showed that hemagglutination and hemolysis induced by uncoated polyplexes were completely eliminated by HA-coating (using both sulfated and non-sulfated HAs).

CHAPTER 7 CONCLUSION AND RECOMMENDATIONS

This work allowed to develop an automated in-line mixing system (AIMS) for reproducible production of large batches of CS-based polyplexes with equivalent bioactivity as compared to manually prepared polyplexes. We found that the mixing speed has not a significant impact on the physico-chemical properties of CS/pDNA polyplexes. However, mixing at higher flow rates resulted in smaller and more homogenous CS/siRNA polyplexes. In additions, it was shown that reducing the concentration of both pDNA and siRNA, results in a reduction in size, PDI and zeta potential of polyplexes. The type of mixer and mixing length showed no or negligible effect on the properties of CS-based polyplexes. AIMS enabled to eliminate day to day small volume preparations, and the risks of batch to batch and inter-user variability.

In a subsequent study, for the first time, tangential flow filtration technique was adopted and optimized to purify large batches of CS-based polyplexes. First, we found that 100 kDa mPES hollow fiber is a proper membrane for permeation of CS molecules (Mn =10 kDa) from polyplexes (z-average = 45-55 nm). We demonstrated that generally TMP has to be maintained below 1.0 psid to prevent clogging of the membrane during the filtration process. Upon establishment of the operational conditions, it was demonstarted that TFF is capable in concentration of polyplexes up to sevenfold while preserving their physico-chemical properties. Furthermore, we demonstrated that a diafiltration volume of 5 is enough to remove up to 98% of free CS (TMP= 0.9 psid, shear rate = 7000 s^{-1}). Our results suggest that CS removal at a low shear rate (7000 s^{-1} with 98% CS removal at 5 DV) is more efficient than a higher shear rate (11000 s^{-1} with 92% CS removal at 5 DV), while there is not a significant difference in recovery yield of polyplexes at 5DV at the shear rates of 7000 s^{-1} and 11000 s^{-1} (81%, and 85% respectively). Also, diafiltration at a lower shear rate is faster due to higher permeate flux. TFF was found suitable for removal of unbound chitosan from the polyplexes while preserving their physicochemical properties, and their biological activity. Finally, decorating the purified polyplexes with HA led to the development of a new class of bioactive complexes with improved hemocompatibility.

This work allowed to develop an automated method for reproducible production of CS-based polyplexes in large batches with equivalent or even improved qualities as compared to manually prepared polyplexes. Establishment of tangential flow filtration technique for purification and concentration of large batches of CS-based polyplexes while preserving their physicochemical

properties and biological activities was another achievement of this work. Finally, this work demonstrated that HA-coating of purified polyplexes led to the development of new formulations with increased bioactivity and hemocompatibility. The accomplishments of this work represent important steps towards future clinical use of CS-based intravenous gene therapies.

Although beyond the scope of this work, the following recommendations are worth considering in the future:

1. *Integration of AIMS and TFF* – In this study, polyplexes were first produced via AIMS, then transferred to the TFF system for either purification or concentration. We programmed and automated both AIMS and TFF *via* the LabView software. One recommendation is to integrate them (by a sub-program) to a bigger platform as a complete production and purification/concentration line. The output vessel of AIMS can be the input (feed) container of the TFF system. This will eliminate manual works, and the risk of contamination.

2. *Optimization of TFF conditions for HA-coated polyplexes* – The main purpose of establishing TFF in this work was to purify the CS/siRNA polyplexes before addition of HA. We also used this technique for filtration of HA-coated complexes in the conditions that were optimal for uncoated polyplexes. Although the size of 10 kDa and 12 kDa HA molecules are close to the CS used (10 kDa), the size range and the viscosity of HA-coated sample is different from the one of uncoated polyplexes. Therefore, it is recommended to investigate the TFF operational parameters (*e.g.* membrane cut-off, TMP, and shear rate needed) for processing of HA-coated complexes.

3. *Assess the colloidal stability of HA-coated complexes* – HA-coated complexes demonstrated excellent hemocompatibility and bioactivity *in vitro*. One recommendation is to test their colloidal stability in physiological conditions (*e.g.* 150 mM NaCl, 25mg/mL BSA or 90% serum), prior transferring them for *in vivo* and clinical administration.

4. *Freeze-dry the purified uncoated and HA-coated samples and check their stability* – For long term storage, HA-coated complexes need to be freeze-dried before delivery to the end user. A recommendation here would be to evaluate their physico-chemical properties, bioactivity and hemocompatibility post freeze-drying.

BIBLIOGRAPHY

Abdelwahed, W., Degobert, G., Stainmesse, S., & Fessi, H. (2006). Freeze-drying of nanoparticles: Formulation, process and storage considerations. *Advanced Drug Delivery Reviews, 58*(15), 1688-1713. doi:DOI 10.1016/j.addr.2006.09.017

Aiba, S. (1989). Studies on Chitosan .2. Solution Stability and Reactivity of Partially N-Acetylated Chitosan Derivatives in Aqueous-Media. *International Journal of Biological Macromolecules, 11*(4), 249-252. doi:Doi 10.1016/0141-8130(89)90077-9

Aiba, S. (1992). Studies on Chitosan .4. Lysozymic Hydrolysis of Partially N-Acetylated Chitosans. *International Journal of Biological Macromolecules, 14*(4), 225-228. doi:Doi 10.1016/S0141-8130(05)80032-7

Al-Dosari, M. S., & Gao, X. (2009a). Nonviral gene delivery: principle, limitations, and recent progress. *AAPS J, 11*(4), 671-681. doi:10.1208/s12248-009-9143-y

Al-Dosari, M. S., & Gao, X. (2009b). Nonviral Gene Delivery: Principle, Limitations, and Recent Progress. *Aaps Journal, 11*(4), 671-681. doi:DOI 10.1208/s12248-009-9143-y

Alameh, M., Dejesus, D., Jean, M., Darras, V., Thibault, M., Lavertu, M., . . . Merzouki, A. (2012). Low molecular weight chitosan nanoparticulate system at low N:P ratio for nontoxic polynucleotide delivery. *Int J Nanomedicine, 7*, 1399-1414. doi:10.2147/IJN.S26571

Alameh, M., Jean, M., Dejesus, D., Buschmann, M. D., & Merzouki, A. (2010). Chitosanase-based method for RNA isolation from cells transfected with chitosan/siRNA nanocomplexes for real-time RT-PCR in gene silencing. *Int J Nanomedicine, 5*, 473-481.

Alameh, M., Lavertu, M., Tran-Khan, N., Chang, C. Y., Lesage, F., Bail, M., . . . Buschmann, M. D. (2017). siRNA delivery with chitosan: influence of chitosan molecular weight, degree of deacetylation and amine to phosphate ratio on in vitro silencing efficiency, hemocompatibility, biodistribution and in vivo efficacy. *Biomacromolecules*.

Albanese, A., & Chan, W. C. (2011). Effect of gold nanoparticle aggregation on cell uptake and toxicity. *ACS Nano, 5*(7), 5478-5489. doi:10.1021/nn2007496

Aliabadi, H. M., Landry, B., Sun, C., Tang, T., & Uludag, H. (2012). Supramolecular assemblies in functional siRNA delivery: Where do we stand? *Biomaterials, 33*(8), 2546-2569. doi:DOI 10.1016/j.biomaterials.2011.11.079

Anchordoquy, T. J., Armstrong, T. K., & Molina, M. D. (2005). Low molecular weight dextrans stabilize nonviral vectors during lyophilization at low osmolalities: Concentrating suspensions by rehydration to reduced volumes. *Journal of Pharmaceutical Sciences, 94*(6), 1226-1236. doi:Doi 10.1002/Jps.20353

Anders, C. B., Baker, J. D., Stahler, A. C., Williams, A. J., Sisco, J. N., Trefry, J. C., . . . Pavel Sizemore, I. E. (2012). Tangential flow ultrafiltration: a "green" method for the size selection and concentration of colloidal silver nanoparticles. *J Vis Exp*(68). doi:10.3791/4167

Andrew, S. M., Titus, J. A., & Zumstein, L. (2001). Dialysis and concentration of protein solutions. *Curr Protoc Immunol, Appendix 3*, Appendix 3H. doi:10.1002/0471142735.ima03hs21

Andrew, S. M., Titus, J. A., & Zumstein, L. (2002). Dialysis and concentration of protein solutions. *Curr Protoc Toxicol, Appendix 3*, A 3H 1-5. doi:10.1002/0471140856.txa03hs10

Ankerfors, C. (2008). *Polyelectrolyte complexes: Their preparation, adsorption behaviour, and effect on paper properties.* (PhD), Royal Institute of Technology (KTH), Stockholm, Sweden.

Ankerfors, C., Ondaral, S., Wagberg, L., & Odberg, L. (2010a). Using jet mixing to prepare polyelectrolyte complexes: Complex properties and their interaction with silicon oxide surfaces. *Journal of Colloid and Interface Science, 351*(1), 88-95. doi:DOI 10.1016/j.jcis.2010.07.027

Ankerfors, C., Ondaral, S., Wagberg, L., & Odberg, L. (2010b). Using jet mixing to prepare polyelectrolyte complexes: complex properties and their interaction with silicon oxide surfaces. *J Colloid Interface Sci, 351*(1), 88-95. doi:10.1016/j.jcis.2010.07.027

Ansari, M. A., Kim, K. Y., Anwar, K., & Kim, S. M. (2012). Vortex micro T-mixer with non-aligned inputs. *Chemical Engineering Journal, 181*, 6.

Balbino, T. A., Azzoni, A. R., & de la Torre, L. G. (2013). Microfluidic devices for continuous production of pDNA/cationic liposome complexes for gene delivery and vaccine therapy. *Colloids Surf B Biointerfaces, 111*, 203-210. doi:10.1016/j.colsurfb.2013.04.003

Ballew, H. W., Martinez, F. J., Markee, C., & Eddleman, R. T. (2002). *The ABCs of filtration and bioprocessing for the third millennium*. Rancho Dominguez, CA, USA: Spectrum Laboratories, Inc.

Basha, G., Novobrantseva, T. I., Rosin, N., Tam, Y. Y. C., Hafez, I. M., Wong, M. K., . . . Cullis, P. R. (2011). Influence of Cationic Lipid Composition on Gene Silencing Properties of Lipid Nanoparticle Formulations of siRNA in Antigen-Presenting Cells. *Molecular Therapy, 19*(12), 2186-2200. doi:Doi 10.1038/Mt.2011.190

Beck, P., Scherer, D., & Kreuter, J. (1990). Separation of Drug-Loaded Nanoparticles from Free Drug by Gel-Filtration. *Journal of Microencapsulation, 7*, 491-496.

Belliveau, N. M., Huft, J., Lin, P. J., Chen, S., Leung, A. K., Leaver, T. J., . . . Cullis, P. R. (2012). Microfluidic Synthesis of Highly Potent Limit-size Lipid Nanoparticles for In Vivo Delivery of siRNA. *Mol Ther Nucleic Acids, 1*, e37. doi:10.1038/mtna.2012.28

Bindig, U., Endisch, C., Fuhrhop, J. H., Komatsu, T., Tsuchida, E., & Siggel, U. (1998). Optimized polyelectrolyte stabilization procedures for polymeric porphyrin assemblies in water allow the analysis of minute photoreactivities. *Journal of Colloid and Interface Science, 199*(2), 123-130. doi:DOI 10.1006/jcis.1997.5311

Boussif, O., Lezoualch, F., Zanta, M. A., Mergny, M. D., Scherman, D., Demeneix, B., & Behr, J. P. (1995). A Versatile Vector for Gene and Oligonucleotide Transfer into Cells in Culture and in-Vivo - Polyethylenimine. *Proceedings of the National Academy of Sciences of the United States of America, 92*(16), 7297-7301. doi:DOI 10.1073/pnas.92.16.7297

Brugnerotto, J., Desbrieres, J., Roberts, G., & Rinaudo, M. (2001). Characterization of chitosan by steric exclusion chromatography. *Polymer, 42*, 7.

Bucur, C. B., Sui, Z., & Schlenoff, J. B. (2006). Ideal mixing in polyelectrolyte complexes and multilayers: Entropy driven assembly. *Journal of the American Chemical Society, 128*(42), 13690-13691. doi:Doi 10.1021/Ja064532c

Bucur, C. B., Sui, Z., & Schlenoff, J. B. (2006). Ideal Mixing in Polyelectrolyte Complexes and Multilayers: Entropy Driven Assembly. *Journal of the American Chemical Society, 128*(42), 13690-13691. doi:10.1021/ja064532c

Buschmann, M. D., Merzouki, A., Lavertu, M., Thibault, M., Jean, M., & Darras, V. (2013). Chitosans for delivery of nucleic acids. *Adv Drug Deliv Rev, 65*(9), 1234-1270. doi:10.1016/j.addr.2013.07.005

Bustin, S. A., Benes, V., Garson, J. A., Hellemans, J., Huggett, J., Kubista, M., . . . Wittwer, C. T. (2009). The MIQE guidelines: minimum information for publication of quantitative real-time PCR experiments. *Clin Chem, 55*(4), 611-622. doi:10.1373/clinchem.2008.112797

Carreno-Gomez, B., & Duncan, R. (1997). Evaluation of the properties of soluble chitosan and chitosan microspheres. *International Journal of Pharmaceutics, 148*, 231-240.

Chaturvedi, K., Ganguly, K., Kulkarni, A. R., Kulkarni, V. H., Nadagouda, M. N., Rudzinski, W. E., & Aminabhavi, T. M. (2011). Cyclodextrin-based siRNA delivery nanocarriers: a state-of-the-art review. *Expert Opinion on Drug Delivery, 8*(11), 1455-1468. doi:Doi 10.1517/17425247.2011.610790

Chen, J. H., Heitmann, J. A., & Hubbe, M. A. (2003). Dependency of polyelectrolyte complex stoichiometry on the order of addition. 1. Effect of salt concentration during streaming current titrations with strong poly-acid and polybase. *Colloids and Surfaces a-Physicochemical and Engineering Aspects, 223*(1-3), 215-230. doi:Doi 10.1016/S0927-7757(03)00222-X

Chiellini, E., Orsini, L. M., & Solaro, R. (2003). Polymeric nanoparticles based on polylactide and related co-polymers. *Macromol. Symp, 197*, 345-354.

Clement, J., Kiefer, K., Kimpfler, A., Garidel, P., & Peschka-Suss, R. (2005). Large-scale production of lipoplexes with long shelf-life. *Eur J Pharm Biopharm, 59*(1), 35-43. doi:10.1016/j.ejpb.2004.06.001

Corbet, C., Ragelle, H., Pourcelle, V., Vanvarenberg, K., Marchand-Brynaert, J., Preat, V., & Feron, O. (2016). Delivery of siRNA targeting tumor metabolism using non-covalent PEGylated chitosan nanoparticles: Identification of an optimal combination of ligand structure, linker and grafting method. *J Control Release, 223*, 53-63. doi:10.1016/j.jconrel.2015.12.020

Correa, S., Choi, K. Y., Dreaden, E. C., Renggli, K., Shi, A., Gu, L., . . . Hammond, P. T. (2016). Highly scalable, closed-loop synthesis of drug-loaded, layer-by-layer nanoparticles. *Adv Funct Mater, 26*(7), 991-1003. doi:10.1002/adfm.201504385

Cross flow filtration Method Handbook. (2014). (Vol. 03/2014 a1675).

Dalwadi, G., Benson, H. A. E., & Chen, Y. (2005). Comparison of diafiltration and tangential flow filtration for purification of nanoparticle suspensions. *Pharmaceutical Research, 22*(12), 2152-2162.

Dalwadi, G., & Sunderland, V. B. (2007). Purification of PEGylated nanoparticles using tangential flow filtration (TFF). *Drug Dev Ind Pharm, 33*(9), 1030-1039. doi:10.1080/03639040601180143

Danielsen, S., Varum, K. M., & Stokke, B. T. (2004). Structural analysis of chitosan mediated DNA condensation by AFM: Influence of chitosan molecular parameters. *Biomacromolecules, 5*(3), 928-936.

Dautzenberg, H. (1997). Polyelectrolyte complex formation in highly aggregating systems. 1. Effect of salt: Polyelectrolyte complex formation in the presence of NaCl. *Macromolecules, 30*(25), 7810-7815. doi:Doi 10.1021/Ma970803f

Dautzenberg, H., Hartmann, J., Grunewald, S., & Brand, F. (1996). Stoichiometry and structure of polyelectrolyte complex particles in diluted solutions. *Berichte Der Bunsen-Gesellschaft-Physical Chemistry Chemical Physics, 100*(6), 1024-1032.

Dautzenberg, H., Zintchenko, A., Konak, C., Reschel, T., Subr, V., & Ulbrich, K. (2001). Polycationic graft copolymers as carriers for oligonucleotide delivery. Complexes of oligonucleotides with polycationic graft copolymers. *Langmuir, 17*(10), 3096-3102. doi:Doi 10.1021/La001779t

Davies, L. A., Nunez-Alonso, G. A., Hebel, H. L., Scheule, R. K., Cheng, S. H., Hyde, S. C., & Gill, D. R. (2010). A novel mixing device for the reproducible generation of nonviral gene therapy formulations. *Biotechniques, 49*(3), 666-668. doi:10.2144/000113498

Davis, M. E., Pun, S. H., Bellocq, N. C., Reineke, T. M., Popielarski, S. R., Mishra, S., & Heidel, J. D. (2004). Self-assembling nucleic acid delivery vehicles via linear, water-soluble, cyclodextrin-containing polymers. *Current Medicinal Chemistry, 11*(2), 179-197. doi:Doi 10.2174/0929867043456179

de Gennes, P. G. (1979). *Scaling Concepts in Polymer Physics*: Cornell University Press.

Degerli, N., & Akpinar, M. A. (2001). A novel concentration method for concentrating solutions of protein extracts based on dialysis techniques. *Analytical Biochemistry, 297*(2), 192-194. doi:DOI 10.1006/abio.2001.5335

Dewey, R. A., Morrissey, G., Cowsill, C. M., Stone, D., Bolognani, F., Dodd, N. J. F., . . . Lowenstein, P. R. (1999). Chronic brain inflammation and persistent herpes simplex virus 1 thymidine kinase expression in survivors of syngeneic glioma treated by adenovirus-mediated gene therapy: Implications for clinical trials. *Nature Medicine, 5*(11), 1256-1263.

Doane, T. L., Chuang, C. H., Hill, R. J., & Burda, C. (2012). Nanoparticle zeta -potentials. *Acc Chem Res, 45*(3), 317-326. doi:10.1021/ar200113c

Dosio, F., Arpicco, S., Stella, B., & Fattal, E. (2016). Hyaluronic acid for anticancer drug and nucleic acid delivery. *Adv Drug Deliv Rev, 97*, 204-236. doi:10.1016/j.addr.2015.11.011

Drogoz, A., David, L., Rochas, C., Domard, A., & Delair, T. (2007). Polyelectrolyte complexes from polysaccharides: formation and stoichiometry monitoring. *Langmuir, 23*(22), 10950-10958. doi:10.1021/la7008545

Ebersold, M. F., & Zydney, A. L. (2004). Separation of protein charge variants by ultrafiltration. *Biotechnol Prog, 20*(2), 543-549. doi:10.1021/bp034264b

Escott, G. M., & Adams, D. J. (1995). Chitinase Activity in Human Serum and Leukocytes. *Infection and Immunity, 63*(12), 4770-4773.

Evani, S. J., & Ramasubramanian, A. K. (2001). Chapter 31: Hemocompatibility of Nanoparticles *Nanobiomaterials Handbook*: CRC Press.

Ewert, K., Slack, N. L., Ahmad, A., Evans, H. M., Lin, A. J., Samuel, C. E., & Safinya, C. R. (2004). Cationic lipid-DNA complexes for gene therapy: Understanding the relationship between complex structure and gene delivery pathways at the molecular level. *Current Medicinal Chemistry, 11*(2), 133-149. doi:Doi 10.2174/0929867043456160

Feng, Q., Lin, S., Zhang, K., Dong, C., Wu, T., Huang, H., . . . Bian, L. (2017). Sulfated hyaluronic acid hydrogels with retarded degradation and enhanced growth factor retention promote hMSC chondrogenesis and articular cartilage integrity with reduced hypertrophy. *Acta Biomater, 53*, 329-342. doi:10.1016/j.actbio.2017.02.015

Filion, D., Lavertu, M., & Buschmann, M. D. (2007). Ionization and solubility of chitosan solutions related to thermosensitive chitosan/glycerol-phosphate systems. *Biomacromolecules, 8*(10), 3224-3234. doi:Doi 10.1021/Bm700520m

Filion, M. C., & Phillips, N. C. (1998). Major limitations in the use of cationic liposomes for DNA delivery. *International Journal of Pharmaceutics, 162*(1-2), 159-170. doi:Doi 10.1016/S0378-5173(97)00423-7

Fox, J. L. (2000). Gene-therapy death prompts broad civil lawsuit. *Nature Biotechnology, 18*(11), 1136-1136. doi:Doi 10.1038/81104

Gao, S., Hein, S., Dagnaes-Hansen, F., Weyer, K., Yang, C., Nielsen, R., . . . Kjems, J. (2014). Megalin-mediated specific uptake of chitosan/siRNA nanoparticles in mouse kidney proximal tubule epithelial cells enables AQP1 gene silencing. *Theranostics, 4*(10), 1039-1051. doi:10.7150/thno.7866

Garcia-Fuentes, M., & Alonso, M. J. (2012). Chitosan-based drug nanocarriers: Where do we stand? *Journal of Controlled Release, 161*(2), 496-504. doi:DOI 10.1016/j.jconrel.2012.03.017

Gennes, P.-G. d. (1979). *Scaling Concepts in Polymer Physics*. New York, USA: Cornell University Press.

Green, D., & Perry, R. (2007). *Perry's Chemical Engineers' Handbook, Eighth Edition*: McGraw-Hill Education.

Grigsby, C. L., Ho, Y. P., Lin, C., Engbersen, J. F., & Leong, K. W. (2013). Microfluidic preparation of polymer-nucleic acid nanocomplexes improves nonviral gene transfer. *Sci Rep, 3*, 3155. doi:10.1038/srep03155

Hammady, T., Nadeau, V., & Hildgen, P. (2006). Microemulsion and diafiltration approaches: an attempt to maximize the global yield of DNA-loaded nanospheres. *Eur J Pharm Biopharm, 62*, 143-154.

Hanauer, M., Pierrat, S., Zins, I., Lotz, A., & Sonnichsen, C. (2007). Separation of nanoparticles by gel electrophoresis according to size and shape. *Nano Lett, 7*(9), 2881-2885. doi:10.1021/nl071615y

Hascall, V. C., Majors, A. K., De La Motte, C. A., Evanko, S. P., Wang, A., Drazba, J. A., . . . Wight, T. N. (2004). Intracellular hyaluronan: a new frontier for inflammation? *Biochim Biophys Acta, 1673*(1-2), 3-12. doi:10.1016/j.bbagen.2004.02.013

Heidel, J. D., Hu, S. W., Liu, X. F., Triche, T., & Davis, M. E. (2004). Cyclodextrin-containing polycations (CDPs) for in vivo delivery of siRNA. *Abstracts of Papers of the American Chemical Society, 227*, U221-U221.

Hirsjarvi, S., Peltonen, L., & Hirvonen, J. (2009). Effect of Sugars, Surfactant, and Tangential Flow Filtration on the Freeze-Drying of Poly(lactic acid) Nanoparticles. *Aaps Pharmscitech, 10*(2), 488-494. doi:DOI 10.1208/s12249-009-9236-z

Holzerny, P., Ajdini, B., Heusermann, W., Bruno, K., Schuleit, M., Meinel, L., & Keller, M. (2012). Biophysical properties of chitosan/siRNA polyplexes: profiling the polymer/siRNA interactions and bioactivity. *J Control Release, 157*(2), 297-304. doi:10.1016/j.jconrel.2011.08.023

Howard, K. A. (2009). Delivery of RNA interference therapeutics using polycation-based nanoparticles. *Advanced Drug Delivery Reviews, 61*(9), 710-720. doi:DOI 10.1016/j.addr.2009.04.001

Howard, K. A., Rahbek, U. L., Liu, X., Damgaard, C. K., Glud, S. Z., Andersen, M. O., . . . Kjems, J. (2006a). RNA interference in vitro and in vivo using a novel chitosan/siRNA nanoparticle system. *Mol Ther, 14*(4), 476-484. doi:10.1016/j.ymthe.2006.04.010

Howard, K. A., Rahbek, U. L., Liu, X. D., Damgaard, C. K., Glud, S. Z., Andersen, M. O., . . . Kjems, J. (2006b). RNA interference in vitro and in vivo using a chitosan/siRNA nanoparticle system. *Molecular Therapy, 14*(4), 476-484. doi:DOI 10.1016/j.ymthe.2006.04.010

Huang, M., Fong, C. W., Khor, E., & Lim, L. Y. (2005). Transfection efficiency of chitosan vectors: Effect of polymer molecular weight and degree of deacetylation. *Journal of Controlled Release, 106*(3), 391-406. doi:DOI 10.1016/j.cornel.2005.05.004

Huang, Q. G., Zhu, F. M., Wu, Q., & Lin, S. G. (2001). The synthesis of high molecular weight polybutene-1 catalyzed by (CpTi)-Ti-star(OBz)(3)/MAO. *Polymer International, 50*(1), 45-48. doi:Doi 10.1002/1097-0126(200101)50:1<45::Aid-Pi531>3.0.Co;2-S

Ikonen, M., Murtomaki, L., & Kontturi, K. (2008). Controlled complexation of plasmid DNA with cationic polymers: Effect of surfactant on the complexation and stability of the complexes. *Colloids and Surfaces B-Biointerfaces, 66*(1), 77-83. doi:DOI 10.1016/j.colsurfb.2008.05.012

Ishii, T., Okahata, Y., & Sato, T. (2001). Mechanism of cell transfection with plasmid/chitosan complexes. *Biochimica Et Biophysica Acta-Biomembranes, 1514*(1), 51-64. doi:Doi 10.1016/S0005-2736(01)00362-5

Issa, M. M., Koping-Hoggard, M., Tommeraas, K., Varum, K. M., Christensen, B. E., Strand, S. P., & Artursson, P. (2006). Targeted gene delivery with trisaccharide-substituted chitosan oligomers in vitro and after lung administration in vivo. *Journal of Controlled Release, 115*(1), 103-112. doi:DOI 10.1016/j.jconrel.2006.06.029

Jackson, W. C., Kuckuck, F., Edwards, B. S., Mammoli, A., Gallegos, C. M., Lopez, G. P., . . . Sklar, L. A. (2002). Mixing small volumes for continuous high-throughput flow cytometry: performance of a mixing Y and peristaltic sample delivery. *Cytometry, 47*(3), 183-191.

Jean, M., Alameh, M., Buschmann, M. D., & Merzouki, A. (2011a). Effective and safe gene-based delivery of GLP-1 using chitosan/plasmid-DNA therapeutic nanocomplexes in an animal model of type 2 diabetes. *Gene Ther, 18*(8), 807-816. doi:10.1038/gt.2011.25

Jean, M., Alameh, M., Buschmann, M. D., & Merzouki, A. (2011b). Effective and safe gene-based delivery of GLP-1 using chitosan/plasmid-DNA therapeutic nanocomplexes in an animal model of type 2 diabetes. *Gene Therapy, 18*(8), 807-816. doi:Doi 10.1038/Gt.2011.25

Jean, M., Alameh, M., De Jesus, D., Thibault, M., Lavertu, M., Darras, V., . . . Merzouki, A. (2012a). Chitosan-based therapeutic nanoparticles for combination gene therapy and gene silencing of in vitro cell lines relevant to type 2 diabetes. *European Journal of Pharmaceutical Sciences, 45*(1-2), 138-149. doi:DOI 10.1016/j.ejps.2011.10.029

Jean, M., Alameh, M., De Jesus, D., Thibault, M., Lavertu, M., Darras, V., . . . Merzouki, A. (2012b). Chitosan-based therapeutic nanoparticles for combination gene therapy and gene silencing of in vitro cell lines relevant to type 2 diabetes. *Eur J Pharm Sci, 45*(1-2), 138-149. doi:10.1016/j.ejps.2011.10.029

Jean, M., Smaoui, F., Lavertu, M., Methot, S., Bouhdoud, L., Buschmann, M. D., & Merzouki, A. (2009). Chitosan-plasmid nanoparticle formulations for IM and SC delivery of recombinant FGF-2 and PDGF-BB or generation of antibodies. *Gene Ther, 16*(9), 1097-1110. doi:10.1038/gt.2009.60

Jeong, J. H., Kim, S. W., & Park, T. G. (2007). Molecular design of functional polymers for gene therapy. *Progress in Polymer Science, 32*(11), 1239-1274. doi:DOI 10.1016/j.progpolymsci.2007.05.019

Ji, A. M., Su, D., Che, O., Li, W. S., Sun, L., Zhang, Z. Y., . . . Xu, F. (2009). Functional gene silencing mediated by chitosan/siRNA nanocomplexes. *Nanotechnology, 20*(40), 405103. doi:10.1088/0957-4484/20/40/405103

Johnson, B. K., & Prud'homme, R. K. (2003). Chemical processing and micromixing in confined impinging jets. *Aiche Journal, 49*(9), 2264-2282. doi:DOI 10.1002/aic.690490905

Johnson, B. K., & Prud’homme, R. K. (2003). Chemical Processing and Micromixing in Confined Impinging Jets. *AIChE Journal, 49*(9), 2264-2282.

Jornitz, M. J., Jornitz, M. W., & Meltzer, T. H. (2007). *Filtration and Purification in the Biopharmaceutical Industry, Second Edition*: CRC Press.

Kabanov, V. A., Zezin, A. B., Kasaikin, V. A., Zakharova, J. A., Litmanovich, E. A., & Ivleva, E. M. (2003). Self-assembly of ionic amphiphiles on polyelectrolyte chains. *Polymer International, 52*(10), 1566-1572. doi:Doi 10.1002/Pi.1340

Kahn, D. W., Butler, M. D., Cohen, D. L., Gordon, M., Kahn, J. W., & Winkler, M. E. (2000). Purification of Plasmid DNA by Tangential Flow Filtration. *BIOTECHNOLOGY AND BIOENGINEERING, 69*.

Kakehi, K., Kinoshita, M., & Yasueda, S. (2003). Hyaluronic acid: separation and biological implications. *J Chromatogr B Analyt Technol Biomed Life Sci, 797*(1-2), 347-355.

Karbownik, M. S., & Nowak, J. Z. (2013). Hyaluronan: towards novel anti-cancer therapeutics. *Pharmacol Rep, 65*(5), 1056-1074.

Kasper, J. C., Schaffert, D., Ogris, M., Wagner, E., & Friess, W. (2011). The establishment of an up-scaled micro-mixer method allows the standardized and reproducible preparation of well-defined plasmid/LPEI polyplexes. *Eur J Pharm Biopharm, 77*(1), 182-185. doi:10.1016/j.ejpb.2010.11.012

Katas, H., & Alpar, H. O. (2006). Development and characterisation of chitosan nanoparticles for siRNA delivery. *J Control Release, 115*(2), 216-225. doi:10.1016/j.jconrel.2006.07.021

Kean, T., & Thanou, M. (2010). Biodegradation, biodistribution and toxicity of chitosan. *Advanced Drug Delivery Reviews, 62*(1), 3-11. doi:DOI 10.1016/j.addr.2009.09.004

Kiang, T., Wen, H., Lim, H. W., & Leong, K. W. (2004). The effect of the degree of chitosan deacetylation on the efficiency of gene transfection. *Biomaterials, 25*(22), 5293-5301. doi:DOI 10.1016/j.biomaterials.2003.12.036

Klausner, E. A., Zhang, Z., Chapman, R. L., Multack, R. F., & Volin, M. V. (2010). Ultrapure chitosan oligomers as carriers for corneal gene transfer. *Biomaterials, 31*(7), 1814-1820. doi:10.1016/j.biomaterials.2009.10.031

Koping-Hoggard, M., Tubulekas, I., Guan, H., Edwards, K., Nilsson, M., Varum, K. M., & Artursson, P. (2001). Chitosan as a nonviral gene delivery system. Structure-property relationships and characteristics compared with polyethylenimine in vitro and after lung administration in vivo. *Gene Therapy, 8*(14), 1108-1121. doi:DOI 10.1038/sj.gt.3301492

Koping-Hoggard, M., Varum, K. M., Issa, M., Danielsen, S., Christensen, B. E., Stokke, B. T., & Artursson, P. (2004). Improved chitosan-mediated gene delivery based on easily dissociated chitosan polyplexes of highly defined chitosan oligomers. *Gene Therapy, 11*(19), 1441-1452. doi:DOI 10.1038/sj.gt.3302312

Kwon, H. Y., Lee, J. Y., Choi, S. W., Jang, Y. S., & Kim, J. H. (2001). Preparation of PLGA nanoparticles containing estrogen by emulsification-diffusion method. *Colloids and Surfaces a-Physicochemical and Engineering Aspects, 182*(1-3), 123-130. doi:Doi 10.1016/S0927-7757(00)00825-6

Lankalapalli, S., & Kolapalli, V. R. M. (2009). Polyelectrolyte complexes: A review of their applicability in drug delivery technology. *Indian Journal of Pharmaceutical Sciences, 71*(5), 481-487.

Latulippe, D. R., & Zydney, A. L. (2010). Radius of gyration of plasmid DNA isoforms from static light scattering. *Biotechnol Bioeng, 107*(1), 134-142. doi:10.1002/bit.22787

Lavertu, M., Methot, S., Tran-Khanh, N., & Buschmann, M. D. (2006). High efficiency gene transfer using chitosan/DNA nanoparticles with specific combinations of molecular weight and degree of deacetylation. *Biomaterials, 27*(27), 4815-4824. doi:10.1016/j.biomaterials.2006.04.029

Lavertu, M., Xia, Z., Serreqi, A. N., Berrada, M., Rodrigues, A., Wang, D., . . . Gupta, A. (2003). A validated 1H NMR method for the determination of the degree of deacetylation of chitosan. *J Pharm Biomed Anal, 32*(6), 1149-1158.

Lazutin, A. A., Semenov, A. N., & Vasilevskaya, V. V. (2012). Polyelectrolyte Complexes Consisting of Macromolecules With Varied Stiffness: Computer Simulation. *Macromolecular Theory and Simulations, 21*(5), 328-339. doi:DOI 10.1002/mats.201100097

Lee, J. B., Zhang, K. X., Tam, Y. Y. C., Tam, Y. K., Belliveau, N. M., Sung, V. Y. C., . . . Cullis, P. R. (2012). Lipid nanoparticle siRNA systems for silencing the androgen receptor in human prostate cancer in vivo. *International Journal of Cancer, 131*(5), E781-E790. doi:Doi 10.1002/Ijc.27361

Leung, A. K., Hafez, I. M., Baoukina, S., Belliveau, N. M., Zhigaltsev, I. V., Afshinmanesh, E., . . . Cullis, P. R. (2012). Lipid Nanoparticles Containing siRNA Synthesized by Microfluidic Mixing Exhibit an Electron-Dense Nanostructured Core. *J Phys Chem C Nanomater Interfaces, 116*(34), 18440-18450. doi:10.1021/jp303267y

Leung, A. K. K., Hafez, I. M., Baoukina, S., Belliveau, N. M., Zhigaltsev, I. V., Afshinmanesh, E., . . . Cullis, P. R. (2012). Lipid Nanoparticles Containing siRNA Synthesized by Microfluidic Mixing Exhibit an Electron-Dense Nanostructured Core (vol 116, pg 18440, 2012). *Journal of Physical Chemistry C, 116*(41), 22104-22104. doi:Doi 10.1021/Jp3088786

Liang, J., Jiang, D., & Noble, P. W. (2016). Hyaluronan as a therapeutic target in human diseases. *Adv Drug Deliv Rev, 97*, 186-203. doi:10.1016/j.addr.2015.10.017

Lim, M. J., Min, S. H., Lee, J. J., Kim, I. C., Kim, J. T., Lee, D. C., . . . Yeom, Y. I. (2006). Targeted therapy of DNA tumor virus-associated cancers using virus-activated transcription factors. *Molecular Therapy, 13*(5), 899-909. doi:DOI 10.1016/j.ymthe.2005.11.023

Limayem, I., Charcosset, C., & Fessi, H. (2004). Purification of nanoparticle suspensions by a concentration/diafiltration process. *Separation and Purification Technology, 38*(1), 1-9.

Liu, H. F., Ma, J., Winter, C., & Bayer, R. (2010). Recovery and purification process development for monoclonal antibody production. *MAbs, 2*(5), 480-499.

Liu, W. G., & De Yao, K. (2002). Chitosan and its derivatives - a promising non-viral vector for gene transfection. *Journal of Controlled Release, 83*(1), 1-11.

Liu, X., Howard, K. A., Dong, M., Andersen, M. O., Rahbek, U. L., Johnsen, M. G., . . . Kjems, J. (2007). The influence of polymeric properties on chitosan/siRNA nanoparticle formulation and gene silencing. *Biomaterials, 28*(6), 1280-1288. doi:10.1016/j.biomaterials.2006.11.004

Liu, X. D., Howard, K. A., Dong, M. D., Andersen, M. O., Rahbek, U. L., Johnsen, M. G., . . . Kjems, J. (2007). The influence of polymeric properties on chitosan/siRNA nanoparticle formulation and gene silencing. *Biomaterials, 28*(6), 1280-1288. doi:DOI 10.1016/j.biomaterials.2006.11.004

Lu, M., Ho, Y. P., Grigsby, C. L., Nawaz, A. A., Leong, K. W., & Huang, T. J. (2014). Three-dimensional hydrodynamic focusing method for polyplex synthesis. *ACS Nano, 8*(1), 332-339. doi:10.1021/nn404193e

Lv, H. T., Zhang, S. B., Wang, B., Cui, S. H., & Yan, J. (2006). Toxicity of cationic lipids and cationic polymers in gene delivery. *Journal of Controlled Release, 114*(1), 100-109. doi:DOI 10.1016/j.jconrel.2006.04.014

Ma, P. L. (2010). *Formation et caractérisation physicochimique des complexes ADN/chitosane pour la thérapie génique.* (Ph.D.), Université de Montréal, École Polytechnique de Montréal, Montreal.

Ma, P. L., Lavertu, M., Winnik, F. M., & Buschmann, M. D. (2009). New insights into chitosan-DNA interactions using isothermal titration microcalorimetry. *Biomacromolecules, 10*(6), 1490-1499. doi:10.1021/bm900097s

MacLaughlin, F. C., Mumper, R. J., Wang, J. J., Tagliaferri, J. M., Gill, I., Hinchcliffe, M., & Rolland, A. P. (1998a). Chitosan and depolymerized chitosan oligomers as condensing carriers for in vivo plasmid delivery. *Journal of Controlled Release, 56*(1-3), 259-272. doi:Doi 10.1016/S0168-3659(98)00097-2

MacLaughlin, F. C., Mumper, R. J., Wang, J. J., Tagliaferri, J. M., Gill, I., Hinchcliffe, M., & Rolland, A. P. (1998b). Chitosan and depolymerized chitosan oligomers as condensing carriers for in vivo plasmid delivery. *Journal of Controlled Release, 56*(1-3), 259–272.

Magnani, A., Silvestri, V., & Barbucci, R. (1999). Hyaluronic acid and sulfated hyaluronic acid in aqueous solution: effect of the sulfation on the protonation and complex formation with Cu2+ and Zn2+ ions. *macromolecular chemistry and physics, 200*, 2003–2014.

Malhotra, M., Kulamarva, A., Sebak, S., Paul, A., Bhathena, J., Mirzaei, M., & Prakash, S. (2009). Ultrafine chitosan nanoparticles as an efficient nucleic acid delivery system targeting neuronal cells. *Drug Dev Ind Pharm, 35*(6), 719-726. doi:10.1080/03639040802526789

Malhotra, M., Lane, C., Tomaro-Duchesneau, C., Saha, S., & Prakash, S. (2011). A novel method for synthesizing PEGylated chitosan nanoparticles: strategy, preparation, and in vitro analysis. *Int J Nanomedicine, 6*, 485-494. doi:10.2147/IJN.S17190

Malhotra, M., Tomaro-Duchesneau, C., Saha, S., Kahouli, I., & Prakash, S. (2013). Development and characterization of chitosan-PEG-TAT nanoparticles for the intracellular delivery of siRNA. *Int J Nanomedicine, 8*, 2041-2052. doi:10.2147/IJN.S43683

Malmo, J., Sorgard, H., Varum, K. M., & Strand, S. P. (2012a). siRNA delivery with chitosan nanoparticles: Molecular properties favoring efficient gene silencing. *Journal of Controlled Release, 158*(2), 261-268. doi:DOI 10.1016/j.jconrel.2011.11.012

Malmo, J., Sorgard, H., Varum, K. M., & Strand, S. P. (2012b). siRNA delivery with chitosan nanoparticles: Molecular properties favoring efficient gene silencing. *J Control Release, 158*(2), 261-268. doi:10.1016/j.jconrel.2011.11.012

Mao, H. Q., Roy, K., Troung-Le, V. L., Janes, K. A., Lin, K. Y., Wang, Y., . . . Leong, K. W. (2001). Chitosan-DNA nanoparticles as gene carriers: synthesis, characterization and transfection efficiency. *Journal of Controlled Release, 70*(3), 399-421. doi:Doi 10.1016/S0168-3659(00)00361-8

Mao, S., Sun, W., & Kissel, T. (2010). Chitosan-based formulations for delivery of DNA and siRNA. *Adv Drug Deliv Rev, 62*(1), 12-27. doi:10.1016/j.addr.2009.08.004

Mao, S. R., Sun, W., & Kissel, T. (2010). Chitosan-based formulations for delivery of DNA and siRNA. *Advanced Drug Delivery Reviews, 62*(1), 12-27. doi:DOI 10.1016/j.addr.2009.08.004

Michaels, A. S., & Miekka, R. G. (1961). Polycation-Polyanion Complexes: Preparation and Properties of Poly-(vinylbenzyltrimethylammonium) Poly-(Styrenesulfonate). *The Journal of Physical Chemistry, 65*(10), 1765-1773.

Millipore. (2003). *Protein Concentration and Diafiltration by Tangential Flow Filtration*. TB032 Rev. C 06/03 03-117, Billerica, MA 01821 U.S.A.

Millipore. (2013). *A Hands-On Guide to Ultrafiltration/Diafiltration Optimization using Pellicon Cassettes*. Billerica, MA USA.

Mortimer, I., Tam, P., MacLachlan, I., Graham, R. W., Saravolac, E. G., & Joshi, P. B. (1999). Cationic lipid-mediated transfection of cells in culture requires mitotic activity. *Gene Therapy, 6*(3), 403-411. doi:DOI 10.1038/sj.gt.3300837

Muller, M. (1974). Sizing, Shaping and Pharmaceutical Applications of Polyelectrolyte Complex Nanoparticles. In Z. A. Rogovin (Ed.), *Advances in polymer science*: Wiley.

Muller, M., Kessler, B., Frohlich, J., Poeschla, S., & Torger, B. (2011). Polyelectrolyte Complex Nanoparticles of Poly(ethyleneimine) and Poly(acrylic acid): Preparation and Applications. *Polymers, 3*(2), 762-778. doi:Doi 10.3390/Polym3020762

Nafee, N., Taetz, S., Schneider, M., Schaefer, U. F., & Lehr, C. M. (2007). Chitosan-coated PLGA nanoparticles for DNA/RNA delivery: Effect of the formulation parameters on complexation and transfection of antisense oligonucleotides. *Nanomedicine-Nanotechnology Biology and Medicine, 3*(3), 173-183. doi:DOI 10.1016/j.nano.2007.03.006

Necas, J., Bartosikova, L., Brauner, P., & Kolar, J. (2008). Hyaluronic acid (hyaluronan): a review. *Veterinarni Medicina, 53*, 397–411.

Nel, A. E., Madler, L., Velegol, D., Xia, T., Hoek, E. M., Somasundaran, P., . . . Thompson, M. (2009). Understanding biophysicochemical interactions at the nano-bio interface. *Nat Mater, 8*(7), 543-557. doi:10.1038/nmat2442

Nguyen, S., Winnik, F. M., & Buschmann, M. D. (2009). Improved reproducibility in the determination of the molecular weight of chitosan by analytical size exclusion chromatography. *Carbohydrate Polymers 75*(3), 6.

Nielsen, E. J., Nielsen, J. M., Becker, D., Karlas, A., Prakash, H., Glud, S. Z., . . . Howard, K. A. (2010). Pulmonary gene silencing in transgenic EGFP mice using aerosolised chitosan/siRNA nanoparticles. *Pharmaceutical Research, 27*(12), 2520-2527. doi:10.1007/s11095-010-0255-y

Nimesh, S., Thibault, M. M., Lavertu, M., & Buschmann, M. D. (2010a). Enhanced gene delivery mediated by low molecular weight chitosan/DNA complexes: effect of pH and serum. *Mol Biotechnol, 46*(2), 182-196. doi:10.1007/s12033-010-9286-1

Nimesh, S., Thibault, M. M., Lavertu, M., & Buschmann, M. D. (2010b). Enhanced Gene Delivery Mediated by Low Molecular Weight Chitosan/DNA Complexes: Effect of pH and Serum. *Molecular Biotechnology, 46*(2), 182-196. doi:DOI 10.1007/s12033-010-9286-1

Novasep. (2016). Hydrophylic Organic Membrane. Retrieved from https://www.bioprocessonline.com/doc/hystreamtrade-membranes-series-0002

Ou, Z. Y., & Muthukumar, M. (2006). Entropy and enthalpy of polyelectrolyte complexation: Langevin dynamics simulations. *Journal of Chemical Physics, 124*(15). doi:Artn 154902

Doi 10.1063/1.2178803

Oupicky, D., Konak, C., Ulbrich, K., Wolfert, M. A., & Seymour, L. W. (2000). DNA delivery systems based on complexes of DNA with synthetic polycations and their copolymers. *Journal of Controlled Release, 65*(1-2), 149-171. doi:Doi 10.1016/S0168-3659(99)00249-7

Paulena, R., Fikara, M., Foleyb, G., Kovácsc, Z., & Czermakc, P. (2012). Optimal feeding strategy of diafiltration buffer in batch membrane processes. *Journal of Membrane Science, 411-412*, 160–172.

Pavan, G. M., Mintzer, M. A., Simanek, E. E., Merkel, O. M., Kissel, T., & Danani, A. (2010). Computational insights into the interactions between DNA and siRNA with "rigid" and "flexible" triazine dendrimers. *Biomacromolecules, 11*(3), 721-730. doi:10.1021/bm901298t

Philipp, B., Dautzenberg, H., Linow, K. J., Kotz, J., & Dawydoff, W. (1989). Poly-Electrolyte Complexes - Recent Developments and Open Problems. *Progress in Polymer Science, 14*(1), 91-172. doi:Doi 10.1016/0079-6700(89)90018-X

Pickenhahn, V. D., Darras, V., Dziopa, F., Biniecki, K., De Crescenzo, G., Lavertu, M., & Buschmann, M. D. (2015). Regioselective Thioacetylation of Chitosan End-Groups for Nanoparticle Gene Delivery Systems. *Chemical Science*.

Platt, V. M., & Szoka, F. C. (2008). Anticancer therapeutics: targeting macromolecules and nanocarriers to hyaluronan or CD44, a hyaluronan receptor. *Molecular Pharmaceutics, 5*, 474–486.

Prakash, S., Malhotra, M., & Rengaswamy, V. (2010). Nonviral siRNA delivery for gene silencing in neurodegenerative diseases. *Methods Mol Biol, 623*, 211-229. doi:10.1007/978-1-60761-588-0_14

Pun, S. H., Bellocq, N. C., Liu, A. J., Jensen, G., Machemer, T., Quijano, E., . . . Davis, M. E. (2004). Cyclodextrin-modified polyethylenimine polymers for gene delivery. *Bioconjugate Chemistry, 15*(4), 831-840. doi:Doi 10.1021/Bc049891g

Ragelle, H., Riva, R., Vandermeulen, G., Naeye, B., Pourcelle, V., Le Duff, C. S., . . . Preat, V. (2014). Chitosan nanoparticles for siRNA delivery: optimizing formulation to increase stability and efficiency. *J Control Release, 176*, 54-63. doi:10.1016/j.jconrel.2013.12.026

Ragelle, H., Vandermeulen, G., & Preat, V. (2013). Chitosan-based siRNA delivery systems. *J Control Release, 172*(1), 207-218. doi:10.1016/j.jconrel.2013.08.005

Raja, M. A., Katas, H., & Jing Wen, T. (2015). Stability, Intracellular Delivery, and Release of siRNA from Chitosan Nanoparticles Using Different Cross-Linkers. *PLoS One, 10*(6), e0128963. doi:10.1371/journal.pone.0128963

Ralf Kuriyel, M. F., and Gary W. Jung. (2008). Advancements in membrane processes for pharmaceutical applications. In A. K. Pabby, S. S. H. Rizvi, & A. M. Sastre (Eds.),

Handbook of Membrane Separations: Chemical, Pharmaceutical, Food, and Biotechnological Applications: Taylor & Francis.

Rao, S. B., & Sharma, C. P. (1997). Use of chitosan as a biomaterial: studies on its safety and hemostatic potential. *Journal of Biomedical Materials Research, 34*, 21-18.

Rinaudo, M. (2006). Chitin and chitosan: Properties and applications. *Prog. Polym. Sci., 31*.

Robertson, J. D., Rizzello, L., Avila-Olias, M., Gaitzsch, J., Contini, C., Magon, M. S., . . . Battaglia, G. (2016). Purification of Nanoparticles by Size and Shape. *Sci Rep, 6*, 27494. doi:10.1038/srep27494

Romoren, K., Pedersen, S., Smistad, G., Evensen, O., & Thu, B. J. (2003). The influence of formulation variables on in vitro transfection efficiency and physicochemical properties of chitosan-based polyplexes. *International Journal of Pharmaceutics, 261*(1-2), 115-127. doi:Doi 10.1016/S0378-5173(03)00301-6

Rungsardthong, U., Ehtezazi, T., Bailey, L., Armes, S. P., Garnett, M. C., & Stolnik, S. (2003). Effect of polymer ionization on the interaction with DNA in nonviral gene delivery systems. *Biomacromolecules, 4*(3), 683-690. doi:Doi 10.1021/Bm025736y

Saptarshi, S. R., Duschl, A., & Lopata, A. L. (2013). Interaction of nanoparticles with proteins: relation to bio-reactivity of the nanoparticle. *J Nanobiotechnology, 11*, 26. doi:10.1186/1477-3155-11-26

Sato, T., Ishii, T., & Okahata, Y. (2001). In vitro gene delivery mediated by chitosan. Effect of pH, serum, and molecular mass of chitosan on the transfection efficiency. *Biomaterials, 22*(15), 2075-2080. doi:Doi 10.1016/S0142-9612(00)00385-9

Schwartz, L. (2003). Diafiltration for Desalting or Buffer Exchange: BioProcess International.

Schwartz, L. (2003). *Diafiltration: A Fast, Efficient Method for Desalting, or Buffer Exchange of Biological Samples*. (PN 33289, 2/03, 2.5k, GN02.0629).

Serway, D., & Tamashiro, W. A. (2010). Purification of Nanoparticles by Hollow Fiber Diafiltration. Retrieved from

Sherman, L., Sleeman, J., Herrlich, P., & Ponta, H. (1994). Hyaluronate receptors: key players in growth, differentiation, migration and tumor progression. *Curr Opin Cell Biol, 6*(5), 726-733.

Shire, S. J., Shahrokh, Z., & Liu, J. (2004). Challenges in the development of high protein concentration formulations. *Journal of Pharmaceutical Sciences, 93*(6), 1390-1402. doi:Doi 10.1002/Jps.20079

Shovsky, A. V., Varga, I., Makuska, R., & Claesson, P. M. (2009). Formation and Stability of Soluble Stochiometric Polyelectrolyte Complexes: Effects of Charge Density and Polyelectrolyte Concentration. *Journal of Dispersion Science and Technology, 30*(6), 980-988. doi:Pii 911745343

Son, K. K., Tkach, D., & Patel, D. H. (2000). Zeta potential of transfection complexes formed in serum-free medium can predict in vitro gene transfer efficiency of transfection reagent. *Biochim Biophys Acta, 1468*(1-2), 11-14.

Standard Test Method for Analysis of Hemolytic Properties of Nanoparticles. (2013). West Conshohocken, PA: ASTM International.

Stella, B., Arpicco, S., Rocco, F., Marsaud, V., Renoir, J. M., Cattel, L., & Couvreur, P. (2007). Encapsulation of gemcitabine lipophilic derivatives into polycyanoacrylate nanospheres and nanocapsules. *International Journal of Pharmaceutics, 344*(1-2), 71-77. doi:DOI 10.1016/j.ijpharm.2007.06.006

Strand, S. P., Danielsen, S., Christensen, B. E., & Varum, K. M. (2005). Influence of chitosan structure on the formation and stability of DNA-chitosan polyelectrolyte complexes. *Biomacromolecules, 6*(6), 3357-3366.

Stroock, A. D., Dertinger, S. K., Ajdari, A., Mezic, I., Stone, H. A., & Whitesides, G. M. (2002). Chaotic mixer for microchannels. *Science, 295*(5555), 647-651. doi:10.1126/science.1066238

Sweeney, S. F., Woehrle, G. H., & Hutchison, J. E. (2006). Rapid purification and size separation of gold nanoparticles via diafiltration. *J Am Chem Soc, 128*(10), 3190-3197. doi:10.1021/ja0558241

Tavakoli Naeini, A., Soliman, O. Y., Alameh, M. G., Lavertu, M., & Buschmann, M. D. (2017). Automated in-line mixing system for large scale production of chitosan-based polyplexes. *J Colloid Interface Sci, 500*, 253-263. doi:10.1016/j.jcis.2017.04.013

Thibault, M., Nimesh, S., Lavertu, M., & Buschmann, M. D. (2010a). Intracellular trafficking and decondensation kinetics of chitosan-pDNA polyplexes. *Mol Ther, 18*(10), 1787-1795. doi:10.1038/mt.2010.143

Thibault, M., Nimesh, S., Lavertu, M., & Buschmann, M. D. (2010b). Intracellular Trafficking and Decondensation Kinetics of Chitosan-pDNA Polyplexes. *Molecular Therapy, 18*(10), 1787-1795. doi:Doi 10.1038/Mt.2010.143

Thunemann, A. F. (2004). *Polyelectrolytes with Defined Molecular Architecture II*: Springer Berlin Heidelberg.

Thunemann, A. F., Muller, M., Dautzenberg, H., Joanny, J. F. O., & Lowen, H. (2004a). Polyelectrolyte Complexes. In M. Schmidt (Ed.), *Polyelectrolytes with Defined Molecular Architecture Ii*: Springer.

Thunemann, A. F., Muller, M., Dautzenberg, H., Joanny, J. F. O., & Lowen, H. (2004b). Polyelectrolyte complexes. *Polyelectrolytes with Defined Molecular Architecture Ii, 166*, 113-171. doi:Doi 10.1007/B11350

Torchilin, V. P., & Trubetskoy, V. S. (1995). Which polymers can make nanoparticulate drug carriers long-circulating? *Advanced Drug Delivery Reviews, 16*, 141-155.

Tousignant, J. D., Gates, A. L., Ingram, L. A., Johnson, C. L., Nietupski, J. B., Cheng, S. H., . . . Scheule, R. K. (2000). Comprehensive analysis of the acute toxicities induced by systemic administration of cationic lipid:plasmid DNA complexes in mice. *Hum Gene Ther, 11*(18), 2493-2513. doi:10.1089/10430340050207984

Trefry, J. C., Monahan, J. L., Weaver, K. M., Meyerhoefer, A. J., Markopolous, M. M., Arnold, Z. S., . . . Pavel, I. E. (2010). Size selection and concentration of silver nanoparticles by

tangential flow ultrafiltration for SERS-based biosensors. *J Am Chem Soc, 132*(32), 10970-10972. doi:10.1021/ja103809c

Tripodo, G., Trapani, A., Torre, M. L., Giammona, G., Trapani, G., & Mandracchia, D. (2015). Hyaluronic acid and its derivatives in drug delivery and imaging: Recent advances and challenges. *Eur J Pharm Biopharm, 97*(Pt B), 400-416. doi:10.1016/j.ejpb.2015.03.032

Truesdell, R. A., Vorobieff, P. V., Sklar, L. A., & Mammoli, A. A. (2003). Mixing of a continuous flow of two fluids due to unsteady flow. *Phys Rev E Stat Nonlin Soft Matter Phys, 67*(6 Pt 2), 066304. doi:10.1103/PhysRevE.67.066304

Tsuchida, E. (1994). Formation of Polyelectrolyte Complexes and Their Structures. *Journal of Macromolecular Science-Pure and Applied Chemistry, A31*(1), 1-15.

Turley, E. A., Noble, P. W., & Bourguignon, L. Y. (2002). Signaling properties of hyaluronan receptors. *J Biol Chem, 277*(7), 4589-4592. doi:10.1074/jbc.R100038200

Valencia, P. M., Farokhzad, O. C., Karnik, R., & Langer, R. (2012). Microfluidic technologies for accelerating the clinical translation of nanoparticles. *Nat Nanotechnol, 7*(10), 623-629. doi:10.1038/nnano.2012.168

Vauthier, C., & Bouchemal, K. (2009). Methods for the Preparation and Manufacture of Polymeric Nanoparticles. *Pharmaceutical Research, 26*(5), 1025-1058. doi:DOI 10.1007/s11095-008-9800-3

Vauthier, C., Cabane, B., & Labarre, D. (2008). How to concentrate nanoparticles and avoid aggregation? *European Journal of Pharmaceutics and Biopharmaceutics, 69*(2), 466-475. doi:DOI 10.1016/j.ejpb.2008.01.025

Veeken, J. (2012). Purification of nanoparticles by hollow fiber diafiltration. *Materials Science and Engineering, 40*, 012035.

Veilleux, D. (2016). *Lyophilisation et concentration de complexes chitosane/ADN et chitosane/ARNic pour la therapie genique.* (Ph.D), University of Montreal, Polytechnique Montrea, Montreal.

Veilleux, D., Nelea, M., Biniecki, K., Lavertu, M., & Buschmann, M. D. (2016). Preparation of Concentrated Chitosan/DNA Nanoparticle Formulations by Lyophilization for Gene Delivery at Clinically Relevant Dosages. *J Pharm Sci, 105*(1), 88-96. doi:10.1016/j.xphs.2015.11.001

Wandrey, C. (1999). Concentration regimes in polyelectrolyte solutions. *Langmuir, 15*(12), 4069-4075. doi:Doi 10.1021/La980895h

Why You Should Consider Hollow Fibres for Ultrafiltration. (2015). Retrieved from http://blog.parker.com/why-you-should-consider-hollow-fibres-for-ultrafiltration

Winkler, J. (2013). Oligonucleotide conjugates for therapeutic applications. *Ther Deliv, 4*(7), 791-809. doi:10.4155/tde.13.47

Xu, L., & Anchordoquy, T. (2011a). Drug Delivery Trends in Clinical Trials and Translational Medicine: Challenges and Opportunities in the Delivery of Nucleic Acid-Based Therapeutics. *Journal of Pharmaceutical Sciences, 100*(1), 38-52. doi:Doi 10.1002/Jps.22243

Xu, L., & Anchordoquy, T. (2011b). Drug delivery trends in clinical trials and translational medicine: challenges and opportunities in the delivery of nucleic acid-based therapeutics. *J Pharm Sci, 100*(1), 38-52. doi:10.1002/jps.22243

Yang, C., Nilsson, L., Cheema, M. U., Wang, Y., Frokiaer, J., Gao, S., . . . Norregaard, R. (2015). Chitosan/siRNA nanoparticles targeting cyclooxygenase type 2 attenuate unilateral ureteral obstruction-induced kidney injury in mice. *Theranostics, 5*(2), 110-123. doi:10.7150/thno.9717

Zaloga, J., Stapf, M., Nowak, J., Pottler, M., Friedrich, R. P., Tietze, R., . . . Alexiou, C. (2015). Tangential Flow Ultrafiltration Allows Purification and Concentration of Lauric Acid-/Albumin-Coated Particles for Improved Magnetic Treatment. *Int J Mol Sci, 16*(8), 19291-19307. doi:10.3390/ijms160819291

Zelphati, O., Nguyen, C., Ferrari, M., Felgner, J., Tsai, Y., & Felgner, P. L. (1998). Stable and monodisperse lipoplex formulations for gene delivery. *Gene Therapy, 5*, 1272–1282.

Zhang, H., & Neau, S. H. (2002). In vitro degradation of chitosan by bacterial enzymes from rat cecal and colonic contents. *Biomaterials, 23*(13), 2761-2766. doi:Pii S0142-9612(02)00011

Zhigaltsev, I. V., Belliveau, N., Hafez, I., Leung, A. K., Huft, J., Hansen, C., & Cullis, P. R. (2012a). Bottom-up design and synthesis of limit size lipid nanoparticle systems with aqueous and triglyceride cores using millisecond microfluidic mixing. *Langmuir, 28*(7), 3633-3640. doi:10.1021/la204833h

Zhigaltsev, I. V., Belliveau, N., Hafez, I., Leung, A. K. K., Huft, J., Hansen, C., & Cullis, P. R. (2012b). Bottom-Up Design and Synthesis of Limit Size Lipid Nanoparticle Systems with Aqueous and Triglyceride Cores Using Millisecond Microfluidic Mixing. *Langmuir, 28*(7), 3633-3640. doi:Doi 10.1021/La204833h

Zhoua, H., Ni, J., Huanga, W., & Zhang, J. (2006). Separation of hyaluronic acid from fermentation broth by tangential flow microfiltration and ultrafiltration. *Separation and Purification Technology, 52*, 29-38.

Zhu, X. S., & Choo, K. H. (2008). A novel approach to determine the molecular overlap of polyelectrolyte using an ultrafiltration membrane. *Colloids and Surfaces a-Physicochemical and Engineering Aspects, 312*(2-3), 231-237. doi:DOI 10.1016/j.colsurfa.2007.06.062

Zintchenko, A., Rother, G., & Dautzenberg, H. (2003). Transition highly aggregated complexes-soluble complexes via polyelectrolyte exchange reactions: Kinetics, structural changes, and mechanism. *Langmuir, 19*(6), 2507-2513. doi:Doi 10.1021/La0265427